ISSN 1949-8462 (online)

World Journal of *Cardiology*

World J Cardiol 2018 September 26; 10(9): 74-122

Published by Baishideng Publishing Group Inc

World Journal of Cardiology

Contents

Monthly Volume 10 Number 9 September 26, 2018

ABOUT COVER

Editorial Board Member of *World Journal of Cardiology*, Ioanna Andreadou, PharmD, PhD, Associate Professor, Department of Pharmaceutical Chemistry, University of Athens School of Pharmacy, Athens , Greece

AIM AND SCOPE

World Journal of Cardiology (*World J Cardiol*, *WJC*, online ISSN 1949-8462, DOI: 10.4330) is a peer-reviewed open access journal that aims to guide clinical practice and improve diagnostic and therapeutic skills of clinicians.

WJC covers topics concerning arrhythmia, heart failure, vascular disease, stroke, hypertension, prevention and epidemiology, dyslipidemia and metabolic disorders, cardiac imaging, pediatrics, nursing, and health promotion. Priority publication will be given to articles concerning diagnosis and treatment of cardiology diseases. The following aspects are covered: Clinical diagnosis, laboratory diagnosis, differential diagnosis, imaging tests, pathological diagnosis, molecular biological diagnosis, immunological diagnosis, genetic diagnosis, functional diagnostics, and physical diagnosis; and comprehensive therapy, drug therapy, surgical therapy, interventional treatment, minimally invasive therapy, and robot-assisted therapy.

We encourage authors to submit their manuscripts to *WJC*. We will give priority to manuscripts that are supported by major national and international foundations and those that are of great basic and clinical significance.

INDEXING/ABSTRACTING

World Journal of Cardiology (*WJC*) is now abstracted and indexed in Emerging Sources Citation Index (Web of Science), PubMed, PubMed Central, Scopus, China National Knowledge Infrastructure (CNKI), and Superstar Journals Database.

NAME OF JOURNAL
World Journal of Cardiology

ISSN
ISSN 1949-8462 (online)

LAUNCH DATE
December 31, 2009

FREQUENCY
Monthly

EDITORIAL BOARD MEMBERS
All editorial board members resources online at http://www.wjgnet.com/1949-8462/editorialboard.htm

EDITORIAL OFFICE
Jin-Lei Wang, Director
World Journal of Cardiology
Baishideng Publishing Group Inc
7901 Stoneridge Drive, Suite 501, Pleasanton, CA 94588, USA
Telephone: +1-925-2238242
Fax: +1-925-2238243
E-mail: editorialoffice@wjgnet.com
Help Desk: http://www.f6publishing.com/helpdesk
http://www.wjgnet.com

PUBLISHER
Baishideng Publishing Group Inc
7901 Stoneridge Drive, Suite 501,
Pleasanton, CA 94588, USA
Telephone: +1-925-2238242
Fax: +1-925-2238243
E-mail: bpgoffice@wjgnet.com
Help Desk: http://www.f6publishing.com/helpdesk
http://www.wjgnet.com

PUBLICATION DATE
September 26, 2018

INSTRUCTIONS TO AUTHORS
http://www.wjgnet.com/bpg/gerinfo/204

ONLINE SUBMISSION
http://www.f6publishing.com

World Journal of Cardiology

Submit a Manuscript: http://www.f6publishing.com

World J Cardiol 2018 September 26; 10(9): 74-86

DOI: 10.4330/wjc.v10.i9.74

ISSN 1949-8462 (online)

REVIEW

Myocardial reperfusion injury and oxidative stress: Therapeutic opportunities

Jaime González-Montero, Roberto Brito, Abraham IJ Gajardo, Ramón Rodrigo

Jaime González-Montero, Roberto Brito, Abraham IJ Gajardo, Ramón Rodrigo, Molecular and Clinical Pharmacology Program, Institute of Biomedical Sciences, Faculty of Medicine, University of Chile, Santiago 70058, Chile

Roberto Brito, Abraham IJ Gajardo, Internal Medicine Department, University of Chile, Clinical Hospital, Santiago 70058, Chile

ORCID number: Jaime González-Montero (0000-0003-0324-2948); Roberto Brito (0000-0001-8205-1984); Abraham IJ Gajardo (0000-0002-6387-3779); Ramón Rodrigo (0000-0003-1724-571X).

Author contributions: All authors equally contributed to this paper with conception and design of the study, literature review and analysis, drafting and critical revision and editing, and final approval of the final version.

Supported by FONDEF grant No. ID15I10285.

Conflict-of-interest statement: No potential conflicts of interest.

Manuscript source: Invited manuscript

Correspondence to: Dr. Ramón Rodrigo. Molecular and Clinical Pharmacology Program, Institute of Biomedical Sciences, Faculty of Medicine, University of Chile, Independencia 1027, Santiago 70058, Chile. rrodrigo@med.uchile.cl
Telephone: +56-2-29786126
Fax: +56-2-29786126

Received: March 27, 2018
Peer-review started: March 28, 2018
First decision: April 11, 2018
Revised: April 28, 2018
Accepted: May 9, 2018
Article in press: May 10, 2018
Published online: September 26, 2018

Abstract

Acute myocardial infarction (AMI) is the leading cause of death worldwide. Its associated mortality, morbidity and complications have significantly decreased with the development of interventional cardiology and percutaneous coronary angioplasty (PCA) treatment, which quickly and effectively restore the blood flow to the area previously subjected to ischemia. Paradoxically, the restoration of blood flow to the ischemic zone leads to a massive production of reactive oxygen species (ROS) which generate rapid and severe damage to biomolecules, generating a phenomenon called myocardial reperfusion injury (MRI). In the clinical setting, MRI is associated with multiple complications such as lethal reperfusion, no-reflow, myocardial stunning, and reperfusion arrhythmias. Despite significant advances in the understanding of the mechanisms accounting for the myocardial ischemia reperfusion injury, it remains an unsolved problem. Although promising results have been obtained in experimental studies (mainly in animal models), these benefits have not been translated into clinical settings. Thus, clinical trials have failed to find benefits from any therapy to prevent MRI. There is major evidence with respect to the contribution of oxidative stress to MRI in cardiovascular diseases. The lack of consistency between basic studies and clinical trials is not solely based on the diversity inherent in epidemiology but is also a result of the methodological weaknesses of some studies. It is quite possible that pharmacological issues, such as doses, active ingredients, bioavailability, routes of administration, co-therapies, startup time of the drug intervention,

and its continuity may also have some responsibility for the lack of consistency between different studies. Furthermore, the administration of high ascorbate doses prior to reperfusion appears to be a safe and rational therapy against the development of oxidative damage associated with myocardial reperfusion. In addition, the association with N-acetylcysteine (a glutathione donor) and deferoxamine (an iron chelator) could improve the antioxidant cardioprotection by ascorbate, making it even more effective in preventing myocardial reperfusion damage associated with PCA following AMI.

Key words: Acute myocardial infarction; Repefusion injury; Oxidative stress; Ascorbate; N-acetylcysteine; Deferoxamine

Core tip: Acute myocardial infarction is the leading cause of death in the world. At least half of the resulting myocardial damage is associated with myocardial reperfusion. Myocardial reperfusion injury is associated with reactive oxygen species production and iron mobilization. Treatment with antioxidants such as ascorbate, N-acetylcysteine, and an iron chelator such as deferoxamine, could prevent the development of this damage.

González-Montero J, Brito R, Gajardo AIJ, Rodrigo R. Myocardial reperfusion injury and oxidative stress: Therapeutic opportunities. *World J Cardiol* 2018; 10(9): 74-86 Available from: URL: http://www.wjgnet.com/1949-8462/full/v10/i9/74.htm DOI: http://dx.doi.org/10.4330/wjc.v10.i9.74

INTRODUCTION

Acute myocardial infarction (AMI) is the leading cause of death worldwide, and it is associated with high morbidity and mortality. The AMI complications have significantly decreased with the development of interventional cardiology and percutaneous coronary angioplasty (PCA) treatment, which quickly and effectively restore the blood flow to the area previously subjected to ischemia[1]. Paradoxically, the restoration of blood flow to the ischemic zone leads to a massive production of reactive oxygen species (ROS), which generate rapid and severe damage to biomolecules, in a phenomenon called myocardial reperfusion injury (MRI)[2,3]. Sources of ROS in reperfusion include the predominant contribution of NADPH oxidases, which are present in many cell types in myocardial tissue. Other sources are xanthine oxidase, uncoupled eNOS and the mitochondrion[4]. In the clinical setting, MRI is associated with multiple complications such as lethal reperfusion, no-reflow phenomenon, myocardial stunning, and reperfusion arrhythmias (Figure 1).

Despite significant advances in the understanding of the mechanisms accounting for MRI, it remains an unsolved problem. Although promising results have been obtained in experimental studies (mainly in animal models) these benefits have not been translated into clinical settings. Clinical trials have failed to find benefits from any therapy to prevent MRI, demonstrating a clear dissociation between the bench and the bedside[5].

Prevention of MRI in the clinical setting has intrinsic difficulties in its approach. First, any therapy oriented to MRI prevention must be administered prior to myocardial reperfusion (in other words, prior to PCA). In addition, it should be applied in doses high enough to counterbalance the rapid and massive ROS production following reperfusion. Moreover, there are many different visions regarding the best biomarker to define MRI in patients, and so clinical trials express their results with different outcomes (such as clinical outcomes, serum cardiac biomarkers, echocardiographic parameters, cardiac magnetic resonance, among many others) which makes the analyses even more difficult. All these elements have made it difficult to develop an effective therapy to prevent MRI in AMI patients. The present review focuses on the cellular and molecular mechanisms of oxidative-stress induced MRI during AMI, and the key points to develop an appropriate strategy to reduce oxidative damage derived from myocardial reperfusion.

PATHOPHYSIOLOGY

MRI is a clinical problem associated with procedures such as thrombolysis, angioplasty, and coronary bypass surgery, which are commonly used to re-establish the blood flow and minimize the damage to the heart due to severe myocardial ischemia[3]. There are three main hypotheses which have been proposed to explain the pathogenesis of ischemia reperfusion (IR) injury: oxidative stress, iron mobilization, and Ca^{2+}-overload[6,7]. All of these mechanisms are most likely related, but it is not known whether they operate simultaneously or one precedes the other (Figure 2).

Oxidative stress

The level of myocardial tissue oxygenation increases following restoration of blood flow, which is initiated with a burst of ROS generation[8]; these ROS are the major initiators of myocardial damage in MRI[3]. Increased ROS production is mainly due to the activation of xanthine oxidase in endothelial cells, mitochondrial electron transport chain reactions in cardiomyocytes, and NADPH oxidase in inflammatory cells[9] (Figure 1).

Oxidative stress occurs when there is an imbalance between the generation of ROS and the antioxidant defense systems in the body so that the latter becomes overwhelmed[10]. ROS include hydrogen peroxide (H_2O_2), the superoxide radical anion, the hydroxyl radical ($OH^{\bullet}$), and peroxynitrite anion ($ONOO^-$), and they have all been shown to increase with reperfusion[11] (Figure 2). As a result of lipid peroxidation, oxidation of DNA and proteins and membrane damage may take place.

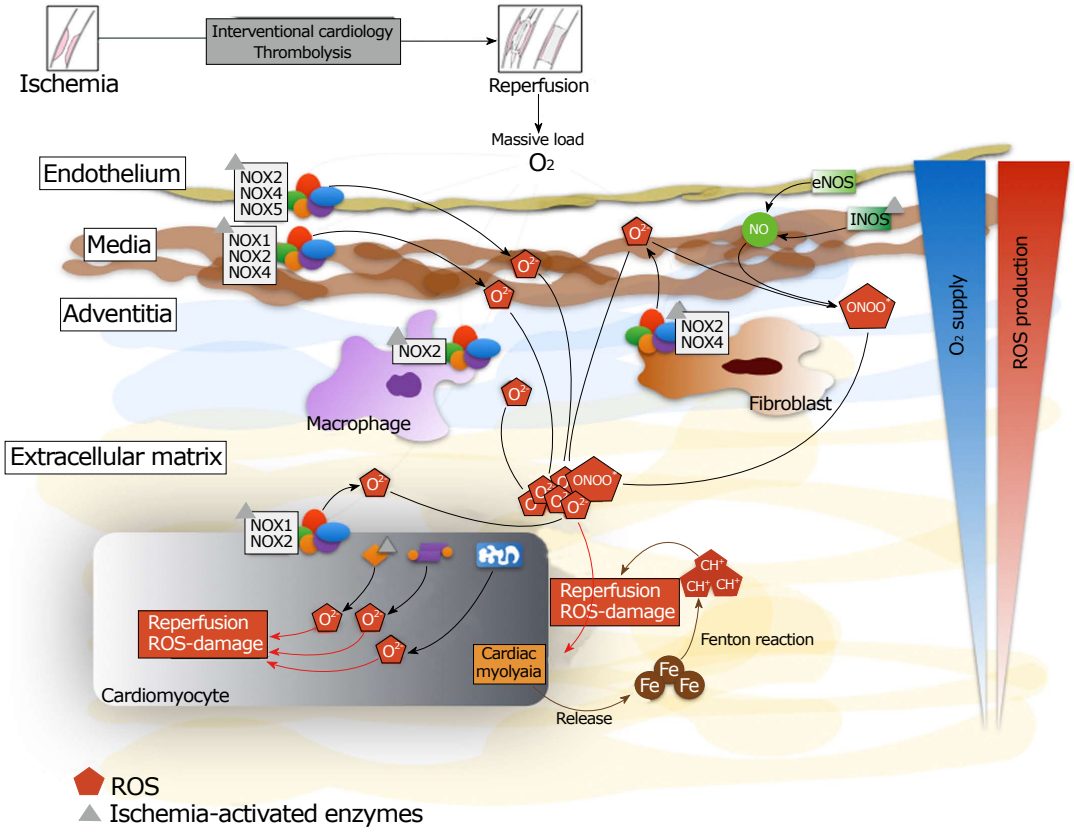

Figure 1 Generation of reactive oxygen species and mobilization of iron after myocardial reperfusion. There is a massive production of reactive oxygen species and iron mobilization by the different cellular types of the myocardial tissue. The iron reacts with superoxide anion to produce hydroxyl radical by the Fenton reaction. Inside cardiomyocyte, there is intracellular production of reactive oxygen species through NADPH oxidase, eNOS uncoupled, xanthine oxidase and mitochondrion. NOX: NADPH oxidase; ROS: Reactive oxygen species; Fe: Iron; eNOS: Endothelial nieric oxide synthases.

This leads to alterations in membrane permeability and to modifications of protein structure and functional changes[12].

ROS sources: In pathophysiological conditions, there are many sources of ROS in myocardial tissue. The most important sources are NADPH oxidases (NOX), uncoupled eNOS, xanthine oxidases and the mitochondrion. NOX catalyzes the one electron reduction of O_2 to generate super-oxide radical anion ($O_2^{\bullet -}$), using NADPH as the source of electrons. This enzyme is largely present in the activated neutrophil, wherein it generates large amounts of toxic $O_2^{\bullet -}$ and other ROS important in bactericidal function[13]. Pathogenic roles of NOX-derived ROS are also verified in human IR injury *in vivo*[14]. It was recently reported that in isolated perfused murine hearts that *NOX1* and/or *NOX2* gene knock-out significantly attenuated MRI (by up to 50% of the final infarct size)[15], thus demonstrating the crucial importance of this enzyme in MRI.

The NO synthases (NOS) are a family of enzymes that convert the amino acid L-arginine to L-citrulline and NO. Endothelial NOS (eNOS) plays a major role in the regulation of vascular function. The eNOS may become uncoupled in the absence of the NOS substrate L-arginine or the cofactor BH4. Uncoupled eNOS results in the production of $O_2^{\bullet -}$ instead of NO[16-18]. This perpetuates a vicious cycle because peroxynitrite, the reaction product of superoxide and NO, leads to further eNOS uncoupling[19]. Furthermore, eNOS uncoupling may play a major role in MRI by increasing ROS production and limiting NO availability[20].

Xanthine oxidase is predominantly present in the vascular endothelium in the normal heart and generates $O2^{\bullet -}$, H_2O_2, and $OH^{\bullet}$ as byproducts of its normal metabolic action[21]. Under pathological conditions, such as tissue ischemia, xanthine dehydrogenase can be converted to Xanthine oxidase. In IR this enzyme catalyzes the formation of uric acid with the coproduction of $O2^{\bullet -}$[22]. Superoxide release results in the recruitment and activation of neutrophils and their adherence to endothelial cells, which stimulates the formation of xanthine oxidase in the endothelium, with further $O2^{\bullet -}$ production[23]

Mitochondria are cellular organelles involved in energy production, so any injury that they may suffer could cause impairment of cellular energy that could lead, depending on the intensity of the injury, to apoptosis or different levels of cellular damage. During ischemia, due

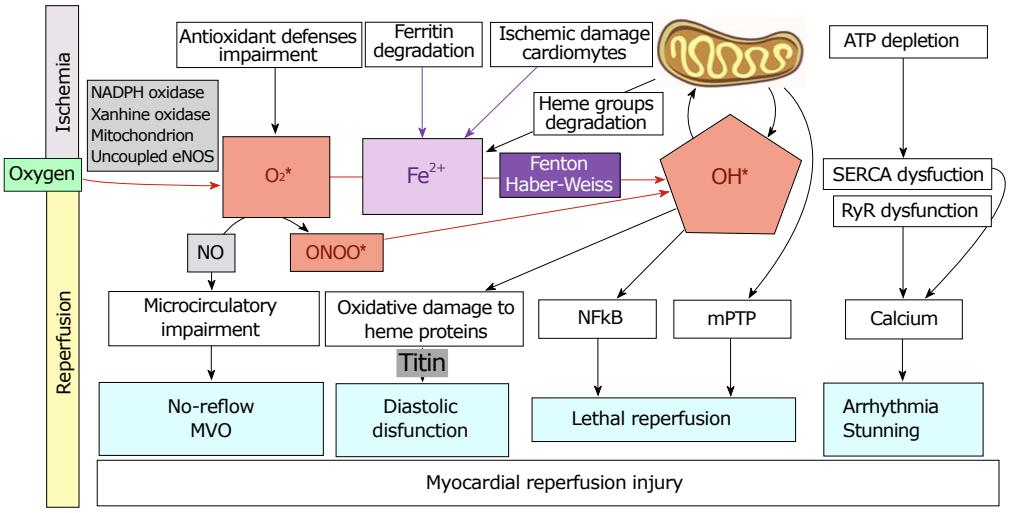

Figure 2 Role of reactive oxygen species and iron mobilization in myocardial reperfusion injury and its clinical implications. MVO: Microvascular obstruction; ONOO*: Peroxynitrite; NO: Nitric oxide; OH *: Radical hydroxyl; Fe: Iron; RyR: Ryanodine receptor channel; SERCA: Sarco/endoplasmic reticulum Ca^{2+}-ATPase.

to the lack of oxygen, the electron transport chain cannot function correctly and therefore ROS are produced at high levels. Additionally, ROS may cause oxidative damage of mitochondrial DNA, impairing mitochondrial function. This damage performs a positive feedback on ROS production that, at the same time, perpetuates mitochondrial damage and ROS synthesis. Oxidative injury to the mitochondrial membrane can also occur, resulting in membrane depolarization and the uncoupling of oxidative phosphorylation, with altered cellular respiration[24]. This can ultimately lead to mitochondrial damage, with release of cytochrome c, activation of caspases, and apoptosis[25].

RNS sources: The ROS are not solely responsible for free radical damage. Reactive nitrogen species (RNS), mainly peroxynitrite anions (ONOO-), also generate RNS-damage, thus producing nitrosative stress. Peroxynitrite results from the interaction between NO and the superoxide anion[4], and NO is synthesized mainly by nitric oxide synthases which have two isoforms in the cardiomyocyte: endothelial (eNOS) and inducible (iNOS). Oxidative and nitrosative damage causes the uncoupling of both NOS isoforms, resulting in the enhanced synthesis of $O2^{\bullet-}$[4].

Evidence supports the view that nitrosative stress plays an important role in the pathogenesis of MRI. While NO itself is not harmful, some of the reaction products (mainly $OH^{\bullet}$) resulting from high ONOO- formation in the cell are highly cytotoxic substances[26]. The production of $O2^{\bullet-}$ is increased during reperfusion, which interacts with NO and leads to the formation of ONOO-, thus triggering the previously described phenomenon[27]. Peroxynitrite not only causes structural damage by attacking macromolecules, but it also leads to myocardial functional impairment[28]. The general view about the mechanisms that lead to nitrosative stress is that IR can induce iNOS expression and that the resulting high concentrations of NO can lead to cardiac injury[26]. The drop in NO concentration occurring during cardiac IR plays an important role in triggering the transcription nuclear factor kappaB (NF-κB) leading to activation and successive induction of iNOS expression during the reperfusion phase[29-31]. Figure 1 shows a diagram of ROS and RNS sources in myocardial tissue.

Iron mobilization

It has been postulated that iron homeostasis could play an important role in the development of MRI in the cardiomyocytes[32,33]. Free iron is deleterious for cells; thus generally it is bound to proteins forming complexes[34]. During ischemia, iron metabolism is impaired, and it is released as free iron. This catalytic free iron can generate ROS through the Fenton reaction, catalyzing the production of ·OH from H_2O_2 and $O_2^{\bullet-}$[35]. It has been reported that susceptibility to injury from H_2O_2 in rat hearts is associated with the magnitude of the intracellular low molecular weight iron pool[36]. Some metals with redox properties have a well-documented role in the development of MRI[37,38]. Following reperfusion, both iron and copper are released to the coronary circulation[32] which can contribute to ROS generation (Figure 2). In patients with thalassemia the iron overload is related to arrhythmias and congestive heart failure, which is the main cause of death among these patients[39]. Iron chelation therapy has significantly improved the survival of patients with thalassemia[40], because iron chelators are effective and safe drugs to treat the iron poisoning[41].

Calcium homeostasis

Oxidative stress modifies phospholipids and proteins leading to lipid peroxidation and thiol-group oxidation; these changes are considered to alter membrane

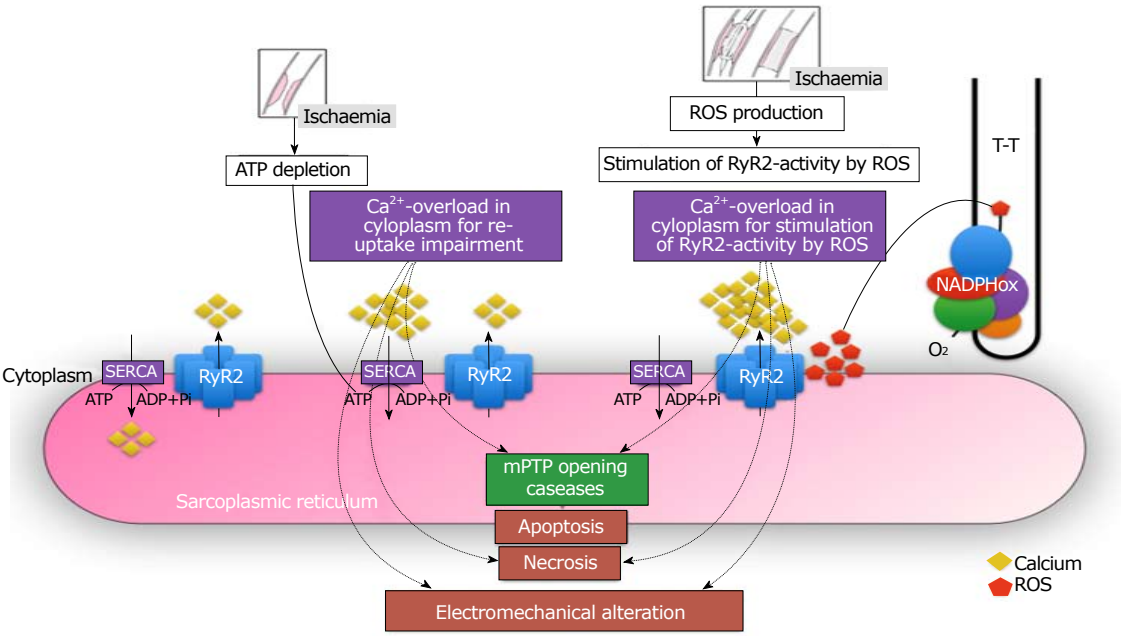

Figure 3 Central role of calcium in the electro-mechanical dissociation of cardiomyocyte after myocardial reperfusion. RyR: Ryanodine receptor channel; SERCA: Sarco / endoplasmic reticulum Ca^{2+}-ATPase; mPTP: Mitochondrial permeability transition pore; Ca: Calcium; ROS: Reactive oxygen species.

permeability and configuration in addition to producing functional modifications of various cellular proteins[42]. Oxidative stress may result in cellular defects including a depression in the sarcolemma Ca^{2+}-pump ATPase that leads to a decreased Ca^{2+}-efflux, and a depression in (Na + K)-ATPase activity that, in turn, leads to an increased Ca^{2+}-influx[43]. Oxidative stress has also been reported to depress the sarcoplasmic reticulum Ca^{2+}-pump ATPase (SERCA) and thus inhibit Ca^{2+} sequestration from the cytoplasm in cardiomyocytes[44]. The depression in Ca^{2+}-regulatory mechanism by ROS ultimately results in intracellular Ca^{2+} ($[Ca^{2+}]i$) overload and cell death. In addition, an increase in $[Ca^{2+}]i$ during ischemia induces the conversion of xanthine dehydrogenase to xanthine oxidase and subsequently results in increased production of $O_2^{\bullet-}$[44].

Recently it has been shown that the function of the channel ryanodine receptor (RyR) is controlled by ROS[45]. It has been demonstrated that NADPH oxidase and the RyR channel could be located adjacent to each other in the T-tubules of cardiomyocytes[46]. Thus, the increase in ROS production after myocardial reperfusion could lead to an increase in RyR channel function, resulting in an intracellular calcium overload, thereby causing activation of pro-apoptotic intracellular pathways, necrosis, and electromechanical alteration. All these mechanisms are summarized in Figure 3.

Redox-sensitive signaling pathways: Not only do ROS exert their actions by directly modifying organic molecules, but ROS are also involved in the regulation of the expression of several genes[47]. NF-κB and AP-1, both of which can experience ROS-mediated activation, stimulate the transcription of several protein mediators, for example, proinflammatory cytokines that activate several cell death pathways[48]. The role of cytokines, chemokines, leukocytes, and acute-phase proteins such as high-sensitivity C-reactive protein in the pathogenesis of MRI has been reported in several studies[49,50]. Oxidative stress, ROS and inflammation are linked in a way that is very difficult to dissect. These phenomena have important molecular bridges that are activated in the presence of ROS[51], leading to the activation of multiple mechanisms that cause heart tissue remodeling and therefore enhance the susceptibility to rhythm disorders. Among those molecules, the most studied has been the transcriptional factor NF-κB, a factor that responds to changes of the cellular oxidative state, ischemia-reperfusion, and inflammatory molecules[52]. When NF-κB is activated, for example in the presence of ROS by phosphorylation of its inhibitory cofactor (Iκ-B), it bonds to a DNA response element and promotes the transcription of genes involved in inflammatory and pro-fibrotic response, for example IL-6, which transforms growth factors TGF-β and TNF-α[53]. Those molecules act in various tissues, but particularly in the heart, producing extracellular matrix remodeling and fibrosis (structural remodeling), which changes the electrophysiological properties of the heart. Several studies have associated NF-κB activation with cardiac dysfunction, ventricular hypertrophy, and maladaptive cardiac growth[54] (Figure 2).

Exposure to low-to-moderate ROS levels should trigger a survival response and reinforce ROS scavengers of the antioxidant defense system to elicit a cardioprotective effect for myocardial reperfusion. The molecular mechanism responsible for this adaptive change involves enhanced antioxidant activity achieved

by up-regulating several housekeeping genes partly under the control of Nrf2 (nuclear factor-erythroid 2-related factor 2); Nrf2 is normally sequestered in the cytosol by Keap[55]. Upon oxidative stimulation, Nrf2 oxidizes or covalently modifies Keap1 thiol groups, which dissociate from Keap1 and undergo nuclear translocation. In the nucleus, Nrf2 binds to antioxidant response elements in target gene promoters[56], which increase the expression of antioxidant enzymes. It has been demonstrated that the constitutive levels/activities of a number of important antioxidants and phase 2 enzymes, such as CAT, GSH-Px, glutathione reductase, glutathione transferase, NADPH-quinone oxidoreductase 1, and heme oxygenase-1 in primary cardiomyocytes are dependent on Nrf2 status. In addition, Nrf2 diminishes the susceptibility of cardiomyocytes to injury elicited by oxidants and electrophilic species[57], making the Nrf2 signaling pathway an important mechanism for myocardial cytoprotection. It is of interest to note that ROS levels could be responsible for the activation of NF-κB and/or Nrf2 pathways.

Clinical implications: Myocardial damage caused by ischemia-reperfusion events are mainly associated with four clinical conditions: lethal reperfusion, myocardial stunning, no-reflow phenomenon, and reperfusion arrhythmias (Figure 2).

Lethal reperfusion is a paradoxical type of MRI caused by the restoration of coronary blood flow after an ischemic episode. It is defined as the death of cardiomyocytes that were viable immediately before myocardial reperfusion. Its main manifestation is as an increased infarct size due to reperfusion, a condition mainly associated with AMI[3]. In the late fifties, it was suggested that myocardial reperfusion contributes part of the histological damage associated with ischemia-reperfusion models. However, for decades it was very complex to determine the precise evolution of necrosis along the transition from ischemia to reperfusion in myocardial tissue[58]. Nowadays, the harmful effects of myocardial reperfusion damage, also known as lethal reperfusion injury, are considered to involve myocardial cell death derived from the restoration of blood flow subsequent to an ischemic process, and to act through mechanisms strongly associated with oxidative stress[3].

Reperfusion arrhythmias clinically represent a major comorbidity of AMI with an 88.7% occurrence rate in certain small clinical trials with continuous monitoring[59]. In addition, postoperative atrial fibrillation (POAF), the most common reperfusion arrhythmia associated with cardiac surgeries, has an incidence ranging between 20%-40%[60]. Myocardial stunning, despite being a reversible damage, is the cause of an impaired ventricular function that leads to increased morbidity. It is derived from a short-term ischemia-reperfusion process that was first reported in the early 1930s[61]. Myocardial stunning is present to a greater or lesser extent in all survivors of AMI. In the late 1980s evidence began to appear suggesting an important role of oxidative stress in the development of myocardial stunning, proposing that the main injury pathway could be an altered calcium homeostasis associated with sarcoplasmic reticulum damage[62]. More recently, clinical studies have strengthened this hypothesis[63], and it has been reported in animal models that interventions aimed to improve antioxidant defenses attenuate myocardial stunning[64,65].

The no-reflow phenomenon is an impaired myocardial perfusion of a specific segment of the coronary system that is not associated with an angiographic occlusion of the respective vessel[66]. Vascular and endothelial damage can occur after the reperfusion of previously blocked coronary circulation. It can be exhibited as a microvascular dysfunction after restoring the flow during either angioplasty or thrombolysis, thus leading to the development of the no-reflow phenomenon[67]. The presence of coronary microvascular dysfunction and this phenomenon are associated with larger infarct size, lower left ventricular ejection fraction, adverse left ventricular remodeling in the remote stage of myocardial infarction, and increased incidences of heart failure and death, compared with patients without no-reflow phenomenon[68]. Some studies using animal models showed that antioxidant strategies are able to reduce this phenomenon[69-71], and this data is consistent with a small clinical trial finding that antioxidant depletion is associated with no-reflow phenomenon in AMI[72]. In addition, recent research in rabbits shows that the suppression of the oxidative stress-sensitive transcription factor NF-κB, a key mediator of inflammation in cardiovascular systems, reduces myocardial no-reflow phenomenon[73].

Recently, our group has reported major clinical benefits with the use of antioxidants in pathologies associated with myocardial reperfusion, such as POAF and AMI. With regard to POAF, we documented a significant decrease in the incidence of this arrhythmia in patients undergoing cardiac surgery with extracorporeal circulation after administration of ascorbate, alpha-tocopherol, and omega-3 polyunsaturated fatty acids, which was accompanied by a significant decrease in oxidative stress biomarkers in auricular tissue and peripheral blood[60].

ROLE OF ANTIOXIDANTS

Despite a molecular basis and *in vitro* evidence supporting the use of antioxidants to prevent MRI, clinical evidence continues to be controversial. In the clinical setting, impaired micro-circulatory reperfusion was improved by ascorbate infusion in patients undergoing elective PCA[74]. Similar results were recently reported by our group[75]. These results suggest a positive role of antioxidants in counteracting the deleterious effects of oxidative stress on microvascular function. On the other hand, the ROS scavenger edaravone when administered to patients with AMI immediately prior to reperfusion, significantly reduced infarct size and

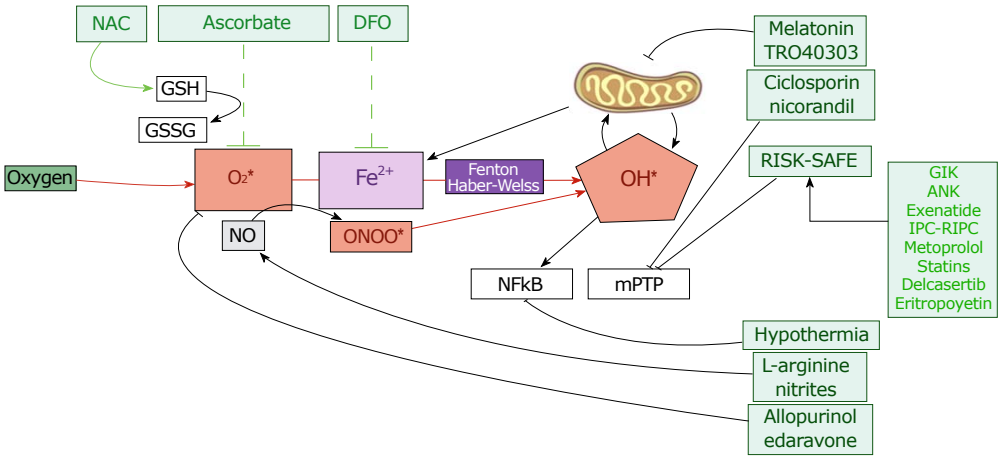

Figure 4 Experimental, pharmacological and clinical approaches to prevent myocardial reperfusion injury at cellular level. RISK: Reperfusion injury salvage kinase pathway; SAFE: Survivor activating factor enhancement pathway; GSH: Reduced glutathione; GSSG: Oxidized glutathione; NAC: N-acetylcysteine; DFO: deferoxamine; ONOO*: Peroxynitrite; NO: Nitric oxide; OH *: Radical hydroxyl; mPTP: Mitochondrial permeability transition pore.

reperfusion arrhythmias[76,77]. Also some experimental studies reported that the use of deferoxamine (DFO) and N-acetylcysteine (NAC) could improve microvascular dysfunction[78,79].

Carotenoids represent another potential pharmacological alternative in the management of MRI[80]. Carotenoids are a widely distributed group of fat-soluble pigments which exert antioxidant, anti-inflammatory, and antiproliferative properties[81]. Several experimental data support potential role of carotenoids in this pathological condition: Tong *et al*[81] demonstrated that pretreatment with lycopene reduced cardiomyocyte death induced by ischemia/reoxygenation *in vitro*, and also reduced myocardial infarct size in an *in vivo* model of AMI[82]. Another carotenoid, crocetin, protected against myocardial reperfusion injury *in vivo* by inhibiting ROS production, reducing eNOS expression and myocardium apoptosis[82]. All-trans retinoic acid presented also protective activity against reperfusion injury both *in vitro* and *in vivo*, probably by down-regulating MAPK signaling[84]. Despite the fact that carotenoids have been useful in preventing MRI in experimental studies and have arisen as a promising pharmacological alternative, further clinical studies and randomized clinical trials are required.

In the following paragraphs we will discuss a new hypothesis for the prevention of MRI through the combined use of ascorbate, NAC, and DFO prior to reperfusion in order to strengthen antioxidant defense systems and so prevent oxidative damage (Figure 4).

Ascorbate

The basis of this hypothesis is to achieve high plasma levels of ascorbate prior to reperfusion in order to strengthen the antioxidant defense system of myocardial tissue. Thus, when oxygen suddenly arrives to the previously ischemia-damaged myocardial tissue-which is the primary substrate for the production of the highly reactive superoxide anion radical-ascorbate may efficiently reduce ROS and prevent oxidative damage[5,8]. To support this hypothesis, we will discuss the main actions of this antioxidant and its pharmacokinetic properties.

Ascorbate is an essential antioxidant that performs its roles in different cell locations by acting in water-soluble components[85,86]. The most studied mechanism in which ascorbate acts is partly based on its ability to directly reduce ROS[87-89]. Besides its ROS scavenger actions, ascorbate exerts a complex modulation of numerous enzymes involved in ROS production, endothelial dysfunction, platelet aggregation, and smooth muscle cell tone[90-92]. The four most important mechanisms in which ascorbate modulates the endothelial function are NADPH down-regulation, and the up-regulation of eNOS, phospholipase A2, and antioxidant enzymes. NADPH oxidase, the most important superoxide source in the cardiovascular system, can be directly down-regulated by ascorbate[91,92]. The mechanism behind this effect has not been completely elucidated. It has been reported that ascorbate could be involved in the transcriptional and post-transcriptional modulation of NADPH oxidase[89,93] as well as in its synthesis[94]. In the presence of oxidative stress, eNOS is mostly in its uncoupled form which leads to endothelial dysfunction. In this context, ascorbate has been shown to increase eNOS activity, by preventing the oxidation of tetrahydrobiopterin and by inhibiting the p47phox subunit expression[95]. Therefore, ascorbate increases NO synthesis, reduces ROS formation and contributes to vascular tone regulation[96-98]. In relation to the up-regulation of antioxidant enzymes, some studies have demonstrated a positive correlation between antioxidant vitamin and antioxidant enzyme activity, particularly SOD. The mechanisms underlying these findings are not well explained, but it is plausible to hypothesize the existence of transcriptional and post-transcriptional events involved in the up-regulation of those antioxidant enzymes[92].

Table 1 Clinical trials

	Study details	Country	*n* Intervention		Main findings	Ref.
AA	Ascorbate previous to elective coronary angioplasty	Italy	28	28	Decrease in oxidative stress and improves reperfusion parameters	[74]
	Ascorbate previous to primary coronary angioplasty in patients with AMI	Chile	53	46	Improve ventricular function and reperfusion No differences in infarct size	[75]
NAC	N-acetylcysteine previous and after primary coronary angioplasty in patients with AMI	Germany	126	126	Decrease in oxidative stress No differences in infarct size	[105]
	N-acetylcysteine and nitroglycerine previous to primary coronary angioplasty in patients with AMI	Australia	67	65	Decrease in infarct size and cardiac damage biomarkers	[116]
DFO	Deferoxamine previous and after coronary angioplasty in patients with AMI	Australia	28	32	Decrease in oxidative stress No differences in infarct size	[114]

Main clinical studies that have used ascorbate, N-acetylcysteine or deferoxamine to prevent reperfusion injury in patients affected by acute myocardial infarction and treated with coronary angioplasty. AA: Ascorbate; NAC: N-acetylcysteine; DFO: Deferoxamine; IR: Ischemia reperfusion; AMI: Acute myocardial infarction.

Ascorbate counteracts and prevents the oxidation of lipids, proteins, and DNA, subsequently protecting their structure and biological function. Together with glutathione, ascorbate constitutes a primary line of defense against ROS[99]. Ascorbate, in aqueous compartments, can recycle α-tocopherol in membranes by reducing the α-tocopheroxyl radical back to α-tocopherol[100]. Accordingly, ascorbate has been shown to recycle α-tocopherol in lipid bilayers[101] and erythrocytes[95].

Ascorbate scavenging is concentration-dependent and requires intravenous administration. This is necessary because ascorbate concentration in plasma is tightly controlled and an excess of ascorbate is excreted as a function of dosage. In fact, even with supplementation approaching maximally tolerated doses, ascorbate plasma concentrations are always < 250 μmol/L. By contrast, intravenously injected ascorbate can safely lead to concentrations of 25-30 mmol/L[102]. It is of interest to mention that intra-arterial administration of high doses of ascorbate has been demonstrated to abolish both *in vivo* and *in vitro* effects of the superoxide anion with respect to the impairment of vascular endothelial function in patients with essential hypertension[103]. Unfortunately, oral doses are not enough to scavenge superoxide anions, thus a beneficial effect should not be expected.

Our group recently developed a randomized clinical trial in patients with AMI undergoing PCA, where massive doses of ascorbate (or placebo) were administered prior to PCA. Patients treated with ascorbate prior to myocardial reperfusion showed a better recovery of ejection fraction at 2-3 mo (measured by cardiac magnetic resonance) and significantly higher myocardial perfusion after PCA (*TIMI*-myocardial perfusion grade) than placebo patients, with no differences in infarct size[75] (Table 1).

N-acetyl-L-cysteine

Ascorbate consumes glutathione (GSH) to exert its antioxidant activity. High doses of ascorbate might be associated with a decrease in cellular GSH reserves[5]. For this reason, N-acetyl-L-cysteine (NAC) - a known GSH-donor-may also have synergistic effects with high doses of ascorbate. In the following paragraphs, we will discuss the potential role of NAC in preventing MRI.

Despite numerous studies and a prolonged track record of clinical trials, the effects of NAC are clouded in controversy and its pharmacological mechanism has not yet been fully clarified. However, there is plenty of evidence regarding its mechanism of action. First of all, NAC's main feature, and also the most studied one, is its capacity to act as a precursor for synthesis of GSH, thus replenishing GSH that has become depleted through the use of this peptide in detoxification routes[104]. However, it is vital to think of NAC as a pro-drug, because actions that are driven by this drug are dependent on its successful conversion to the antioxidant and detoxifying agent, GSH. Another frequently mentioned property of NAC is its intrinsic antioxidant activity. Nevertheless, the evidence regarding the antioxidant potential of NAC suggests that it does not have a noteworthy direct antioxidant activity[105].

NAC acts indirectly through chelation of metal ions such as catalytic iron[106,107] giving it the capability of mediating Fenton's reaction, thus ameliorating the possibility of the formation of hydroxyl radicals. This property is due to the fact that NAC forms conjugates with some metals. However, the importance of this mechanism in driving any protective effects compared to intracellular GSH replenishing is still unclear. Current evidence agrees on the capability of NAC to act as an inhibitor of NF-κB[108], a transcription factor that plays a critical role in inflammation, immunity, cell proliferation, differentiation, and survival. In conclusion, molecular mechanisms by which NAC exerts its diverse effects are complex and still unclear. Although it has been shown that NAC interacts with numerous biochemical pathways, its main mechanism involves serving as a precursor of cysteine and replenishing cellular GSH levels[104].

NAC has been widely used in different experimental and clinical settings to counteract oxidative stress. It has been demonstrated that NAC in combination with nitroglycerin and streptokinase is associated with significantly less oxidative stress and improved preservation of left ventricular function[109]. However, it has also been reported that a high-dose of NAC prior to PCA, although it reduces oxidative stress, does not provide an additional advantage in the prevention of MRI[110]. Additionally, an interesting study published in 2006 shows that administration of NAC in combination with streptokinase significantly diminishes oxidative stress and improves left ventricular function in patients with AMI[111]. A recent study using a rat model of myocardial ischemia-reperfusion injury demonstrates that treatment with continuous infusion of NAC (150 mg/kg per hour) starting 30 min before occlusion and lasting for 2 h (or until 1 h after the start of reperfusion) produces a significant limitation of the infarct and allows the recovery of the decreased total glutathione when compared to control[112]. Recently has been published the NACIAM trial by Pasupathy *et al*[113], that demonstrated a protective effect with the use of high doses of NAC in combination with a nitric oxide donor in patients with AMI (Table 1). This important study shows that NAC has a powerful protective effect when used in combination and previous to myocardial reperfusion. In summary, due to the known antioxidant and cardioprotective effect and its role as GSH-donor, it is plausible to suggest that NAC might have a synergistic effect with high doses of ascorbate and deferoxamine to prevent MRI.

Deferoxamine

Given the known role of iron in the lethal reperfusion, iron chelators have been tested to ameliorate this injury. One of the most frequently used drugs for this purpose is DFO. The first reports of its use to improve cardiac function in myocardium iron overload by directly removing iron from the myocardium[114] date from 1980s[115]. In animal models of AMI, the use of DFO has exhibited positive results. Some studies performed in dogs reported a decrease in the infarct size when they used DFO during the reperfusion, suggesting that iron-catalyzed production of ROS contributes to cardiomyocyte necrosis in the setting of MRI[116,117]. Studies have described improved recovery of myocardial function after ischemia, by using iron chelation[36,118]. The results obtained from animal models of MRI have suggested the use of iron chelators in the human model with partial results to date. Paraskevaidis *et al*[119] suggested DFO infusion was able to reduce myocardial stunning after elective coronary artery bypass grafting and to improve long-term ejection fraction. In a recent clinical study, Chan *et al*[120] randomized patients with STEMI to intravenous deferoxamine before coronary angioplasty and then for 12 h *vs* placebo (Table 1). The serum iron levels and lipid peroxidation biomarkers were reduced in the DFO-group without differences in the infarct size. The role of iron and ascorbate in the MRI has become of increasing interest in the last few years. It has been demonstrated that the combined use of DFO and ascorbate prevent reperfusion arrhythmias[121].

As has been previously discussed, cumulated evidence from both experimental and clinical studies leads us to support the view that a novel combined antioxidant strategy could limit MRI and its consequences. This novel hypothesis is based on the combined use of antioxidants prior to the reperfusion therapy in order to limit the oxidative challenge during reperfusion. The key points of this novel intervention are: (1) To achieve high plasma concentrations of ascorbate through massive intravenous doses to counteract the ROS and RNS production; (2) the use of NAC to prevent GSH depletion; and (3) the use of DFO to diminish the catalytic free iron levels in order to prevent the ROS production by the Fenton reaction.

Accordingly, in our laboratory recent studies of the murine Langendorff model have been conducted to determine the effect of antioxidants in MRI. We are now studying the effect of ascorbate, NAC, and DFO used alone and in association. Under these conditions, we expect a lower vulnerability of the myocardial tissue to the reperfusion injury associated with oxidative stress. This protective effect could be expressed by a lower infarct size, reduced post-reperfusion arrhythmias and myocardial stunning occurrence, and improved microvascular function. Finally, at present, there is no evidence available from any trial that has applied this antioxidant protocol to diminish MRI. Table 1 shows a summary of the main clinical studies that have used antioxidants to prevent MRI in patients with AMI.

CONCLUSION

There is major evidence with respect to the contribution of oxidative stress to MRI in cardiovascular diseases. Despite the many significant advances in the understanding of the mechanisms of MRI, it remains an unsolved problem. There is a lack of consistency between basic studies and clinical trials aimed to reduce MRI through antioxidant therapies. Although promising results have been obtained in experimental studies (mainly in animal models), these benefits have not been translated into clinical settings. It is noteworthy that the administration of high ascorbate doses prior to reperfusion and also NAC administration appear to be safe and rational therapies against the development of oxidative damage associated with myocardial reperfusion. Furthermore, ascorbate association with NAC and DFO could improve the beneficial effect of ascorbate, making it even more effective in preventing myocardial reperfusion damage associated with PCA following AMI.

REFERENCES

1 **Roe MT**, Halabi AR, Mehta RH, Chen AY, Newby LK, Harrington RA, Smith SC Jr, Ohman EM, Gibler WB, Peterson ED.

Documented traditional cardiovascular risk factors and mortality in non-ST-segment elevation myocardial infarction. *Am Heart J* 2007; **153**: 507-514 [PMID: 17383286 DOI: 10.1016/j.ahj.2006.12.018]
2 **Vanden Hoek TL**, Li C, Shao Z, Schumacker PT, Becker LB. Significant levels of oxidants are generated by isolated cardiomyocytes during ischemia prior to reperfusion. *J Mol Cell Cardiol* 1997; **29**: 2571-2583 [PMID: 9299379 DOI: 10.1006/jmcc.1997.0497]
3 **Yellon DM**, Hausenloy DJ. Myocardial reperfusion injury. *N Engl J Med* 2007; **357**: 1121-1135 [PMID: 17855673 DOI: 10.1056/NEJMra071667]
4 **Rodrigo R**. Oxidative stress and antioxidants: their role in human disease. Nova Biomedical Books, 2009 [cited 2018 Mar 26]: 358
5 **Rodrigo R**, Libuy M, Feliú F, Hasson D. Molecular basis of cardioprotective effect of antioxidant vitamins in myocardial infarction. *Biomed Res Int* 2013; **2013**: 437613 [PMID: 23936799 DOI: 10.1155/2013/437613]
6 **Ferrari R**. The role of mitochondria in ischemic heart disease. *J Cardiovasc Pharmacol* 1996; **28** Suppl 1: S1-10 [PMID: 8891865 DOI: 10.1097/00005344-199600003-00002]
7 **Jahangiri A**, Leifert WR, Kind KL, McMurchie EJ. Dietary fish oil alters cardiomyocyte Ca2+ dynamics and antioxidant status. *Free Radic Biol Med* 2006; **40**: 1592-1602 [PMID: 16632119 DOI: 10.1016/j.freeradbiomed.2005.12.026]
8 **Rodrigo R**, Prieto JC, Castillo R. Cardioprotection against ischaemia/reperfusion by vitamins C and E plus n-3 fatty acids: molecular mechanisms and potential clinical applications. *Clin Sci* (Lond) 2013; **124**: 1-15 [PMID: 22963444 DOI: 10.1042/CS20110663]
9 **Chamiec T**, Herbaczyńska-Cedro K, Ceremuzyński L. Effects of antioxidant vitamins C and E on signal-averaged electrocardiogram in acute myocardial infarction. *Am J Cardiol* 1996; **77**: 237-241 [PMID: 8607400 DOI: 10.1016/S0002-9149(97)89385-X]
10 **Juránek I**, Bezek S. Controversy of free radical hypothesis: reactive oxygen species--cause or consequence of tissue injury? *Gen Physiol Biophys* 2005; **24**: 263-278 [PMID: 16308423]
11 **Eaton P**, Clements-Jewery H. Peroxynitrite: *in vivo* cardioprotectant or arrhythmogen? *Br J Pharmacol* 2008; **155**: 972-973 [PMID: 18806818 DOI: 10.1038/bjp.2008.372]
12 **Zimmerman JJ**. Defining the role of oxyradicals in the pathogenesis of sepsis. *Crit Care Med* 1995; **23**: 616-617 [PMID: 7712748 DOI: 10.1097/00003246-199504000-00003]
13 **Brandes RP**, Kreuzer J. Vascular NADPH oxidases: molecular mechanisms of activation. *Cardiovasc Res* 2005; **65**: 16-27 [PMID: 15621030 DOI: 10.1016/j.cardiores.2004.08.007]
14 **Loukogeorgakis SP**, van den Berg MJ, Sofat R, Nitsch D, Charakida M, Haiyee B, de Groot E, MacAllister RJ, Kuijpers TW, Deanfield JE. Role of NADPH oxidase in endothelial ischemia/reperfusion injury in humans. *Circulation* 2010; **121**: 2310-2316 [PMID: 20479156 DOI: 10.1161/CIRCULATIONAHA.108.814731]
15 **Braunersreuther V**, Montecucco F, Asrih M, Pelli G, Galan K, Frias M, Burger F, Quinderé AL, Montessuit C, Krause KH, Mach F, Jaquet V. Role of NADPH oxidase isoforms NOX1, NOX2 and NOX4 in myocardial ischemia/reperfusion injury. *J Mol Cell Cardiol* 2013; **64**: 99-107 [PMID: 24051369 DOI: 10.1016/j.yjmcc.2013.09.007]
16 **Vásquez-Vivar J**, Kalyanaraman B, Martásek P, Hogg N, Masters BS, Karoui H, Tordo P, Pritchard KA Jr. Superoxide generation by endothelial nitric oxide synthase: the influence of cofactors. *Proc Natl Acad Sci USA* 1998; **95**: 9220-9225 [PMID: 9689061 DOI: 10.1073/pnas.95.16.9220]
17 **Xia Y**, Zweier JL. Direct measurement of nitric oxide generation from nitric oxide synthase. *Proc Natl Acad Sci USA* 1997; **94**: 12705-12710 [PMID: 9356514 DOI: 10.1073/pnas.94.23.12705]
18 **Chalupsky K**, Cai H. Endothelial dihydrofolate reductase: critical for nitric oxide bioavailability and role in angiotensin II uncoupling of endothelial nitric oxide synthase. *Proc Natl Acad Sci USA* 2005; **102**: 9056-9061 [PMID: 15941833 DOI: 10.1073/pnas.0409594102]
19 **Schulz E**, Jansen T, Wenzel P, Daiber A, Münzel T. Nitric oxide, tetrahydrobiopterin, oxidative stress, and endothelial dysfunction in hypertension. *Antioxid Redox Signal* 2008; **10**: 1115-1126 [PMID: 18321209 DOI: 10.1089/ars.2007.1989]
20 **Landmesser U**, Dikalov S, Price SR, McCann L, Fukai T, Holland SM, Mitch WE, Harrison DG. Oxidation of tetrahydrobiopterin leads to uncoupling of endothelial cell nitric oxide synthase in hypertension. *J Clin Invest* 2003; **111**: 1201-1209 [PMID: 12697739 DOI: 10.1172/JCI14172]
21 **Friedl HP**, Smith DJ, Till GO, Thomson PD, Louis DS, Ward PA. Ischemia-reperfusion in humans. Appearance of xanthine oxidase activity. *Am J Pathol* 1990; **136**: 491-495 [PMID: 2316621]
22 **Granger DN**. Role of xanthine oxidase and granulocytes in ischemia-reperfusion injury. *Am J Physiol* 1988; **255**: H1269-H1275 [PMID: 3059826 DOI: 10.1152/ajpheart.1988.255.6.H1269]
23 **Wang X**, Han M, Bao J, Tu W, Dai Z. A superoxide anion biosensor based on direct electron transfer of superoxide dismutase on sodium alginate sol-gel film and its application to monitoring of living cells. *Anal Chim Acta* 2012; **717**: 61-66 [PMID: 22304816 DOI: 10.1016/j.aca.2011.12.045]
24 **Nathan AT**, Singer M. The oxygen trail: tissue oxygenation. *Br Med Bull* 1999; **55**: 96-108 [PMID: 10695081 DOI: 10.1258/0007142991902312]
25 **Macdonald J**, Galley HF, Webster NR. Oxidative stress and gene expression in sepsis. *Br J Anaesth* 2003; **90**: 221-232 [PMID: 12538380 DOI: 10.1093/bja/aeg034]
26 **Darra E**, Rungatscher A, Carcereri de Prati A, Podesser BK, Faggian G, Scarabelli T, Mazzucco A, Hallström S, Suzuki H. Dual modulation of nitric oxide production in the heart during ischaemia/reperfusion injury and inflammation. *Thromb Haemost* 2010; **104**: 200-206 [PMID: 20508903 DOI: 10.1160/TH09-08-0554]
27 **Rodrigo R**, Vinay J, Castillo R, Cereceda M, Asenjo R, Zamorano J, Araya J, Castillo-Koch R, Espinoza J, Larraín E. Use of vitamins C and E as a prophylactic therapy to prevent postoperative atrial fibrillation. *Int J Cardiol* 2010; **138**: 221-228 [PMID: 19446899 DOI: 10.1016/j.ijcard.2009.04.043]
28 **Ferdinandy P**, Danial H, Ambrus I, Rothery RA, Schulz R. Peroxynitrite is a major contributor to cytokine-induced myocardial contractile failure. *Circ Res* 2000; **87**: 241-247 [PMID: 10926876 DOI: 10.1161/01.RES.87.3.241]
29 **Kanno S**, Lee PC, Zhang Y, Ho C, Griffith BP, Shears LL 2nd, Billiar TR. Attenuation of myocardial ischemia/reperfusion injury by superinduction of inducible nitric oxide synthase. *Circulation* 2000; **101**: 2742-2748 [PMID: 10851213 DOI: 10.1161/01.CIR.101.23.2742]
30 **Suzuki H**, Colasanti M. Cross-talk between constitutive and inducible nitric oxide synthases. *Circulation* 2001; **103**: E81-E81 [PMID: 11294818 DOI: 10.1161/01.CIR.103.14.e81]
31 **Kitamoto S**, Egashira K, Kataoka C, Koyanagi M, Katoh M, Shimokawa H, Morishita R, Kaneda Y, Sueishi K, Takeshita A. Increased activity of nuclear factor-kappaB participates in cardiovascular remodeling induced by chronic inhibition of nitric oxide synthesis in rats. *Circulation* 2000; **102**: 806-812 [PMID: 10942751 DOI: 10.1161/01.CIR.102.7.806]
32 **Chevion M**, Jiang Y, Har-El R, Berenshtein E, Uretzky G, Kitrossky N. Copper and iron are mobilized following myocardial ischemia: possible predictive criteria for tissue injury. *Proc Natl Acad Sci USA* 1993; **90**: 1102-1106 [PMID: 8430081 DOI: 10.1073/pnas.90.3.1102]
33 **Korkmaz S**, Barnucz E, Loganathan S, Li S, Radovits T, Hegedus P, Zubarevich A, Hirschberg K, Weymann A, Puskás LG, Ózsvári B, Faragó N, Kanizsai I, Fábián G, Gyuris M, Merkely B, Karck M, Szabó C, Szabó G. Q50, an iron-chelating and zinc-complexing agent, improves cardiac function in rat models of ischemia/reperfusion-induced myocardial injury. *Circ J* 2013; **77**: 1817-1826 [PMID: 23575364 DOI: 10.1253/circj.CJ-12-1162]
34 **Esposito BP**, Breuer W, Sirankapracha P, Pootrakul P, Hershko C, Cabantchik ZI. Labile plasma iron in iron overload: redox activity and susceptibility to chelation. *Blood* 2003; **102**: 2670-2677 [PMID: 12805056 DOI: 10.1182/blood-2003-03-0807]
35 **Merkofer M**, Kissner R, Hider RC, Brunk UT, Koppenol WH. Fenton chemistry and iron chelation under physiologically relevant conditions: Electrochemistry and kinetics. *Chem Res Toxicol* 2006;

19: 1263-1269 [PMID: 17040095 DOI: 10.1021/tx060101w]
36 **Voogd A**, Sluiter W, Koster JF. The increased susceptibility to hydrogen peroxide of the (post-)ischemic rat heart is associated with the magnitude of the low molecular weight iron pool. *Free Radic Biol Med* 1994; **16**: 453-458 [PMID: 8005530 DOI: 10.1016/0891-5849(94)90122-8]
37 **Pucheu S**, Coudray C, Tresallet N, Favier A, de Leiris J. Effect of iron overload in the isolated ischemic and reperfused rat heart. *Cardiovasc Drugs Ther* 1993; **7**: 701-711 [PMID: 8241014 DOI: 10.1007/BF00877824]
38 **Tang WH**, Wu S, Wong TM, Chung SK, Chung SS. Polyol pathway mediates iron-induced oxidative injury in ischemic-reperfused rat heart. *Free Radic Biol Med* 2008; **45**: 602-610 [PMID: 18549825 DOI: 10.1016/j.freeradbiomed.2008.05.003]
39 **Zurlo MG**, De Stefano P, Borgna-Pignatti C, Di Palma A, Piga A, Melevendi C, Di Gregorio F, Burattini MG, Terzoli S. Survival and causes of death in thalassaemia major. *Lancet* 1989; **2**: 27-30 [PMID: 2567801 DOI: 10.1016/S0140-6736(89)90264-X]
40 **Xia S**, Zhang W, Huang L, Jiang H. Comparative efficacy and safety of deferoxamine, deferiprone and deferasirox on severe thalassemia: a meta-analysis of 16 randomized controlled trials. *PLoS One* 2013; **8**: e82662 [PMID: 24376563 DOI: 10.1371/journal.pone.0082662]
41 **Hoffbrand AV**, Taher A, Cappellini MD. How I treat transfusional iron overload. *Blood* 2012; **120**: 3657-3669 [PMID: 22919029 DOI: 10.1182/blood-2012-05-370098]
42 **Hool LC**. The L-type Ca(2+) channel as a potential mediator of pathology during alterations in cellular redox state. *Heart Lung Circ* 2009; **18**: 3-10 [PMID: 19119068 DOI: 10.1016/j.hlc.2008.11.004]
43 **Dixon IM**, Hata T, Dhalla NS. Sarcolemmal Na(+)-K(+)-ATPase activity in congestive heart failure due to myocardial infarction. *Am J Physiol* 1992; **262**: C664-C671 [PMID: 1312780 DOI: 10.1152/ajpcell.1992.262.3.C664]
44 **Sasaki M**, Joh T. Oxidative stress and ischemia-reperfusion injury in gastrointestinal tract and antioxidant, protective agents. *J Clin Biochem Nutr* 2007; **40**: 1-12 [PMID: 18437208 DOI: 10.3164/jcbn.40.1]
45 **Donoso P**, Sanchez G, Bull R, Hidalgo C. Modulation of cardiac ryanodine receptor activity by ROS and RNS. *Front Biosci* (Landmark Ed) 2011; **16**: 553-567 [PMID: 21196188 DOI: 10.2741/3705]
46 **Prosser BL**, Ward CW, Lederer WJ. X-ROS signaling: rapid mechano-chemo transduction in heart. *Science* 2011; **333**: 1440-1445 [PMID: 21903813 DOI: 10.1126/science]
47 **Kim YH**, Lim DS, Lee JH, Shim WJ, Ro YM, Park GH, Becker KG, Cho-Chung YS, Kim MK. Gene expression profiling of oxidative stress on atrial fibrillation in humans. *Exp Mol Med* 2003; **35**: 336-349 [PMID: 14646586 DOI: 10.1038/emm.2003.45]
48 **Bowie A**, O'Neill LA. Oxidative stress and nuclear factor-kappaB activation: a reassessment of the evidence in the light of recent discoveries. *Biochem Pharmacol* 2000; **59**: 13-23 [PMID: 10605930 DOI: 10.1016/S0006-2952(99)00296-8]
49 **Chung MK**, Martin DO, Sprecher D, Wazni O, Kanderian A, Carnes CA, Bauer JA, Tchou PJ, Niebauer MJ, Natale A, Van Wagoner DR. C-reactive protein elevation in patients with atrial arrhythmias: inflammatory mechanisms and persistence of atrial fibrillation. *Circulation* 2001; **104**: 2886-2891 [PMID: 11739301 DOI: 10.1161/hc4901.101760]
50 **Lamm G**, Auer J, Weber T, Berent R, Ng C, Eber B. Postoperative white blood cell count predicts atrial fibrillation after cardiac surgery. *J Cardiothorac Vasc Anesth* 2006; **20**: 51-56 [PMID: 16458214 DOI: 10.1053/j.jvca.2005.03.026]
51 **Pavlović D**, Đorđević V, Kocić G. A "cross-talk" between oxidative stress and REDOX cell signaling. *Med Biol* 2002; **9**: 131-137
52 **Chandra J**, Samali A, Orrenius S. Triggering and modulation of apoptosis by oxidative stress. *Free Radic Biol Med* 2000; **29**: 323-333 [PMID: 11035261 DOI: 10.1016/S0891-5849(00)00302-6]
53 **Liakopoulos OJ**, Schmitto JD, Kazmaier S, Bräuer A, Quintel M, Schoendube FA, Dörge H. Cardiopulmonary and systemic effects of methylprednisolone in patients undergoing cardiac surgery. *Ann Thorac Surg* 2007; **84**: 110-8; discussion 118-9 [PMID: 17588396 DOI: 10.1016/j.athoracsur.2007.01.003]
54 **Opie LH**, Commerford PJ, Gersh BJ, Pfeffer MA. Controversies in ventricular remodelling. *Lancet* 2006; **367**: 356-367 [PMID: 16443044 DOI: 10.1016/S0140-6736(06)68074-4]
55 **Rodrigo R**, Libuy M, Feliú F, Hasson D. Oxidative stress-related biomarkers in essential hypertension and ischemia-reperfusion myocardial damage. *Dis Markers* 2013; **35**: 773-790 [PMID: 24347798 DOI: 10.1155/2013/974358]
56 **Kobayashi M**, Yamamoto M. Molecular mechanisms activating the Nrf2-Keap1 pathway of antioxidant gene regulation. *Antioxid Redox Signal* 2005; **7**: 385-394 [PMID: 15706085 DOI: 10.1089/ars.2005.7.385]
57 **Zhu H**, Jia Z, Misra BR, Zhang L, Cao Z, Yamamoto M, Trush MA, Misra HP, Li Y. Nuclear factor E2-related factor 2-dependent myocardiac cytoprotection against oxidative and electrophilic stress. *Cardiovasc Toxicol* 2008; **8**: 71-85 [PMID: 18463988 DOI: 10.1007/s12012-008-9016-0]
58 **Piper HM**, García-Dorado D, Ovize M. A fresh look at reperfusion injury. *Cardiovasc Res* 1998; **38**: 291-300 [PMID: 9709390 DOI: 10.1016/S0008-6363(98)00033-9]
59 **Tatli E**, Alicik G, Buturak A, Yilmaztepe M, Aktoz M. Arrhythmias following revascularization procedures in the course of acute myocardial infarction: are they indicators of reperfusion or ongoing ischemia? *ScientificWorldJournal* 2013; **2013**: 160380 [PMID: 23431252 DOI: 10.1155/2013/160380]
60 **Rodrigo R**, Korantzopoulos P, Cereceda M, Asenjo R, Zamorano J, Villalabeitia E, Baeza C, Aguayo R, Castillo R, Carrasco R, Gormaz JG. A randomized controlled trial to prevent post-operative atrial fibrillation by antioxidant reinforcement. *J Am Coll Cardiol* 2013; **62**: 1457-1465 [PMID: 23916928 DOI: 10.1016/j.jacc.2013.07.014]
61 **Tennant R**, Wiggers CJ. The effects of coronary occlusion on myocardial contraction. Am J Physiol Content. *American Physiological Society* 1935; **112**: 351-361 [DOI: 10.1152/ajplegacy.1935.112.2.351]
62 **Bolli R**. Mechanism of myocardial "stunning". *Circulation* 1990; **82**: 723-738 [PMID: 2203553 DOI: 10.1161/01.CIR.82.3.723]
63 **Laky D**, Parascan L, Cândea V. Myocardial stunning. Morphological studies in acute experimental ischemia and intraoperatory myocardial biopsies. *Rom J Morphol Embryol* 2008; **49**: 153-158 [PMID: 18516320]
64 **Kals J**, Starkopf J, Zilmer M, Pruler T, Pulges K, Hallaste M, Kals M, Pulges A, Soomets U. Antioxidant UPF1 attenuates myocardial stunning in isolated rat hearts. *Int J Cardiol* 2008; **125**: 133-135 [PMID: 17395289 DOI: 10.1016/j.ijcard.2007.01.032]
65 **Crystal GJ**, Malik G, Yoon SH, Kim SJ. Isoflurane late preconditioning against myocardial stunning is associated with enhanced antioxidant defenses. *Acta Anaesthesiol Scand* 2012; **56**: 39-47 [PMID: 22103751 DOI: 10.1111/j.1399-6576.2011.02583.x]
66 **Kloner RA**, Ganote CE, Jennings RB. The "no-reflow" phenomenon after temporary coronary occlusion in the dog. *J Clin Invest* 1974; **54**: 1496-1508 [PMID: 4140198 DOI: 10.1172/JCI107898]
67 **Movahed MR**, Butman SM. The pathogenesis and treatment of no-reflow occurring during percutaneous coronary intervention. *Cardiovasc Revasc Med* 2008; **9**: 56-61 [PMID: 18206640 DOI: 10.1016/j.carrev.2007.08.005]
68 **Bouleti C**, Mewton N, Germain S. The no-reflow phenomenon: State of the art. *Arch Cardiovasc Dis* 2015; **108**: 661-674 [PMID: 26616729 DOI: 10.1016/j.acvd.2015.09.006]
69 **Oyanagui Y**, Sato S. Superoxide dismutases and anti-oxidants protected mice from no-reflow and necrotic damage induced by ischemia. *Free Radic Res Commun* 1993; **18**: 147-157 [PMID: 8319925 DOI: 10.3109/10715769309147488]
70 **Shimizu M**, Sjöquist PO, Wang QD, Rydén L. Effects of the angiotensin AT1 receptor blocker candesartan on myocardial ischemic/reperfusion injury. *J Am Soc Nephrol* 1999; **10 Suppl 11**: S137-S142 [PMID: 9892154]
71 **Molyneux CA**, Glyn MC, Ward BJ. Oxidative stress and cardiac microvascular structure in ischemia and reperfusion: the protective effect of antioxidant vitamins. *Microvasc Res* 2002; **64**: 265-277 [PMID: 12204651 DOI: 10.1006/mvre.2002.2419]
72 **Matsumoto H**, Inoue N, Takaoka H, Hata K, Shinke T, Yoshikawa R, Masai H, Watanabe S, Ozawa T, Yokoyama M. Depletion of

antioxidants is associated with no-reflow phenomenon in acute myocardial infarction. *Clin Cardiol* 2004; **27**: 466-470 [PMID: 15346844 DOI: 10.1002/clc.4960270809]

73 **Zeng M**, Yan H, Chen Y, Zhao HJ, Lv Y, Liu C, Zhou P, Zhao B. Suppression of NF-κB reduces myocardial no-reflow. *PLoS One* 2012; **7**: e47306 [PMID: 23056624 DOI: 10.1371/journal.pone.0047306]

74 **Basili S**, Tanzilli G, Mangieri E, Raparelli V, Di Santo S, Pignatelli P, Violi F. Intravenous ascorbic acid infusion improves myocardial perfusion grade during elective percutaneous coronary intervention: relationship with oxidative stress markers. *JACC Cardiovasc Interv* 2010; **3**: 221-229 [PMID: 20170881 DOI: 10.1016/j.jcin.2009.10.025]

75 **Ramos C**, Brito R, González-Montero J, Valls N, Gormaz JG, Prieto JC, Aguayo R, Puentes Á, Noriega V, Pereira G, Palavecino T, Rodrigo R. Effects of a novel ascorbate-based protocol on infarct size and ventricle function in acute myocardial infarction patients undergoing percutaneous coronary angioplasty. *Arch Med Sci* 2017; **13**: 558-567 [PMID: 28507569 DOI: 10.5114/aoms.2016.59713]

76 **Valls N**, Gormaz JG, Aguayo R, González J, Brito R, Hasson D, Libuy M, Ramos C, Carrasco R, Prieto JC, Dussaillant G, Puentes Á, Noriega V, Rodrigo R. Amelioration of persistent left ventricular function impairment through increased plasma ascorbate levels following myocardial infarction. *Redox Rep* 2016; **21**: 75-83 [PMID: 26066587 DOI: 10.1179/1351000215Y.0000000018]

77 **Tsujita K**, Shimomura H, Kaikita K, Kawano H, Hokamaki J, Nagayoshi Y, Yamashita T, Fukuda M, Nakamura Y, Sakamoto T, Yoshimura M, Ogawa H. Long-term efficacy of edaravone in patients with acute myocardial infarction. *Circ J* 2006; **70**: 832-837 [PMID: 16799234 DOI: 10.1253/circj.70.832]

78 **Defraigne JO**, Pincemail J, Detry O, Franssen C, Meurisse M, Limet R. Preservation of cortical microcirculation after kidney ischemia-reperfusion: value of an iron chelator. *Ann Vasc Surg* 1994; **8**: 457-467 [PMID: 7811583 DOI: 10.1007/BF02133066]

79 **Brunet J**, Boily MJ, Cordeau S, Des Rosiers C. Effects of N-acetylcysteine in the rat heart reperfused after low-flow ischemia: evidence for a direct scavenging of hydroxyl radicals and a nitric oxide-dependent increase in coronary flow. *Free Radic Biol Med* 1995; **19**: 627-638 [PMID: 8529922 DOI: 10.1016/0891-5849(95)00077-B]

80 **Ciccone MM**, Cortese F, Gesualdo M, Carbonara S, Zito A, Ricci G, De Pascalis F, Scicchitano P, Riccioni G. Dietary intake of carotenoids and their antioxidant and anti-inflammatory effects in cardiovascular care. *Mediators Inflamm* 2013; **2013**: 782137 [PMID: 24489447 DOI: 10.1155/2013/782137]

81 **Tong C**, Peng C, Wang L, Zhang L, Yang X, Xu P, Li J, Delplancke T, Zhang H, Qi H. Intravenous Administration of Lycopene, a Tomato Extract, Protects against Myocardial Ischemia-Reperfusion Injury. *Nutrients* 2016; **8**: 138 [PMID: 26950150 DOI: 10.3390/nu8030138]

82 **Wang Y**, Chung SJ, McCullough ML, Song WO, Fernandez ML, Koo SI, Chun OK. Dietary carotenoids are associated with cardiovascular disease risk biomarkers mediated by serum carotenoid concentrations. *J Nutr* 2014; **144**: 1067-1074 [PMID: 24744306 DOI: 10.3945/jn.113.184317]

83 **Wang Y**, Sun J, Liu C, Fang C. Protective effects of crocetin pretreatment on myocardial injury in an ischemia/reperfusion rat model. *Eur J Pharmacol* 2014; **741**: 290-296 [PMID: 25176181 DOI: 10.1016/j.ejphar.2014.07.052]

84 **Zhu Z**, Zhu J, Zhao X, Yang K, Lu L, Zhang F, Shen W, Zhang R. All-Trans Retinoic Acid Ameliorates Myocardial Ischemia/Reperfusion Injury by Reducing Cardiomyocyte Apoptosis. *PLoS One* 2015; **10**: e0133414 [PMID: 26186635 DOI: 10.1371/journal.pone.0133414]

85 **Levine M**, Rumsey SC, Daruwala R, Park JB, Wang Y. Criteria and recommendations for vitamin C intake. *JAMA* 1999; **281**: 1415-1423 [PMID: 10217058 DOI: 10.1001/jama.281.15.1415]

86 **Wang X**, Quinn PJ. The location and function of vitamin E in membranes (review). *Mol Membr Biol* 2000; **17**: 143-156 [PMID: 11128973 DOI: 10.1080/09687680010000311]

87 **Heller R**, Werner-Felmayer G, Werner ER. Alpha-Tocopherol and endothelial nitric oxide synthesis. *Ann N Y Acad Sci* 2004; **1031**: 74-85 [PMID: 15753135 DOI: 10.1196/annals.1331.007]

88 **Heller R**, Werner-Felmayer G, Werner ER. Antioxidants and endothelial nitric oxide synthesis. Eur J Clin Pharmacol. *Springer-Verlag* 2006; **62** (S1): 21-28 [DOI: 10.1007/s00228-005-0009-7]

89 **Gille L**, Staniek K, Nohl H. Effects of tocopheryl quinone on the heart: model experiments with xanthine oxidase, heart mitochondria, and isolated perfused rat hearts. *Free Radic Biol Med* 2001; **30**: 865-876 [PMID: 11295529 DOI: 10.1016/S0891-5849(01)00475-0]

90 **Ramlawi B**, Otu H, Mieno S, Boodhwani M, Sodha NR, Clements RT, Bianchi C, Sellke FW. Oxidative stress and atrial fibrillation after cardiac surgery: a case-control study. *Ann Thorac Surg* 2007; **84**: 1166-1172; discussion 1172-1173 [PMID: 17888965 DOI: 10.1016/j.athoracsur.2007.04.12]

91 **Newaz MA**, Yousefipour Z, Nawal NN. Modulation of nitric oxide synthase activity in brain, liver, and blood vessels of spontaneously hypertensive rats by ascorbic acid: protection from free radical injury. *Clin Exp Hypertens* 2005; **27**: 497-508 [PMID: 16081342 DOI: 10.1081/CEH-200067681]

92 **Guney M**, Oral B, Demirin H, Karahan N, Mungan T, Delibas N. Protective effects of vitamins C and E against endometrial damage and oxidative stress in fluoride intoxication. *Clin Exp Pharmacol Physiol* 2007; **34**: 467-474 [PMID: 17439417 DOI: 10.1111/j.1440-1681.2007.04596.x]

93 **Gille L**, Gregor W, Staniek K, Nohl H. Redox-interaction of alpha-tocopheryl quinone with isolated mitochondrial cytochrome bc1 complex. *Biochem Pharmacol* 2004; **68**: 373-381 [PMID: 15194009 DOI: 10.1016/j.bcp.2004.03.031]

94 **Ulker S**, McKeown PP, Bayraktutan U. Vitamins reverse endothelial dysfunction through regulation of eNOS and NAD(P)H oxidase activities. *Hypertension* 2003; **41**: 534-539 [PMID: 12623955 DOI: 10.1161/01.HYP.0000057421.28533.37]

95 **May JM**, Qu ZC, Mendiratta S. Protection and recycling of alpha-tocopherol in human erythrocytes by intracellular ascorbic acid. *Arch Biochem Biophys* 1998; **349**: 281-289 [PMID: 9448716 DOI: 10.1006/abbi.1997.0473]

96 **Taddei S**, Virdis A, Ghiadoni L, Salvetti A. Endothelial dysfunction in hypertension: fact or fancy? *J Cardiovasc Pharmacol* 1998; **32** Suppl 3: S41-S47 [PMID: 9883747]

97 **Newaz MA**, Nawal NN, Rohaizan CH, Muslim N, Gapor A. alpha-Tocopherol increased nitric oxide synthase activity in blood vessels of spontaneously hypertensive rats. *Am J Hypertens* 1999; **12**: 839-844 [PMID: 10480480 DOI: 10.1016/S0895-7061(99)00022-9]

98 **Wu F**, Schuster DP, Tyml K, Wilson JX. Ascorbate inhibits NADPH oxidase subunit p47phox expression in microvascular endothelial cells. *Free Radic Biol Med* 2007; **42**: 124-131 [PMID: 17157199 DOI: 10.1016/j.freeradbiomed.2006.10.033]

99 **Gao F**, Yao CL, Gao E, Mo QZ, Yan WL, McLaughlin R, Lopez BL, Christopher TA, Ma XL. Enhancement of glutathione cardioprotection by ascorbic acid in myocardial reperfusion injury. *J Pharmacol Exp Ther* 2002; **301**: 543-550 [PMID: 11961055 DOI: 10.1124/jpet.301.2.543]

100 **Packer JE**, Slater TF, Willson RL. Direct observation of a free radical interaction between vitamin E and vitamin C. *Nature* 1979; **278**: 737-738 [PMID: 431730 DOI: 10.1038/278737a0]

101 **Niki E**, Noguchi N, Tsuchihashi H, Gotoh N. Interaction among vitamin C, vitamin E, and beta-carotene. *Am J Clin Nutr* 1995; **62**: 1322S-1326S [PMID: 7495227 DOI: 10.1093/ajcn/62.6.1322S]

102 **Levine M**, Padayatty SJ, Espey MG. Vitamin C: a concentration-function approach yields pharmacology and therapeutic discoveries. *Adv Nutr* 2011; **2**: 78-88 [PMID: 22332036 DOI: 10.3945/an.110.000109]

103 **Schneider MP**, Delles C, Schmidt BM, Oehmer S, Schwarz TK, Schmieder RE, John S. Superoxide scavenging effects of N-acetylcysteine and vitamin C in subjects with essential hypertension. *Am J Hypertens* 2005; **18**: 1111-1117 [PMID: 16109326 DOI: 10.1016/j.amjhyper.2005.02.006]

104 **Rushworth GF**, Megson IL. Existing and potential therapeutic uses for N-acetylcysteine: the need for conversion to intracellular glutathione for antioxidant benefits. *Pharmacol Ther* 2014; **141**: 150-159 [PMID: 24080471 DOI: 10.1016/j.pharmthera.2013.09.006]

105 **Winterbourn CC**, Metodiewa D. Reactivity of biologically

important thiol compounds with superoxide and hydrogen peroxide. *Free Radic Biol Med* 1999; **27**: 322-328 [PMID: 10468205 DOI: 10.1016/S0891-5849(99)00051-9]

106 **Lodge JK**, Traber MG, Packer L. Thiol chelation of Cu2+ by dihydrolipoic acid prevents human low density lipoprotein peroxidation. *Free Radic Biol Med* 1998; **25**: 287-297 [PMID: 9680174 DOI: 10.1016/S0891-5849(98)00048-3]

107 **Joshi D**, Mittal DK, Shrivastava S, Shukla S. Protective role of thiol chelators against dimethylmercury induced toxicity in male rats. *Bull Environ Contam Toxicol* 2010; **84**: 613-617 [PMID: 20401649 DOI: 10.1007/s00128-010-9982-3]

108 **Lu Y**, Qin W, Shen T, Dou L, Man Y, Wang S, Xiao C, Li J. The antioxidant N-acetylcysteine promotes atherosclerotic plaque stabilization through suppression of RAGE, MMPs and NF-κB in ApoE-deficient mice. *J Atheroscler Thromb* 2011; **18**: 998-1008 [PMID: 21873804 DOI: 10.5551/jat.8870]

109 **Arstall MA**, Yang J, Stafford I, Betts WH, Horowitz JD. N-acetylcysteine in combination with nitroglycerin and streptokinase for the treatment of evolving acute myocardial infarction. Safety and biochemical effects. *Circulation* 1995; **92**: 2855-2862 [PMID: 7586252 DOI: 10.1161/01.CIR.92.10.2855]

110 **Thiele H**, Hildebrand L, Schirdewahn C, Eitel I, Adams V, Fuernau G, Erbs S, Linke A, Diederich KW, Nowak M, Desch S, Gutberlet M, Schuler G. Impact of high-dose N-acetylcysteine versus placebo on contrast-induced nephropathy and myocardial reperfusion injury in unselected patients with ST-segment elevation myocardial infarction undergoing primary percutaneous coronary intervention. The LIPSIA-N-ACC (Prospective, Single-Blind, Placebo-Controlled, Randomized Leipzig Immediate PercutaneouS Coronary Intervention Acute Myocardial Infarction N-ACC) Trial. *J Am Coll Cardiol* 2010; **55**: 2201-2209 [PMID: 20466200 DOI: 10.1016/j.jacc.2009.08.091]

111 **Yesilbursa D**, Serdar A, Senturk T, Serdar Z, Sağ S, Cordan J. Effect of N-acetylcysteine on oxidative stress and ventricular function in patients with myocardial infarction. *Heart Vessels* 2006; **21**: 33-37 [PMID: 16440146 DOI: 10.1007/s00380-005-0854-4]

112 **Abe M**, Takiguchi Y, Ichimaru S, Tsuchiya K, Wada K. Comparison of the protective effect of N-acetylcysteine by different treatments on rat myocardial ischemia-reperfusion injury. *J Pharmacol Sci* 2008; **106**: 571-577 [PMID: 18385540 DOI: 10.1254/jphs.FP0071664]

113 **Pasupathy S**, Tavella R, Grover S, Raman B, Procter NEK, Du YT, Mahadavan G, Stafford I, Heresztyn T, Holmes A, Zeitz C, Arstall M, Selvanayagam J, Horowitz JD, Beltrame JF. Early Use of N-acetylcysteine With Nitrate Therapy in Patients Undergoing Primary Percutaneous Coronary Intervention for ST-Segment-Elevation Myocardial Infarction Reduces Myocardial Infarct Size (the NACIAM Trial [N-acetylcysteine in Acute Myocardial Infarction]). *Circulation* 2017; **136**: 894-903 [PMID: 28634219 DOI: 10.1161/CIRCULATIONAHA.117.027575]

114 **Kolnagou A**, Kleanthous M, Kontoghiorghes GJ. Reduction of body iron stores to normal range levels in thalassaemia by using a deferiprone/deferoxamine combination and their maintenance thereafter by deferiprone monotherapy. *Eur J Haematol* 2010; **85**: 430-438 [PMID: 20662901 DOI: 10.1111/j.1600-0609.2010.01499.x]

115 **Freeman AP**, Giles RW, Berdoukas VA, Walsh WF, Choy D, Murray PC. Early left ventricular dysfunction and chelation therapy in thalassemia major. *Ann Intern Med* 1983; **99**: 450-454 [PMID: 6625375 DOI: 10.7326/0003-4819-99-4-450]

116 **Reddy BR**, Kloner RA, Przyklenk K. Early treatment with deferoxamine limits myocardial ischemic/reperfusion injury. *Free Radic Biol Med* 1989; **7**: 45-52 [PMID: 2753395 DOI: 10.1016/0891-5849(89)90099-3]

117 **Lesnefsky EJ**, Repine JE, Horwitz LD. Deferoxamine pretreatment reduces canine infarct size and oxidative injury. *J Pharmacol Exp Ther* 1990; **253**: 1103-1109 [PMID: 2359019]

118 **Williams RE**, Zweier JL, Flaherty JT. Treatment with deferoxamine during ischemia improves functional and metabolic recovery and reduces reperfusion-induced oxygen radical generation in rabbit hearts. *Circulation* 1991; **83**: 1006-1014 [PMID: 1847847 DOI: 10.1161/01.CIR.83.3.1006]

119 **Paraskevaidis IA**, Iliodromitis EK, Vlahakos D, Tsiapras DP, Nikolaidis A, Marathias A, Michalis A, Kremastinos DT. Deferoxamine infusion during coronary artery bypass grafting ameliorates lipid peroxidation and protects the myocardium against reperfusion injury: immediate and long-term significance. *Eur Heart J* 2005; **26**: 263-270 [PMID: 15618054 DOI: 10.1093/eurheartj/ehi028]

120 **Chan W**, Taylor AJ, Ellims AH, Lefkovits L, Wong C, Kingwell BA, Natoli A, Croft KD, Mori T, Kaye DM, Dart AM, Duffy SJ. Effect of iron chelation on myocardial infarct size and oxidative stress in ST-elevation-myocardial infarction. *Circ Cardiovasc Interv* 2012; **5**: 270-278 [PMID: 22496085 DOI: 10.1161/CIRCINTERVENTIONS.111.966226]

121 **Karahaliou A**, Katsouras C, Koulouras V, Nikas D, Niokou D, Papadopoulos G, Nakos G, Sideris D, Michalis L. Ventricular arrhythmias and antioxidative medication: experimental study. *Hellenic J Cardiol* 2008; **49**: 320-328 [PMID: 18846922]

P- Reviewer: Ciccon MM, Sun CK, Schoenhagen P **S- Editor**: Ji FF
L- Editor: A **E- Editor**: Wu YXJ

World Journal of Cardiology

Submit a Manuscript: http://www.f6publishing.com

World J Cardiol 2018 September 26; 10(9): 87-96

DOI: 10.4330/wjc.v10.i9.87

ISSN 1949-8462 (online)

MINIREVIEWS

Established and novel pathophysiological mechanisms of pericardial injury and constrictive pericarditis

Vinasha Ramasamy, Bongani M Mayosi, Edward D Sturrock, Mpiko Ntsekhe

Vinasha Ramasamy, Bongani M Mayosi, Edward D Sturrock, Mpiko Ntsekhe, Institute of Infectious Disease and Molecular Medicine, University of Cape Town, Observatory 7925, South Africa

Vinasha Ramasamy, Edward D Sturrock, Department of Integrative Biomedical Sciences, University of Cape Town, Observatory 7925, South Africa

Bongani M Mayosi, Mpiko Ntsekhe, Division of Cardiology, University of Cape Town, Observatory 7925, South Africa

ORCID number: Vinasha Ramasamy (0000-0002-3336-5773); Bongani M Mayosi (0000-0001-6641-8950); Edward D Sturrock (0000-0003-2032-7636); Mpiko Ntsekhe (0000-0002-0851-7675).

Author contributions: All authors contributed to the manuscript.

Supported by The University of Cape Town's Research Committee (URC) and the South African National Research Foundation (NRF).

Conflict-of-interest statement: No potential conflicts of interest relevant to this article were reported.

Manuscript source: Unsolicited manuscript

Correspondence to: Mpiko Ntsekhe, FACC, MD, MPhil, PhD, Professor, Division of Cardiology, University of Cape Town, Anzio Road, Observatory 7925,
South Africa. mpiko.ntsekhe@uct.ac.za
Telephone: +27-21-4046183

Received: February 8, 2018
Peer-review started: February 8, 2018
First decision: April 4, 2018
Revised: April 6, 2018
Accepted: April 18, 2018
Article in press: April 22, 2018
Published online: September 26, 2018

Abstract

This review article aims to: (1) discern from the literature the immune and inflammatory processes occurring in the pericardium following injury; and (2) to delve into the molecular mechanisms which may play a role in the progression to constrictive pericarditis. Pericarditis arises as a result of a wide spectrum of pathologies of both infectious and non-infectious aetiology, which lead to various degrees of fibrogenesis. Current understanding of the sequence of molecular events leading to pathological manifestations of constrictive pericarditis is poor. The identification of key mechanisms and pathways common to most fibrotic events in the pericardium can aid in the design and development of novel interventions for the prevention and management of constriction. We have identified through this review various cellular events and signalling cascades which are likely to contribute to the pathological fibrotic phenotype. An initial classical pattern of inflammation arises as a result of insult to the pericardium and can exacerbate into an exaggerated or prolonged inflammatory state. Whilst the implication of major drivers of inflammation and fibrosis such as tumour necrosis factor and transforming growth factor β were foreseeable, the identification of pericardial deregulation of other mediators (basic fibroblast growth factor, galectin-3 and the tetrapeptide Ac-SDKP) provides important avenues for further research.

Key words: Inflammatory pericarditis; Autoimmune disease; Tuberculous pericarditis; Fibrosis mechanism; Constrictive pericarditis

Core tip: Constrictive pericarditis arises as a complication of pericarditis from a wide range of aetiologies. A comprehensive understanding of the fibrotic process eventually leading to pathological symptoms is currently lacking.Through this review of the literature, we have identified various molecular mediators which are likely to play a role in the establishment of constriction and which warrant further studies.

Ramasamy V, Mayosi BM, Sturrock ED, Ntsekhe M. Established and novel pathophysiological mechanisms of pericardial injury and constrictive pericarditis. *World J Cardiol* 2018; 10(9): 87-96 Available from: URL: http://www.wjgnet.com/1949-8462/full/v10/i9/87.htm DOI: http://dx.doi.org/10.4330/wjc.v10.i9.87

INTRODUCTION

Pericarditis describes the clinical syndrome that occurs in response to injury of the pericardium. Following an episode of pericarditis, the natural history of the disease is variable and unpredictable. In a significant proportion of patients there is progression from acutely inflamed pericardium to chronic thickening, fibrosis, and fusion of the two pericardial layers with often dire consequences for patients. The molecular mechanisms involved in the inflammatory and immune mediated injury during pericarditis and the mechanisms involved in progression to constrictive pericarditis are poorly understood[1]. Such an understanding may be important to the design and development of interventions which are able to interrupt and prevent maladaptive and deleterious pericardial responses.

We conducted a comprehensive review of the available literature to summarize what is currently known about (1) immune and inflammation-mediated pericardial injury in a range of different causes of pericarditis; and (2) the molecular mechanisms involved in both pericarditis and subsequent post inflammatory progression to fibrosis and constrictive pericarditis.

SEARCH STRATEGY

The literature search was conducted in Pubmed, Embase, ScienceDirect and Google Scholar to identify journal articles for the review that had been published up to July 2017. In order to identify papers describing inflammatory and fibrotic processes occurring in the different types of pericarditis, the following search terms were used: "Pericarditis"and ("inflammation" or "fibrosis" or "constrictive" or "constriction"). The search was repeated for the common types of pericarditis described using the following search terms in the search criteria described above: "(uraemic or uremic)", "tuberculous", "malignant", "radiation", "autoimmune", "viral", "infectious", "post surgery" and "myocardial infarction"[2]. Literature regarding different animal models of pericarditis was obtained using the search terms: "animal model" and "pericarditis". Papers were then filtered according to their titles and content for the identification of relevant literature.

NORMAL PERICARDIUM

The pericardium is double layered flask-like sac which encloses the heart through its attachments to the great vessels, namely the vena cava, aorta, and pulmonary artery and vein. It is lined on the outside by the parietal pericardium, which is a fibrous layer of connective tissue rich in elastic fibres and collagenous fibres. This fibrosa is supplied by a network of blood and lymphatic vessels that contains macrophages and fibroblasts. The inner visceral pericardium is a single serous layer composed of flat, irregular, ciliated mesothelial cells resting on a thin basement membrane and separated from the fibrous layer by a thin sub-mesothelial space[3,4]. These two layers of the pericardium are 1-2 mm thick and give rise to a cavity which contains on average 15 to 35 mL of pericardial fluid, under normal physiological conditions[5]. Pericardial fluid is formed from ultrafiltration of plasma and comprises largely globular proteins, phospholipids and surfactant-like prostaglandins[6].

PATHOPHYSIOLOGICAL RESPONSE OF THE PERICARDIUM TO INJURY

Pericarditis

The pathophysiological response of the pericardium to injury is characterized by intense inflammation with or without effusion, and the clinical syndrome of pericarditis. Pericarditis is a common disorder[7] that can result from both an infectious and non-infectious aetiology and presents clinically as pericarditis with and without effusion. Causes of pericarditis include viral, bacterial, fungal, uraemic, post-acute myocardial infarction, neoplastic, post-cardiac surgery, following mediastinal irradiation and as a consequence of systemic autoimmune diseases[2]. The major complications of pericarditis are cardiac tamponade with and without hemodynamic instability in the short term, constrictive pericarditis in the long term and death[5]. The latter is usually the consequence of chronic inflammation, thickening, adhesion, fibrosis and obliteration of the pericardial space.

CLINICAL MODELS OF POST INFLAMMATORY PERICARDITIS

Uraemic pericarditis

Uraemic pericarditis is a complication of acute and chronic renal failure, which can arise prior to, and on dialysis treatment. The condition was prevalent before the widespread use of dialysis and was commonly associated with a poor prognosis and high mortality.

Currently, with modern dialysis, it has a highly improved prognosis and survival rate[8]. The mechanism of the development of pericarditis in uraemic disease is poorly understood. Although pericarditis is more frequent in cases of severe uraemia, there is no correlation between blood urea and creatinine levels and the appearance of pericarditis[9]. Uraemic pericarditis is usually exudative with protein and large numbers of mononuclear cells in the pericardial fluid[10]. Serous or haemorrhagic effusions are common and typically evolve into a fibrinous state. This fibrotic state often manifests as a rough granular surface with irregular, scattered adhesions between parietal and visceral pericardium in a "bread and butter" pattern[8,11]. However, densely adherent pericarditis and gross pericardial thickening with organizing fibrinous pericarditis have been found at autopsy in cases of uraemic disease[12].

Radiation pericarditis

Radiation pericarditis occurs as a complication of radiation therapy of malignant mediastinal tissues and organs, most commonly breast cancer or mediastinal Hodgkin's disease. Radiation pericarditis was a common adverse outcome when large areas of the heart were exposed to high doses of radiation therapy, but the advent of chemo- and immuno- therapy has decreased the incidence of the condition[13]. Both acute and late post radiation pericardial injuries have been described. Acutely, radiation toxicity can cause micro-vascular damage and episodic pericardial ischemia, which in turn leads to permeable neovascularization and fibrous deposition. Later, activated fibroblasts express increasing type Ⅰ collagen levels, with subsequent focal massive hyalinization, adhesions of the epicardium and thickening pericardium[14,15]. There is also evidence of impaired drainage of extracellular fluid from the pericardium, a chronic fibrinous exudative pericarditis and vascular and lymphatic fibrosis[16].

The degree of inflammation and thickening in radiation pericarditis corresponds to the X-ray exposure, with marked thickening observed more at the site of irradiation. This suggests a cellular injury and necrosis induced inflammatory response as a result of the acute radiation of actively proliferating cells, potentially mesothelial cells of the pericardium. On a molecular level, increased collagen synthesis and the pathological remodelling of the pericardium post radiation have been associated with the activation of various growth factors and cytokines including transforming growth factor β (TGF-β) and connective tissue growth factor (CTGF)[17].

Autoimmune disease pericarditis

Pericardial involvement can arise in various autoimmune diseases, most commonly systemic lupus erythematosus (SLE), rheumatoid arthritis (RA) and systemic sclerosis (SSc)[2].

SLE is a chronic inflammatory disease with a broad range of clinical manifestations and a variable disease course. The exact aetiology of SLE is still unclear, but it is likely to be mediated by antibodies and immune complexes (IC) which typically contribute to the clinical manifestation of SLE. Immune complexes can result in complement activation and inflammation and they have been detected in the pericardial fluid in SLE[18]. While pericarditis is the most common cardiac manifestation of SLE, constrictive pericarditis is a rare occurrence[19].

RA is a chronic inflammatory disorder that primarily affects joints. Symptomatic pericarditis arises in less than 10% of patients with severe disease and is often associated with a poor prognosis[20]. The pericardial involvement is usually a diffuse pericardial effusion, sometimes associated with leukocyte infiltration and often positive for rheumatoid factor and immune complexes. Constrictive pericarditis is not common in RA and can arise despite second-line therapy. Thickened pericardia with collagenous fibrous tissue and organising fibrin, fibrinous exudate and leukocyte infiltration have been described[21]. Asymptomatic pericardial effusions occur in upto 30%-50% of patients with RA and represents the most common cardiac manifestation of the disease.

Systemic sclerosis is a systemic autoimmune disease characterized by aberrant fibroblast activity resulting in dense fibrosis of visceral organs and skin. Pericardial manifestations include pericardial effusions, fibrous pericarditis, pericardial adhesions or constrictive pericarditis. Clinical manifestations of pericardial pathology are apparent in over 5%-16% of cases. The pathogenesis of pericardial effusions in SSc is believed to differ from the inflammatory pathway triggered by auto-antibodies and immune complexes of SLE and RA as evidenced by the "non-inflammatory" profile of the pericardial fluid. Instead, the release of basic fibroblast growth factor (bFGF) and histamine by mast cells may contribute to the pathophysiological manifestations[22,23].

The inflammatory basis of autoimmune pericarditis, centered around the role of the inflammasome, has recently been reviewed by Xu *et al*[24].

Post myocardial infarction pericarditis

Pericarditis is a common sequelae of transmural myocardial infarction (MI) and arises "early" as pericarditis epistenocardica or as a "delayed" presentation in the form of Dressler syndrome[25].

The acute form of pericarditis is often diagnosed 1-4 d post MI[26] and is sometimes accompanied by a pericardial effusion. Vascular injury and myocardial necrosis have been associated with increased incidence of pericarditis, suggesting an inflammatory response to injury[27,28]. Fibrous deposits and adhesions often develop in the visceral and parietal pericardium covering the area of infarction but may also involve wider and more diffuse pericardial surfaces[29].

Dressler syndrome (DS) commonly arises around

two weeks post MI. It is an uncommon presentation since the advent of early reperfusion therapy with thrombolytic therapy and primary percutaneous intervention, and with the widespread use of heparin. DS is presumably a recurrent immune-inflammatory syndrome arising from the release of auto-myocardial antigens from necrosis of myocardial tissues. The formation of immune complexes are believed to trigger a hypersensitivity reaction from molecular mimicry and cross-reactions[25,30]. Indeed, the presence of increased anti-myocardial antibodies following myocardial injury has been previously suggested and supports a possible autoimmune pathogenesis[31].

Post cardiac surgery pericarditis

Pericarditis can present as a midterm or late complication of cardiac surgery. Post surgery pericarditis often bears restrictive haemodynamic characteristics despite an open pericardium and can occur as early as 2 wk following surgery[32]. Adhesions and fibrous patches in the pericardium lead to constrictive pericarditis and cause symptoms of dyspnoea, and signs of congestive cardiac failure. Whilst the exact mechanism for the development of pericardial fibrosis following surgery is obscure, the presence of blood in the pericardial cavity may play a role, with failure to drain bloody effusions being a risk factor for the development of fibrosis. Blood in the pericardium may result in irritation of the serosal layer and inflammation[33]. However, pericardial fibrosis in the absence of bloody effusions after surgery has also been documented[34].

Post infectious pericarditis

A range of infectious organisms can affect the pericardium, but the most common causes are viruses (coxsakie viruses, influenza virus and enteric cytopathogenic human orphan virus, among others) and bacteria (*Staphylococcus* and *Streptococcus, Haemophilus,* and *M. tuberculosis*).

Bacterial (purulent) pericarditis which is a life threatening condition is characterised by gross pus in the pericardium or microscopically purulent effusion[35]. It is an uncommon occurrence in the developed world, due to widespread antibiotic usage. However, tuberculous pericarditis is a leading cause of pericarditis in Sub Saharan Africa and is discussed separately below[36].

Viral pericarditis, on the other hand, is a common manifestation and is often self-limiting, in that only a small number of patients develop fibrous complications. Viral antigens lead to an inflammatory response of lymphocytic predominance which often results in effusions. Cytotoxic and T and/or B cell-driven immune-mediated mechanisms of inflammation have been described in different types of viral infections[1]. Increased levels of IL-6 and IL-8 have also been described in both serum and pericardial fluid in viral pericarditis, with a marked local increase in the pericardial cavity[37,38]. An increase in pericardial TNF-α levels has also been measured in the pericardial fluid by Ristić *et al*[37], whilst TGF-β levels were only elevated in serum. However, conflicting Interferon-γ (IFN-γ) deregulation has been reported by the two studies, with a strongly elevated levels described by Pankuweit *et al*[38], whilst no differences were reported by Ristić *et al*[37]. This is probably due to the small sample size used in the latter study. Further, Karatolios *et al*[39] measured increased pericardial and serum levels of vascular endothelial growth factor (VEGF) in viral pericarditis as well as decreased bFGF levels in the pericardial fluid. Elevated serum cardiac troponin Ⅰ (cTn Ⅰ) levels have been observed in viral pericarditis and have been associated with ST-segment elevation, and pericardial effusion. Whilst, this increase is often more pronounced with increased myocardial inflammation, it did not affect the prognosis and the development of tamponade and fibrosis[40].

Tuberculous pericarditis

Tuberculous (TB) pericarditis accounts for roughly 4% of cases of acute pericarditis in the developed world. However, in developing countries with a high prevalence of tuberculosis, around 70% of cases of large pericardial effusion are attributable to TB[41,42]. Further, HIV co-infection has not only increased the number of TB pericarditis cases, but has also changed its clinical manifestations and therapeutic considerations[43].

The spread of Mycobacterium tuberculosis (MTb) to the pericardium occurs either through retrograde lymphatic spread or through haematogenous spread from primary sites of infection[36,44]. The inflammatory process in TB pericarditis follows a sequence of pathological events. An early fibrinous exudate is formed with leucocytosis, and early granuloma formation as a response to the high mycobacterial abundance, followed by a sero-sanguineous effusion with a predominantly lymphocytic exudate. The effusion gradually recedes whilst the granulomatous architecture is organised to restrict mycobacterial spread. Fibrin, collagen and extracellular matrix (ECM) deposition lead to pericardial thickening and fibrosis[36].

Infection of the pericardium with the bacilli elicits an immune response, stimulating lymphocytes to release cytokines which activate macrophages and influence granuloma formation. This initial reaction presents pathologically with polymorphonuclear leucocytosis and granuloma formation[45]. Marked elevations of IL-10 and IFN-γ accompanied by low levels of bioactive TGF-β levels in tuberculous pericardial fluid suggest a Th-1 mediated delayed type hypersensitivity response to the pathogen[46]. Similarly, Reuter *et al*[47] measured significantly increased IFN-γ levels in the pericardial fluid and observed large numbers of mesothelial cells in tuberculous pericardial aspirates.

A role for complement fixing antimyolemmal antibodies has also been suggested in the development of exudative tuberculous pericarditis through cardiocyte cytolysis[48]. More recently, it was shown that the tetrapeptide N-acetyl-seryl-aspartyl-lysyl-proline (Ac-

SDKP) and galectin-3 could be detected in tuberculous pericardial fluid. The reduction in Ac-SDKP levels in TB pericardial effusion has been suggested to contribute to the development of fibrosis associated with TB pericarditis[49].

Elevated pericardial adenosine deaminase (ADA) activity and lysozyme levels have also been associated with TB pericarditis, and are of significant value in the diagnosis of TB pericarditis[47]. High ADA levels are also prognostic for the development of constrictive pericarditis[50].

Malignant pericarditis

Both primary (mesotheliomas, sarcomas, fibromas) and secondary (carcinoma, lymphoma, and carcinoid) neoplasms can be accompanied by pericardial inflammation. However, neoplastic pericarditis arises mostly from secondary disorders as a result of tumour spread and metastasis through lymphatic and haematogenous spread[51]. Effusions are common in neoplastic pericarditis and can be bloody. Malignant cells can also be present in the pericardium but almost 50% of symptomatic pericarditis cases have negative cytological results for malignant cells[52]. However, malignancies are commonly widespread when pericardial symptoms become apparent and malignant invasion of the heart and the deposition of fibrous tissue often lead to constriction[53]. Sub-acute inflammation with lymphocytic accumulation and mesothelial hyperplasia has been described in primary pericardial mesothelioma[54].

Ristić *et al*[37] measured elevated serum and pericardial levels of IL-6 and TGF-β in malignant pericarditis as compared to bypass surgery controls. TNF-α and IFN-γ levels were however not affected. A study by Pankuweit *et al*[38], found that IFN-γ levels in effusions were found to be slightly lower than in the serum. In accordance with Ristić *et al*[38] IL-6 and IL-8 levels were markedly increased in pericardial fluid as compared to the serum, suggesting a local initiation of the inflammatory response. Cardiac embryonic antigen is useful in the diagnosis of malignant pericarditis and levels above 5 ng/mL are found in the majority of cases[55].

ANIMAL MODELS OF PERICARDITIS

Several animal models of pericarditis have been described whereby the onset of inflammation was triggered by diverse mechanisms. A severe inflammatory reaction has been described in the pericardium of sheep injected with a bacterial toxin and Freund's adjuvant. A cellular mesothelial response was observed with changes to the morphology and disturbance to the architecture, followed by detachment from neighbouring cells and desquamation. An accompanying increase in vascular permeability resulted in the accumulation of large numbers of inflammatory cells and the exudation of fibrin. An increased collagen turnover was apparent after 6 d and the appearance of adhesions occurred as early as 2 wk post injection[56].

Coxsackie B viruses are known to cause perimyocarditis, an acute inflammation of the pericardium and the underlying myocardium[57]. In Coxsackie B3 induced perimyocarditis in mice, an early onset of myocardial injury and necrosis has been observed, followed by marked pericardial fibrosis[58]. In this particular study, the sub-epicardial myocardial tissues appeared to mostly contribute to the fibrotic process, with infiltration by macrophages, lymphocytes and polymorphonuclear leukocytes observed in the myocardial layer. However, in Coxsackie B4 pericarditis in mice, fibrotic lesions occurred independently of, or in conjunction with adjacent myocardial lesions. Similar patterns of inflammation were observed in the mesothelial cells with necrosis, cellular infiltration, inflammatory cell infiltration and fibrinous exudate. The inflammatory processes are likely to be as a result of infection of mesothelial cells by the virus, since viral antigens have been detected in the mesothelial cells[59]. Interleukin-33 (IL-33) induced eosinophilic pericarditis has also been implicated in Coxsackie B infection[60].

IFN-γ and TGF-β knockout (KO) mice bear gross histological and haemodynamic characteristics of pericarditis. Pericarditis in the IFN-γ mice presented as a thick and stiff pericardium which formed adhesions to surrounding structures. Mesothelial hyperplasia in the pericardium was accompanied by a morphological change to a cuboidal shape. In addition to the predominant mononuclear cell infiltration, the pericardial inflammatory infiltrate of the IFN-γ KO mice had marked eosinophilia. Similarly, cardiac myocytes bordering areas of inflammation in the TGF-β KO mice presented with eosinophilic inclusions and contained large nucleoli[61,62].

THE FIBROTIC PROCESS AND CONSTRICTIVE PERICARDITIS

Constrictive pericarditis

Constrictive pericarditis is a clinical syndrome, characterised by a thickened and non-compliant pericardium, which restricts cardiac filling[63]. The most apparent pathological features of constrictive pericarditis are inflammation and fibrotic thickening of the thin and elastic parietal and visceral pericardial linings. The pericardium commonly bears areas of inflammation of the serosa, scarring, and fibro-calcification[63].

Constrictive pericarditis may result from severe acute inflammation or recurrent less severe inflammatory events over a highly variable time course from the period of injury[64]. While the predictors of progression to constriction following acute pericarditis are poorly understood the incidence of constrictive pericarditis is significantly dependent on the aetiology of the pericarditis. Whilst idiopathic and viral pericarditis have a low incidence of constrictive complications (0.8/1000 person-years), tuberculous (31.7/1000 person-years) and purulent pericarditis (52.74/1000 person-years) are associated with the highest rates of progression to

Table 1 Summary of Inflammatory and fibrotic cytokines and growth factors (detected in pericardial fluid) likely to modulate the pathophysiological processes leading to chronic fibrosis in the pericardium

Inflammatory/ fibrotic mediator	Major roles in Inflammation and fibrosis	References
TGF-β	Anti-inflammatory mediator ECM deposition and remodelling	[17,37,46,61]
CTGF	Myofibroblast activation ECM deposition and remodelling	[17]
TNF-α	Inducer and regulator of inflammation Macrophage and Natual Killer cell recruitment	[37,38]
IL-6	Late role in inflammatory cascade Adaptive Immune system activation	[37,38]
IL-8	Later role in inflammatory cascade Neutrophil cell recruitment	[37,38]
IL-10	Inflammatory mediator	[46]
IFN-γ	Immune response modulation Macrophage and Natual Killer cell activation Anti-fibrotic	[37-39,46,62]
VEGF	Angiogenesis and fibrosis promotion Fibrosis resolution	[39]
bFGF	ECM deposition	[23,39]
Ac-SDKP	Major role in the inhibition of fibrosis	[49]
Galectin-3	Myofibroblast activation ECM deposition	[49]

TGF-β: Growth factor β; CTGF: Connective tissue growth factor; TNF-α: Tumor necrosis factor-α; IFN-γ: Interferon-γ; VEGF: Vascular endothelial growth factor; bFGF: Basic fibroblast growth factor; ECM: Extracellular matrix.

pericardial constriction[7].

Molecular mechanisms of fibrosis

Although the molecular processes leading to fibrogenesis are likely to be unique for different pathologies, some key mechanisms and pathways are common to most fibrotic events[65]. The fibrotic cascade of events is triggered upon insult to epithelial or endothelial cells which results in the activation of the coagulation cascade. The initial inflammatory response is characterised by the release of various pro-inflammatory cytokines, including tumour necrosis factor-α, TNF-α[66,67]. TNF-α is a pleiotropic cytokine with a central role in the activation and recruitment of immune cells and the regulation of pro-inflammatory cytokine production[68]. Activated leukocytes then proceed to release pro-fibrotic cytokines such as IL-13 and TGF-β which drive EMT and ECM component production. TGF-β, is a key mediator of the fibrotic response and it acts *via* canonical (Smad-dependent) and non-canonical (non-Smad-based) signalling pathways to coordinate an ECM accumulation through increased synthesis as well as a decreased degradation of ECM components[69-71].

Molecular mechanisms of pericardial fibrosis

Molecular mechanisms of pericardial constriction remain to be fully elucidated but are likely to follow a classical pattern of pericardial inflammation mediated by various cytokines (Table 1), including TNF-α, followed by abnormal healing with an exaggerated TGF-β mediated profibrotic response leading to pericardial fibrosis. Both experimental mice models of acute pericarditis and pericardial fluid from patients with tuberculous effusive constrictive pericarditis (associated with a high incidence of pericarditis), demonstrate a mixed picture of both pro-inflammatory IFN-γ, and anti inflammatory cytokines IL-8, and IL-10[72], but their exact roles are as yet unclear.

Patterns of inflammation and fibrosis in the pericardium suggest that both myocardial and pericardial cells play a role in the pathogenesis of pericarditis and constriction. A change in mesothelial cell morphology has been consistently described in various forms of pericarditis. Further, a loss of the mesothelial cell architecture, as well as mesothelial desquamation often accompanies constrictive pericarditis (Figure 1). The transition from a "flat" to a "cuboidal" shape has been associated with an "activation" of mesothelial cells and a distinct enzymatic profile of the cells with functions being geared towards oxidative stress and inflammatory responses[73,74]. Activated mesothelial cells secrete chemokines and adhesion molecules to aid in the recruitment and migration of leukocytes across the mesothelium. They are also known to mediate the inflammatory process and produce ECM components[75]. Further, mesothelial cells can undergo phenotypic changes similar to epithelial-to-mesenchymal transition to adopt fibroblast-like morphology and function in the healing serosa[4,76]. The active regulation of both pro- and anti-inflammatory mediators by mesothelial cells suggests a key role for the cells in maintaining pericardial homeostasis and also in the pathogenesis of pericardial fibrosis. Pericardial interstitial cells (PICs) have also been implicated in the production of ECM and calcification in the pericardium[77].

PICs have a comparable immune-phenotype to

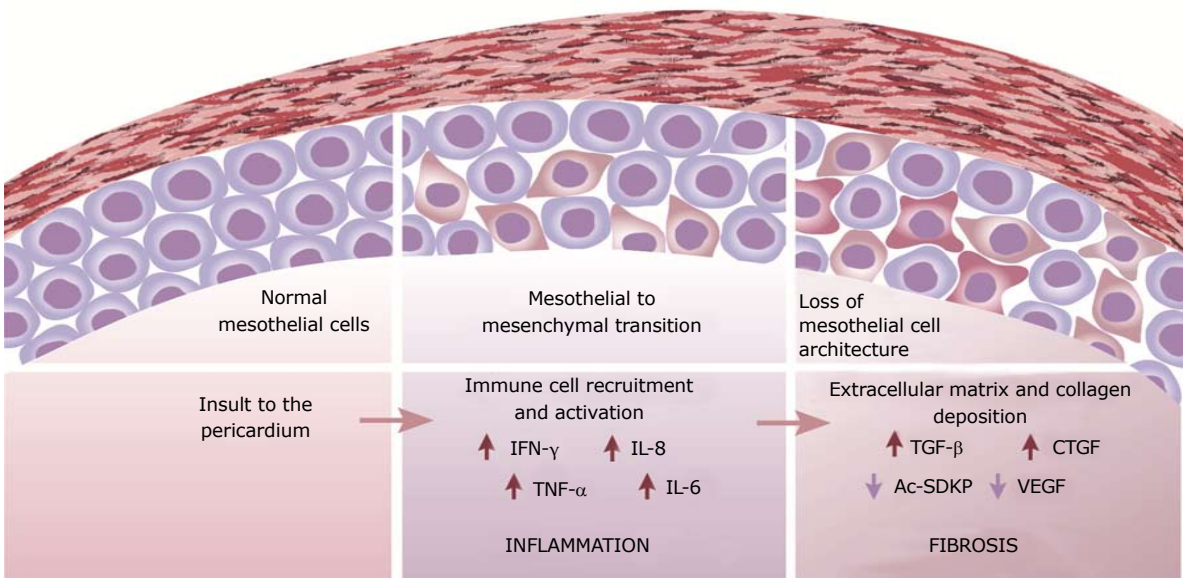

Figure 1 Molecular mediators involved in the inflammatory and fibrotic processes arising in constrictive pericarditis. Ac-SDKP: N-acetyl-seryl-aspartyl-lysyl-proline; TGF-β: Growth factor β; TNF-α: Tumor necrosis factor-α; CTGF: Connective tissue growth factor; IFN-γ: Interferon-γ; VEGF: Vascular endothelial growth factor.

mesenchymal stem cells. PICs cultured from fibro-calcific human samples could be differentiated into myofibroblasts and osteoblasts which are central to the development of fibrosis and the production of extra-osseous calcification. TGF-β and bone morphogenetic protein 2 (BMP-2) were associated with the trans-differentiation process. TGF-β increased PIC mRNA expression of collagens Ⅰ and Ⅲ whilst decreasing the matrix metalloprotease-2 and -9 mRNA levels which are important for elastin degradation, thus regulating the fibrotic process by modulating fibrosis related gene expression[77].

TGF-β is a master regulator of extracellular matrix component expression and the development of fibrosis. Increased pericardial fluid and serum levels of TGF-β have been described in various forms of pericarditis and have been associated with increased collagen synthesis. It is thus safe to say that TGF-β might play a key role in the development of fibrosis in the pericardium. Interestingly, Ristic *et al*[37] did not detect any increase in TGF-β levels in viral pericardial fluid and this could account for the low proportion of constrictive pericarditis arising in this group.

Ac-SDKP, which is known to decrease TGF-β signalling by decreasing TGF-β transcription and the phosphorylation of Smad2 and Smad3 and their translocation to the nucleus[78-81], may play a role in the pathway to pericardial fibrosis. Patients with TB pericarditis, have been found to have diminished Ac-SDKP levels compared to particpants without pericarditis undergoing cardiac sugery[49]. Lowered Ac-SDKP levels could arise from an increase in angiotensin converting enzyme (ACE) activity, which is known to degrade Ac-SDKP[82,83]. An increase in ACE serum levels has been reported in granulomatous conditions including Mtb infection, and is believed to arise from an overflow of ACE production by the macrophages and phagocytes in the granulomatous lesions into the circulation. Thus increased ACE levels, resulting in increased enzymatic cleavage of Ac-SDKP and a subsequent dampening in its anti-fibrotic potential, could potentially contribute to the pathogenesis of constriction.

Finally, an increase in CTGF was associated with ECM deposition and pericardial remodelling[17]. This is not surprising as CTGF expression is known to be induced by TGF-β in cardiac fibroblasts and cardiac myocytes, whereby it contributes to the expression of fibronectin, collagen type Ⅰ and plasminogen activator inhibitor-1[84]. Interestingly a decrease in VEGF was observed in viral pericarditis which rarely results in a constrictive pericarditis. Whilst VEGF mediated angiogenesis is known to be important for the promotion of fibrosis, it also plays a role in fibrosis resolution[85]. Indeed, an angio-fibrotic switch of VEGF and CTGF has been described in proliferative diabetic retinopathy, whereby the VEGF to CTGF ratio closely dictates the progression to fibrosi[86,87]. CTGF has also been shown to bind to VEGF and to inhibit its angiogenic functions[88]. Hence, it is possible that such CTGF-VEGF interplay is also involved in the progression to fibrosis in the pericardium. This would further explain the high VEGF levels coinciding with low levels of bFGF in viral pericardial fluid.

CONCLUSION

In this review, we have highlighted that the pericardium is subjected to noxious injury from a wide spectrum of infections and non infections causes and that the pathogenesis of pericarditis in each instance may differ in significant ways. Importantly the progression from

pericarditis, to the development of pericardial fibrosis varies significantly by etiology. A classical pattern of inflammation in the pericardium mediated by various cytokines is likely to occur as a result of most types of insult. However, the unfolding of events leading to the development of fibrosis post-inflammation is harder to accurately predict. Nevertheless, this review has allowed us to postulate various cellular events and signalling cascades which are likely to contribute, albeit to different extents in varying types of pericarditis, to the pathological fibrotic phenotype. Whilst the role of common players such as TGF-β and TNF-α in the inflammatory process can be quite easily predicted, their complex range of functions makes them unattractive targets in the management and treatment of constrictive pericarditis. However, the identification of other pro-and anti-fibrotic mediators such as Galectin-3, Ac-SDKP and bFGF, with a narrower range of functions could represent new avenues for the treatment of pericarditis. Research aimed at developing a better understanding of molecular mechanisms involved in the progression of pericarditis to fibrosis may be able to (1) identify high risk patients for progression to constrictive pericarditis through novel markers of fibrosis; and (2) identify novel targets for therapy to interrupt the progression to fibrosis and prevent the development of constrictive pericarditis.

ACKNOWLEDGEMENTS

Research in MN's, BMM's and EDS's research groups is supported by the National Research Foundation, South Africa. We would like to acknowledge S.L. Schwager for crtical reading of the manuscript.

REFERENCES

1 **Adler Y**, Charron P, Imazio M, Badano L, Baron-Esquivias G, Bogaert J, Brucato A, Gueret P, Klingel K, Lionis C, Maisch B, Mayosi B, Pavie A, Ristic AD, Sabaté Tenas M, Seferovic P, Swedberg K, Tomkowski W; Società Europea di Cardiologia. 2015 ESC Guidelines for the diagnosis and management of pericardial diseases. Task Force for the Diagnosis and Management of Pericardial Diseases of the European Society of Cardiology (ESC). *G Ital Cardiol* (Rome) 2015; **16**: 702-738 [PMID: 26667949 DOI: 10.1714/2088.22592]

2 **Maisch B**, Seferović PM, Ristić AD, Erbel R, Rienmüller R, Adler Y, Tomkowski WZ, Thiene G, Yacoub MH; Task Force on the Diagnosis and Management of Pricardial Diseases of the European Society of Cardiology. Guidelines on the diagnosis and management of pericardial diseases executive summary; The Task force on the diagnosis and management of pericardial diseases of the European society of cardiology. *Eur Heart J* 2004; **25**: 587-610 [PMID: 15120056 DOI: 10.1016/j.ehj.2004.02.002]

3 **Ishihara T**, Ferrans VJ, Jones M, Boyce SW, Kawanami O, Roberts WC. Histologic and ultrastructural features of normal human parietal pericardium. *Am J Cardiol* 1980; **46**: 744-753 [PMID: 7435384 DOI: 10.1016/0002-9149(80)90424-5]

4 **Mutsaers SE**. Mesothelial cells: their structure, function and role in serosal repair. *Respirology* 2002; **7**: 171-191 [PMID: 12153683 DOI: 10.1046/j.1440-1843.2002.00404.x]

5 **Little WC**, Freeman GL. Pericardial disease. *Circulation* 2006; **113**: 1622-1632 [PMID: 16567581 DOI: 10.1161/CIRCULATIONAHA.105.561514]

6 **Spodick DH**. Macrophysiology, microphysiology, and anatomy of the pericardium: a synopsis. *Am Heart J* 1992; **124**: 1046-1051 [PMID: 1529878 DOI: 10.1016/0002-8703(92)90990-D]

7 **Imazio M**, Gaita F, LeWinter M. Evaluation and Treatment of Pericarditis: A Systematic Review. *JAMA* 2015; **314**: 1498-1506 [PMID: 26461998 DOI: 10.1001/jama.2015.12763]

8 **de Gouveia RH**, Santos C, Santi R, Nesi G. Lessons from the past: Uremic pericarditis. *Cor Vasa* 2018; **60:** e101-e103 [DOI: 10.1016/j.crvasa.2016.09.001]

9 **Kumar S**, Lesch M. Pericarditis in renal disease. *Prog Cardiovasc Dis* 1980; **22**: 357-369 [PMID: 6987712 DOI: 10.1016/0033-0620(80)90028-6]

10 **Reyman TA**. Subacute constrictive uremic pericarditis. *Am J Med* 1969; **46**: 972-975 [PMID: 5797917 DOI: 10.1016/0002-9343(69)90098-9]

11 **Lindsay J Jr**, Crawley IS, Callaway GM Jr. Chronic constrictive pericarditis following uremic hemopericardium. *Am Heart J* 1970; **79**: 390-395 [PMID: 5413174 DOI: 10.1016/0002-8703(70)90426-6]

12 **Bailey GL**, Hampers CL, Hager EB, Merrill JP. Uremic pericarditis. Clinical features and management. *Circulation* 1968; **38**: 582-591 [PMID: 5673609 DOI: 10.1161/01.CIR.38.3.582]

13 **Schultz-Hector S**, Trott KR. Radiation-induced cardiovascular diseases: is the epidemiologic evidence compatible with the radiobiologic data? *Int J Radiat Oncol Biol Phys* 2007; **67**: 10-18 [PMID: 17189062 DOI: 10.1016/j.ijrobp.2006.08.071]

14 **Botti RE**, Driscol TE, Pearson OH, Smith JC. Radiation myocardial fibrosis simulating constrictive pericarditis. A review of the literature and a case report. *Cancer* 1968; **22**: 1254-1261 [PMID: 5705787 DOI: 10.1002/1097-0142(196811)22:6<1254::AID-CNCR2820220624>3.0.CO;2-9]

15 **Morton DL**, Glancy DL, Joseph WL, Adkins PC. Management of patients with radiation-induced pericarditis with effusion: a note on the development of aortic regurgitation in two of them. *Chest* 1973; **64**: 291-297 [PMID: 4127171 DOI: 10.1378/chest.64.3.291]

16 **Taunk NK**, Haffty BG, Kostis JB, Goyal S. Radiation-induced heart disease: pathologic abnormalities and putative mechanisms. *Front Oncol* 2015; **5**: 39 [PMID: 25741474 DOI: 10.3389/fonc.2015.00039]

17 **Yarnold J**, Brotons MC. Pathogenetic mechanisms in radiation fibrosis. *Radiother Oncol* 2010; **97**: 149-161 [PMID: 20888056 DOI: 10.1016/j.radonc.2010.09.002]

18 **Quismorio FP Jr**. Immune complexes in the pericardial fluid in systemic lupus erythematosus. *Arch Intern Med* 1980; **140**: 112-114 [PMID: 6965447 DOI: 10.1001/archinte.1980.00330130114028]

19 **Jacobson EJ**, Reza MJ. Constrictive pericarditis in systemic lupus erythematosus. Demonstration of immunoglobulins in the pericardium. *Arthritis Rheum* 1978; **21**: 972-974 [PMID: 367381 DOI: 10.1002/art.1780210815]

20 **Mankad R,** Ball CA, Myasoedova E, Matteson EL. Non-atherosclerotic cardiac manifestations of rheumatoid arthritis [Internet]. Handbook of Cardiovascular Disease Management in Rheumatoid Arthritis. Springer; 2017; 19–38. Available from: URL: http://link.springer.com.ezproxy.uct.ac.za/content/pdf/10.1007/978-3-319-26782-1_2.pdf

21 **Voskuyl AE**. The heart and cardiovascular manifestations in rheumatoid arthritis. *Rheumatology* (Oxford) 2006; **45** Suppl 4: iv4-iv7 [PMID: 16980723 DOI: 10.1093/rheumatology/kel313]

22 **Lambova S**. Cardiac manifestations in systemic sclerosis. *World J Cardiol* 2014; **6**: 993-1005 [PMID: 25276300 DOI: 10.4330/wjc.v6.i9.993]

23 **Byers RJ**, Marshall DA, Freemont AJ. Pericardial involvement in systemic sclerosis. *Ann Rheum Dis* 1997; **56**: 393-394 [PMID: 9227172 DOI: 10.1136/ard.56.6.393]

24 **Xu B**, Harb SC, Cremer PC. New Insights into Pericarditis: Mechanisms of Injury and Therapeutic Targets. *Curr Cardiol Rep* 2017; **19**: 60 [PMID: 28528454 DOI: 10.1007/s11886-017-0866-6]

25 **Feola A**, De Stefano N, Della Pietra B. Pericarditis Epistenocardica or Dressler Syndrome? An Autopsy Case. *Case Rep Med* 2015; **2015**: 215340 [PMID: 26240567 DOI: 10.1155/2015/215340]

26 **Hombach V**, Grebe O, Merkle N, Waldenmaier S, Höher M, Kochs

M, Wöhrle J, Kestler HA. Sequelae of acute myocardial infarction regarding cardiac structure and function and their prognostic significance as assessed by magnetic resonance imaging. *Eur Heart J* 2005; **26**: 549-557 [PMID: 15713695 DOI: 10.1093/eurheartj/ehi147]
27 **Dorfman TA**, Aqel R. Regional pericarditis: a review of the pericardial manifestations of acute myocardial infarction. *Clin Cardiol* 2009; **32**: 115-120 [PMID: 19301285 DOI: 10.1002/clc.20444]
28 **Sugiura T**, Iwasaka T, Takayama Y, Matsutani M, Hasegawa T, Takahashi N, Inada M. Factors associated with pericardial effusion in acute Q wave myocardial infarction. *Circulation* 1990; **81**: 477-481 [PMID: 2297857 DOI: 10.1161/01.CIR.81.2.477]
29 **Roberts WC**. Pericardial heart disease: its morphologic features and its causes. *Proc* (Bayl Univ Med Cent) 2005; **18**: 38-55 [PMID: 16200146 DOI: 10.1080/08998280.2005.11928030]
30 **Bendjelid K**, Pugin J. Is Dressler syndrome dead? *Chest* 2004; **126**: 1680-1682 [PMID: 15539743 DOI: 10.1378/chest.126.5.1680]
31 **Robinson J**, Brigden W. Immunological Studies in the Post-Cardiotomy Syndrome. *Br Med J* 1963; **2**: 706-709 [PMID: 14043728 DOI: 10.1136/bmj.2.5359.706]
32 **Cohen MV**, Greenberg MA. Constrictive pericarditis: early and late complication of cardiac surgery. *Am J Cardiol* 1979; **43**: 657-661 [PMID: 420115 DOI: 10.1016/0002-9149(79)90028-6]
33 **Matsuyama K**, Matsumoto M, Sugita T, Nishizawa J, Yoshioka T, Tokuda Y, Ueda Y. Clinical characteristics of patients with constrictive pericarditis after coronary bypass surgery. *Jpn Circ J* 2001; **65**: 480-482 [PMID: 11407725 DOI: 10.1253/jcj.65.480]
34 **Gaudino M**, Anselmi A, Pavone N, Massetti M. Constrictive pericarditis after cardiac surgery. *Ann Thorac Surg* 2013; **95**: 731-736 [PMID: 23266135 DOI: 10.1016/j.athoracsur.2012.08.059]
35 **Pankuweit S**, Ristić AD, Seferović PM, Maisch B. Bacterial pericarditis: diagnosis and management. *Am J Cardiovasc Drugs* 2005; **5**: 103-112 [PMID: 15725041 DOI: 10.2165/00129784-200505020-00004]
36 **Mayosi BM**, Burgess LJ, Doubell AF. Tuberculous pericarditis. *Circulation* 2005; **112**: 3608-3616 [PMID: 16330703 DOI: 10.1161/CIRCULATIONAHA.105.543066]
37 **Ristić AD**, Pankuweit S, Maksimović R, Moosdorf R, Maisch B. Pericardial cytokines in neoplastic, autoreactive, and viral pericarditis. *Heart Fail Rev* 2013; **18**: 345-353 [PMID: 22850905 DOI: 10.1007/s10741-012-9334-y]
38 **Pankuweit S**, Wädlich A, Meyer E, Portig I, Hufnagel G, Maisch B. Cytokine activation in pericardial fluids in different forms of pericarditis. *Herz* 2000; **25**: 748-754 [PMID: 11200123 DOI: 10.1007/PL00001993]
39 **Karatolios K**, Moosdorf R, Maisch B, Pankuweit S. Cytokines in pericardial effusion of patients with inflammatory pericardial disease. *Mediators Inflamm* 2012; **2012**: 382082 [PMID: 22577248 DOI: 10.1155/2012/382082]
40 **Imazio M**, Demichelis B, Cecchi E, Belli R, Ghisio A, Bobbio M, Trinchero R. Cardiac troponin I in acute pericarditis. *J Am Coll Cardiol* 2003; **42**: 2144-2148 [PMID: 14680742 DOI: 10.1016/j.jacc.2003.02.001]
41 **Syed FF**, Mayosi BM. A modern approach to tuberculous pericarditis. *Prog Cardiovasc Dis* 2007; **50**: 218-236 [PMID: 17976506 DOI: 10.1016/j.pcad.2007.03.002]
42 **Fowler NO**. Tuberculous pericarditis. *JAMA* 1991; **266**: 99-103 [PMID: 2046135 DOI: 10.1001/jama.1991.03470010103039]
43 **Ntsekhe M**, Mayosi BM. Tuberculous pericarditis with and without HIV. *Heart Fail Rev* 2013; **18**: 367-373 [PMID: 22427006 DOI: 10.1007/s10741-012-9310-6]
44 **Myers RB**, Spodick DH. Constrictive pericarditis: clinical and pathophysiologic characteristics. *Am Heart J* 1999; **138**: 219-232 [PMID: 10426832 DOI: 10.1016/S0002-8703(99)70105-5]
45 **Mutyaba AK**, Ntsekhe M. Tuberculosis and the Heart. *Cardiol Clin* 2017; **35**: 135-144 [PMID: 27886784 DOI: 10.1016/j.ccl.2016.08.007]
46 **Ntsekhe M**, Matthews K, Syed FF, Deffur A, Badri M, Commerford PJ, Gersh BJ, Wilkinson KA, Wilkinson RJ, Mayosi BM. Prevalence, hemodynamics, and cytokine profile of effusive-constrictive pericarditis in patients with tuberculous pericardial effusion. *PLoS One* 2013; **8**: e77532 [PMID: 24155965 DOI: 10.1371/journal.pone.0077532]
47 **Reuter H**, Burgess L, van Vuuren W, Doubell A. Diagnosing tuberculous pericarditis. *QJM* 2006; **99**: 827-839 [PMID: 17121764 DOI: 10.1093/qjmed/hcl123]
48 **Maisch B**, Maisch S, Kochsiek K. Immune reactions in tuberculous and chronic constrictive pericarditis. Clinical data and diagnostic significance of antimyocardial antibodies. *Am J Cardiol* 1982; **50**: 1007-1013 [PMID: 6753555 DOI: 10.1016/0002-9149(82)90409-X]
49 **Ntsekhe M,** Matthews K, Wolske J, Badri M, Wilkinson KA, Wilkinson RJ, Sturrock ED, Mayosi BM. Scientific letter: Ac-SDKP (N-acetyl-seryl-aspartyl-lysyl-proline) and Galectin-3 levels in tuberculous pericardial effusion: implications for pathogenesis and prevention of pericardial constriction. *Heart* 2012; **98**: 1326–1328 [DOI: 10.1136/heartjnl-2012-302196]
50 **Burgess LJ**, Reuter H, Carstens ME, Taljaard JJ, Doubell AF. The use of adenosine deaminase and interferon-gamma as diagnostic tools for tuberculous pericarditis. *Chest* 2002; **122**: 900-905 [PMID: 12226030 DOI: 10.1378/chest.122.3.900]
51 **Troughton RW**, Asher CR, Klein AL. Pericarditis. *Lancet* 2004; **363**: 717-727 [PMID: 15001332 DOI: 10.1016/S0140-6736(04)15648-1]
52 **Wilkes JD**, Fidias P, Vaickus L, Perez RP. Malignancy-related pericardial effusion. 127 cases from the Roswell Park Cancer Institute. *Cancer* 1995; **76**: 1377-1387 [PMID: 8620412 DOI: 10.1002/1097-0142(19951015)76:8<1377::AID-CNCR2820760813>3.0.CO;2-M]
53 **Thurber DL**, Edwards JE, Achor RW. Secondary malignant tumors of the pericardium. *Circulation* 1962; **26**: 228-241 [PMID: 14037856 DOI: 10.1161/01.CIR.26.2.228]
54 **Smets P**, Guettrot-Imbert G, Hermet M, Delevaux I, Kemeny JL, Aumaître O, André M. Recurrent pericarditis related to primary pericardial malignant mesothelioma. *Rev Med Interne* 2013; **34**: 573-576 [PMID: 23773902 DOI: 10.1016/j.revmed.2013.04.021]
55 **Tatsuta M**, Yamamura H, Yamamoto R, Ichii M, Iishi H, Noguchi S. Carcinoembryonic antigens in the pericardial fluid of patients with malignant pericarditis. *Oncology* 1984; **41**: 328-330 [PMID: 6472769 DOI: 10.1159/000225848]
56 **Leak LV**, Ferrans VJ, Cohen SR, Eidbo EE, Jones M. Animal model of acute pericarditis and its progression to pericardial fibrosis and adhesions: ultrastructural studies. *Am J Anat* 1987; **180**: 373-390 [PMID: 3425565 DOI: 10.1002/aja.1001800408]
57 **Smith WG**. Coxsackie B myopericarditis in adults. *Am Heart J* 1970; **80**: 34-46 [PMID: 5426837 DOI: 10.1016/0002-8703(70)90035-9]
58 **Matsumori A**, Kawai C. Coxsackie virus B3 perimyocarditis in BALB/c mice: experimental model of chronic perimyocarditis in the right ventricle. *J Pathol* 1980; **131**: 97-106 [PMID: 6253611 DOI: 10.1002/path.1711310202]
59 **Tsui CY**, Burch GE. Coxsackie virus B4 pericarditis in mice. *Br J Exp Pathol* 1971; **52**: 47-50 [PMID: 4926537]
60 **Abston ED**, Barin JG, Cihakova D, Bucek A, Coronado MJ, Brandt JE, Bedja D, Kim JB, Georgakopoulos D, Gabrielson KL, Mitzner W, Fairweather D. IL-33 independently induces eosinophilic pericarditis and cardiac dilation: ST2 improves cardiac function. *Circ Heart Fail* 2012; **5**: 366-375 [PMID: 22454393 DOI: 10.1161/CIRCHEARTFAILURE.111.963769]
61 **Afanasyeva M**, Georgakopoulos D, Fairweather D, Caturegli P, Kass DA, Rose NR. Novel model of constrictive pericarditis associated with autoimmune heart disease in interferon-gamma-knockout mice. *Circulation* 2004; **110**: 2910-2917 [PMID: 15505106 DOI: 10.1161/01.CIR.0000147538.92263.3A]
62 **Kulkarni AB**, Ward JM, Yaswen L, Mackall CL, Bauer SR, Huh CG, Gress RE, Karlsson S. Transforming growth factor-beta 1 null mice. An animal model for inflammatory disorders. *Am J Pathol* 1995; **146**: 264-275 [PMID: 7856732]
63 **Goldstein JA**. Cardiac tamponade, constrictive pericarditis, and restrictive cardiomyopathy. *Curr Probl Cardiol* 2004; **29**: 503-567 [PMID: 15365561 DOI: 10.1016/j.cpcardiol.2004.03.002]
64 **Syed FF**, Schaff HV, Oh JK. Constrictive pericarditis--a curable diastolic heart failure. *Nat Rev Cardiol* 2014; **11**: 530-544 [PMID: 25072910 DOI: 10.1038/nrcardio.2014.100]
65 **Leask A**, Abraham DJ. TGF-beta signaling and the fibrotic response. *FASEB J* 2004; **18**: 816-827 [PMID: 15117886 DOI:

10.1096/fj.03-1273rev]
66 **Wynn TA**. Common and unique mechanisms regulate fibrosis in various fibroproliferative diseases. *J Clin Invest* 2007; **117**: 524-529 [PMID: 17332879 DOI: 10.1172/JCI31487]
67 **Wynn TA**. Cellular and molecular mechanisms of fibrosis. *J Pathol* 2008; **214**: 199-210 [PMID: 18161745 DOI: 10.1002/path.2277]
68 **Parameswaran N**, Patial S. Tumor necrosis factor-α signaling in macrophages. *Crit Rev Eukaryot Gene Expr* 2010; **20**: 87-103 [PMID: 21133840 DOI: 10.1615/CritRevEukarGeneExpr.v20.i2.10]
69 **Branton MH**, Kopp JB. TGF-beta and fibrosis. *Microbes Infect* 1999; **1**: 1349-1365 [PMID: 10611762 DOI: 10.1016/S1286-4579(99)00250-6]
70 **Moustakas A**, Souchelnytskyi S, Heldin CH. Smad regulation in TGF-beta signal transduction. *J Cell Sci* 2001; **114**: 4359-4369 [PMID: 11792802]
71 **Zhang YE**. Non-Smad pathways in TGF-beta signaling. *Cell Res* 2009; **19**: 128-139 [PMID: 19114990 DOI: 10.1038/cr.2008.328]
72 **Fairweather D**, Frisancho-Kiss S, Yusung SA, Barrett MA, Davis SE, Gatewood SJ, Njoku DB, Rose NR. Interferon-gamma protects against chronic viral myocarditis by reducing mast cell degranulation, fibrosis, and the profibrotic cytokines transforming growth factor-beta 1, interleukin-1 beta, and interleukin-4 in the heart. *Am J Pathol* 2004; **165**: 1883-1894 [PMID: 15579433 DOI: 10.1016/S0002-9440(10)63241-5]
73 **Vogiatzidis K**, Zarogiannis SG, Aidonidis I, Solenov EI, Molyvdas PA, Gourgoulianis KI, Hatzoglou C. Physiology of pericardial fluid production and drainage. *Front Physiol* 2015; **6**: 62 [PMID: 25852564 DOI: 10.3389/fphys.2015.00062]
74 **Whitaker D**, Papadimitriou JM, Walters MN. The mesothelium: a cytochemical study of "activated" mesothelial cells. *J Pathol* 1982; **136**: 169-179 [PMID: 6279811 DOI: 10.1002/path.1711360302]
75 **Mutsaers SE**, Birnie K, Lansley S, Herrick SE, Lim CB, Prêle CM. Mesothelial cells in tissue repair and fibrosis. *Front Pharmacol* 2015; **6**: 113 [PMID: 26106328 DOI: 10.3389/fphar.2015.00113]
76 **Yáñez-Mó M**, Lara-Pezzi E, Selgas R, Ramírez-Huesca M, Domínguez-Jiménez C, Jiménez-Heffernan JA, Aguilera A, Sánchez-Tomero JA, Bajo MA, Alvarez V, Castro MA, del Peso G, Cirujeda A, Gamallo C, Sánchez-Madrid F, López-Cabrera M. Peritoneal dialysis and epithelial-to-mesenchymal transition of mesothelial cells. *N Engl J Med* 2003; **348**: 403-413 [PMID: 12556543 DOI: 10.1056/NEJMoa020809]
77 **Liu X,** Tan M, Gong D, Han L, Lu F, Huang S, Xu Z. Characteristics of pericardial interstitial cells and their implications in pericardial fibrocalcification. *J Mol Cell Cardiol* 2012; **53**: 780–789 [DOI: 10.1016/j.yjmcc.2012.09.008]
78 **Castoldi G**, di Gioia CR, Bombardi C, Perego C, Perego L, Mancini M, Leopizzi M, Corradi B, Perlini S, Zerbini G, Stella A. Prevention of myocardial fibrosis by N-acetyl-seryl-aspartyl-lysyl-proline in diabetic rats. *Clin Sci* (Lond) 2009; **118**: 211-220 [PMID: 20310083 DOI: 10.1042/CS20090234]
79 **Kanasaki K**, Koya D, Sugimoto T, Isono M, Kashiwagi A, Haneda M. N-Acetyl-seryl-aspartyl-lysyl-proline inhibits TGF-beta-mediated plasminogen activator inhibitor-1 expression via inhibition of Smad pathway in human mesangial cells. *J Am Soc Nephrol* 2003; **14**: 863-872 [PMID: 12660320 DOI: 10.1097/01.ASN.0000057544.95569.EC]
80 **Pokharel S**, van Geel PP, Sharma UC, Cleutjens JP, Bohnemeier H, Tian XL, Schunkert H, Crijns HJ, Paul M, Pinto YM. Increased myocardial collagen content in transgenic rats overexpressing cardiac angiotensin-converting enzyme is related to enhanced breakdown of N-acetyl-Ser-Asp-Lys-Pro and increased phosphorylation of Smad2/3. *Circulation* 2004; **110**: 3129-3135 [PMID: 15520311 DOI: 10.1161/01.CIR.0000147180.87553.79]
81 **Lin CX**, Rhaleb NE, Yang XP, Liao TD, D'Ambrosio MA, Carretero OA. Prevention of aortic fibrosis by N-acetyl-seryl-aspartyl-lysyl-proline in angiotensin II-induced hypertension. *Am J Physiol Heart Circ Physiol* 2008; **295**: H1253-H1261 [PMID: 18641275 DOI: 10.1152/ajpheart.00481.2008]
82 **Azizi M**, Junot C, Ezan E, Ménard J. Angiotensin I-converting enzyme and metabolism of the haematological peptide N-acetyl-seryl-aspartyl-lysyl-proline. *Clin Exp Pharmacol Physiol* 2001; **28**: 1066-1069 [PMID: 11903317 DOI: 10.1046/j.1440-1681.2001.03560.x]
83 **Inoue K**, Ikemura A, Tsuruta Y, Watanabe K, Tsutsumiuchi K, Hino T, Oka H. Quantification of N-acetyl-seryl-aspartyl-lysyl-proline in hemodialysis patients administered angiotensin-converting enzyme inhibitors by stable isotope dilution liquid chromatography-tandem mass spectrometry. *J Pharm Biomed Anal* 2011; **54**: 765-771 [PMID: 21074346 DOI: 10.1016/j.jpba.2010.10.009]
84 **Chen MM**, Lam A, Abraham JA, Schreiner GF, Joly AH. CTGF expression is induced by TGF- beta in cardiac fibroblasts and cardiac myocytes: a potential role in heart fibrosis. *J Mol Cell Cardiol* 2000; **32**: 1805-1819 [PMID: 11013125 DOI: 10.1006/jmcc.2000.1215]
85 **Yang L**, Kwon J, Popov Y, Gajdos GB, Ordog T, Brekken RA, Mukhopadhyay D, Schuppan D, Bi Y, Simonetto D, Shah VH. Vascular endothelial growth factor promotes fibrosis resolution and repair in mice. *Gastroenterology* 2014; **146**: 1339-1350.e1 [PMID: 24503129 DOI: 10.1053/j.gastro.2014.01.061]
86 **Van Geest RJ**, Lesnik-Oberstein SY, Tan HS, Mura M, Goldschmeding R, Van Noorden CJ, Klaassen I, Schlingemann RO. A shift in the balance of vascular endothelial growth factor and connective tissue growth factor by bevacizumab causes the angiofibrotic switch in proliferative diabetic retinopathy. *Br J Ophthalmol* 2012; **96**: 587-590 [PMID: 22289291 DOI: 10.1136/bjophthalmol-2011-301005]
87 **Kuiper EJ**, Van Nieuwenhoven FA, de Smet MD, van Meurs JC, Tanck MW, Oliver N, Klaassen I, Van Noorden CJ, Goldschmeding R, Schlingemann RO. The angio-fibrotic switch of VEGF and CTGF in proliferative diabetic retinopathy. *PLoS One* 2008; **3**: e2675 [PMID: 18628999 DOI: 10.1371/journal.pone.0002675]
88 **Inoki I**, Shiomi T, Hashimoto G, Enomoto H, Nakamura H, Makino K, Ikeda E, Takata S, Kobayashi K, Okada Y. Connective tissue growth factor binds vascular endothelial growth factor (VEGF) and inhibits VEGF-induced angiogenesis. *FASEB J* 2002; **16**: 219-221 [PMID: 11744618 DOI: 10.1096/fj.01-0332fje]

P- Reviewer: Movahed A, Sabate M **S- Editor**: Cui LJ
L- Editor: A **E- Editor**: Wu YXJ

World Journal of Cardiology

Submit a Manuscript: http://www.f6publishing.com

World J Cardiol 2018 September 26; 10(9): 97-109

DOI: 10.4330/wjc.v10.i9.97

ISSN 1949-8462 (online)

ORIGINAL ARTICLE

Basic Study

NBCe1 Na^+-$HCO3^-$ cotransporter ablation causes reduced apoptosis following cardiac ischemia-reperfusion injury *in vivo*

Kanimozhi Vairamani, Vikram Prasad, Yigang Wang, Wei Huang, Yinhua Chen, Mario Medvedovic, John N Lorenz, Gary E Shull

Kanimozhi Vairamani, Division of Oncology, Cancer and Blood Diseases Institute, Cincinnati Children's Hospital Medical Center, Cincinnati, OH 45229-3026, United States

Vikram Prasad, Department of Pediatrics, Cincinnati Children's Hospital Medical Center, University of Cincinnati, Cincinnati, OH 45229-3039, United States

Yigang Wang, Wei Huang, Department of Pathology, University of Cincinnati, College of Medicine, Cincinnati, OH 45267-0529, United States

Yinhua Chen, Division of Developmental Biology, Cincinnati Children's Hospital Medical Center, Cincinnati, OH 45229-3039, United States

Mario Medvedovic, Department of Environmental Health, University of Cincinnati, College of Medicine, Cincinnati, OH 45267-0056, United States

John N Lorenz, Department of Pharmacology and Systems Physiology, University of Cincinnati, College of Medicine, Cincinnati, OH 45267-0575, United States

Gary E Shull, Department of Molecular Genetics, Biochemistry and Microbiology, University of Cincinnati, College of Medicine, Cincinnati, OH 45267-0524, United States

ORCID number: Kanimozhi Vairamani (0000-0002-1596-7762); Vikram Prasad (0000-0002-8852-3986); Yigang Wang (0000-0002-0872-1860); Wei Huang (0000-0003-3046-4220); Yinhua Chen (0000-0002-7954-8452); Mario Medvedovic (0000-0003-4510-3102); John N Lorenz (0000-0003-2161-9833); Gary E Shull (0000-0002-1719-234X).

Author contributions: Shull GE, Vairamani K, Wang Y and Lorenz JN designed and coordinated the research; Shull GE and Vairamani K wrote the paper; Wang Y, Vairamani K and Huang W performed the ischemia reperfusion studies; Lorenz JN performed the cardiovascular physiology studies; Medvedovic M, Vairamani K and Shull GE performed the RNA Seq analysis; Prasad V and Chen Y established the animal model and provided important critiques of the study; all authors approved the final version of the manuscript.

Supported by NIH grants, No. HL061974 (to Gary E Shull), No. R01HL136025 (to Yigang Wang), No. P30ES006096 (to Mario Medvedovic); funds from the Center for Clinical and Translational Science and Training, University of Cincinnati (to Gary E Shull); and a Research Innovation Seed Grant from the University of Cincinnati (to Gary E Shull and John N Lorenz).

Institutional review board statement: Because human subjects or tissues were not used in this study, approval from the Institutional review board was not required. Ethical issues relating to the animal protocol were reviewed and approved by the Institutional Animal Care and Use Committee of the University of Cincinnati.

Institutional animal care and use committee statement: All procedures involving animals were reviewed and approved by the Institutional Animal Care and Use Committee (IACUC) of the University of Cincinnati (protocol number: 15-07-27-01).

Conflict-of-interest statement: The authors have no conflict of interest related to this manuscript.

ARRIVE guidelines statement: The authors have read the ARRIVE guidelines, and the manuscript was prepared according these guidelines.

Manuscript source: Invited manuscript

Correspondence to: Gary E Shull, PhD, Professor, Department

of Molecular Genetics, Biochemistry and Microbiology, University of Cincinnati, College of Medicine, 231 Albert Sabin Way, Cincinnati, OH 45267-0524,
United States. shullge@ucmail.uc.edu
Telephone: +1-513-5580056
Fax: +1-513-5581885

Received: April 6, 2018
Peer-review started: April 7, 2018
First decision: June 5, 2018
Revised: July 5, 2018
Accepted: July 15, 2018
Article in press: July 17, 2018
Published online: September 26, 2018

Abstract

AIM

To investigate the hypothesis that cardiomyocyte-specific loss of the electrogenic NBCe1 Na^+-HCO_3^- cotransporter is cardioprotective during *in vivo* ischemia-reperfusion (IR) injury.

METHODS

An NBCe1 (*Slc4a4* gene) conditional knockout mouse (KO) model was prepared by gene targeting. Cardiovascular performance of wildtype (WT) and cardiac-specific NBCe1 KO mice was analyzed by intraventricular pressure measurements, and changes in cardiac gene expression were determined by RNA Seq analysis. Response to *in vivo* IR injury was analyzed after 30 min occlusion of the left anterior descending artery followed by 3 h of reperfusion.

RESULTS

Loss of NBCe1 in cardiac myocytes did not impair cardiac contractility or relaxation under basal conditions or in response to β-adrenergic stimulation, and caused only limited changes in gene expression patterns, such as those for electrical excitability. However, following ischemia and reperfusion, KO heart sections exhibited significantly fewer apoptotic nuclei than WT sections.

CONCLUSION

These studies indicate that cardiac-specific loss of NBCe1 does not impair cardiovascular performance, causes only minimal changes in gene expression patterns, and protects against IR injury *in vivo* .

Key words: Deep sequencing; Ischemic; Apoptosis; *Slc4a4*; NBCe1

Core tip: The NBCe1 Na^+-HCO_3^- cotransporter and NHE1 Na^+/H^+ exchanger both mediate Na^+-loading and intracellular pH regulation in cardiomyocytes. Inhibition of NHE1 protects against ischemia-reperfusion (IR) injury, and evidence suggests that loss of NBCe1 activity could also be cardioprotective. We have developed a conditional NBCe1 knockout mouse model and have used it to determine the effects of NBCe1 ablation in cardiac muscle. These studies demonstrate that loss of NBCe1 does not impair cardiac performance. However, cardiomyocyte apoptosis following IR injury *in vivo* is much lower in hearts that lack NBCe1, thus indicating that loss of NBCe1 is cardioprotective.

Vairamani K, Prasad V, Wang Y, Huang W, Chen Y, Medvedovic M, Lorenz JN, Shull GE. NBCe1 Na^+-HCO_3^- cotransporter ablation causes reduced apoptosis following cardiac ischemia-reperfusion injury *in vivo*. *World J Cardiol* 2018; 10(9): 97-109 Available from: URL: http://www.wjgnet.com/1949-8462/full/v10/i9/97.htm DOI: http://dx.doi.org/10.4330/wjc.v10.i9.97

INTRODUCTION

Regulation of intracellular pH (pH_i) in cardiac myocytes is critical for cardiac function[1-4]. Cardiomyocytes express a sarcolemmal Na^+/H^+ exchanger (NHE1), two Na^+-HCO_3^- cotransporters, and a number of Na^+-independent electroneutral Cl^-/HCO_3^- exchangers[1,2,5]. The Cl^-/HCO_3^- exchangers extrude HCO_3^- in exchange for Cl^- and therefore serve as acid-loading mechanisms[1,2]. In addition, they facilitate Na^+-loading by operating in concert with the Na^+-dependent acid extruders[6] and have the potential to contribute to CO_2 disposal[7]. The sarcolemmal Na^+/H^+ exchanger and Na^+-HCO_3^- cotransporters are activated by intracellular acidification and serve to alkalinize the cell by extruding H^+ or bringing in HCO_3^-[1,2]. Because their acid-base transport activities are coupled with uptake of Na^+, these transporters stimulate Ca^{2+}-loading via effects on the Na^+/Ca^{2+} exchanger[4], which in turn can affect contractility[8].

The effects of NHE1 activity on Na^+- and Ca^{2+}-loading and on ischemia-reperfusion (IR) injury in heart, using both inhibitors[9-13] and a gene-targeted mouse model[14], are well established. The cardiac functions of the Na^+-HCO_3^- cotransporters and their relevance to disease processes are less understood. Two Na^+/HCO_3^- cotransporters, one electrogenic (NBCe1) and one electroneutral (NBCn1), are expressed in mammalian hearts. Based on RNA seq data[5,7], NBCe1 mRNA expression in mouse heart is about double that of NBCn1 and data available in the EMBL-EBI Expression Atlas (https://www.ebi.ac.uk/gxa/home) shows that this is also the case in the human heart. NBCe1 has been localized to the lateral sarcolemma, intercalated disc, and t-tubules of cardiomyocytes[1], and it has been suggested that the presence of NBCe1 in the t-tubule may contribute to electrical events involved in excitation-contraction coupling[1]. Inhibition of NBCe1 has been shown to reduce infarct size and improve ventricular function during reperfusion of the isolated rodent heart[15,16], and the expression of NBCe1 is elevated in hearts of human patients with heart failure[15]. In a rat model of pressure overload hypertrophy,

both NBCe1 and NBCn1 mRNAs were elevated[17]. These observations suggest that increased Na^+-HCO_3^- cotransport activity may be a contributing factor during pathological conditions like heart failure, myocardial infarction, and ischemic injury.

Mice with a targeted global disruption of the *Slc4a4* gene exhibit severe metabolic acidosis, absorptive and secretory defects, growth retardation, hyperaldosteronism, splenomegaly, and abnormal dentition, and they die before weaning[18]. Because of the severe phenotype it was not possible to examine the cardiac functions of NBCe1 using the global KO. The studies performed to assess cardio-protective effects of inhibiting NBCe1 in the heart have been performed using an anti-NBCe1 antibody[15,16] or the compound S0859, reported to be a common inhibitor of all NBCs[16]. To better understand the functions of NBCe1 in heart, we generated cardiomyocyte-specific conditional NBCe1 KO mice. The cardiovascular functions of WT and KO mice were analyzed *in vivo* under basal conditions and in response to β-adrenergic stimulation. To determine if the loss of NBCe1 is protective against IR injury *in vivo*, WT and NBCe1 KO mice were subjected to ligation of the left anterior descending artery followed by a period of reperfusion.

MATERIALS AND METHODS

Generation of a conditional NBCe1 knockout mouse model

Design and construction of the targeting vector, gene targeting of embryonic stem (ES) cells, and subsequent steps needed to generate mice carrying a floxed allele of NBCe1 were performed by the Animal Models Core Facility of the University of Cincinnati. The targeting construct was prepared with LoxP sites flanking coding exon 12 for transcripts ENSMUST00000148750 and ENSMUST00000156238 of the *Slc4a4* gene, both of which have an upstream non-coding exon. It should be noted that there are multiple transcripts for the *Slc4a4* gene and that the numbering of exons differs in some transcripts. However, because the targeted exon is an essential exon in all transcripts, the model can be used for conditional deletion of *Slc4a4* transcripts in any tissue. The targeted exon is 134 nucleotides in length, begins with the codons for the amino acid sequence GVLESFLGT and ends with the codons for the amino acid sequence FERLLFNFS. Because it also contains two nucleotides of the next codon, deletion of this exon causes any transcripts that might be produced to go out of frame, thus eliminating all codons following that for amino acid 499, which include sequences that encode the transmembrane domains necessary for ion transport.

To prepare the targeting construct, LoxP sites were inserted at the ends of a 1.2 kb genomic DNA fragment containing exon 12. The proximal LoxP site was 709 nucleotides upstream of exon 12, and the distal LoxP site was 393 nucleotides downstream of exon 12. A neomycin resistance gene (neo), which allowed for positive selection of ES cells, was inserted just inside the distal LoxP site and was flanked by flippase recognition target (FRT) sites, which allowed its removal at a later step. The 5′ arm of the targeting construct was a 3.4 kb fragment from sequences in intron 11 that immediately preceded the insertion site of the proximal LoxP site, and the 3′ arm was a 2.3 kb fragment from intron 12 that immediately followed the insertion site of the distal LoxP site. Each of the genomic fragments used to prepare the construct were amplified by polymerase chain reaction (PCR) from mouse genomic DNA. A thymidine kinase gene was included after the 3′ arm in order to allow negative selection of ES cells. The targeting construct was electroporated into ES cells derived from 129/SvJ mice and targeted ES cells were identified by long-range PCR and used to generate chimeric mice. When germline transmission of the targeted allele was achieved, the mice were bred with C57Bl6 mice expressing FLP recombinase to remove the Neo gene. For cardiac myocyte-specific deletion of *Slc4a4* exon 12, the mice were bred with a C57Bl6 mouse carrying the Cre recombinase gene driven by the β-myosin promoter, which is an effective strategy for Cre-mediated recombination beginning during embryonic development in cardiac myocytes[19].

All procedures using animals conformed to guidelines published by the National Institutes of Health (Guide for the Care and Use of Laboratory Animals) and were approved by the Institutional Animal Care and Use Committee at the University of Cincinnati. Mice were used in this study, as it is the best mammalian model for preparing genetic modifications and appropriate techniques are available for analysis of cardiovascular performance and response to *in vivo* IR injury. All appropriate measures were taken to minimize pain or discomfort. Mice were maintained in a specific pathogen free, temperature controlled barrier facility, with a 12 h light-dark cycle, and access to food and water ad libitum.

Genotype analysis

PCR genotyping of mice carrying the floxed allele was performed using DNA from tail biopsies and the following primers: Forward primer: 5′-TGGTGGC TTAAATTGCAAATGGC-3′; Reverse primer: 5′-CATAAC CCACTAAGTCCAGTACG-3′. These primers flank the proximal LoxP site and yield a 176-base pair PCR product for the wild-type *Slc4a4* allele, and a 223-base pair PCR product for the floxed allele, with the increase in size being due to the LoxP site. An additional PCR reaction was performed to determine the presence or absence of the *Cre* transgene.

Quantitative PCR analysis of the degree of knockdown of functional NBCe1 mRNA

To determine the degree of knockdown of NBCe1 mRNA

in KO (*Slc4a4*$^{flx/flx(Cre)}$) relative to WT (*Slc4a4*$^{flx/flx}$) hearts, quantitative reverse transcriptase-PCR analysis (qRT-PCR) was performed using an ABI 7300 Real Time PCR system as described previously[7]. cDNA was prepared from mRNA isolated from whole heart of 4 mo old male mice (n = 6 for each genotype) and was PCR amplified using a forward primer (5'-TTCAGGCTCTCTCTGCGATT-3') from coding exon 11 and reverse primer from coding exon 12 (5'-CTCAAGATGGTAAGCGGTTGA-3').

Analysis of left ventricular function and blood pressure

Cardiovascular performance was determined using intraventricular and intra-arterial pressure measurements as described previously[20,21]. The mice (2-3 mo old; n = 4 male and 4 female *Slc4a4*$^{flx/flx}$ and 8 *Slc4a4*$^{flx/flx(Cre)}$) were anesthetized with a mixture of ketamine and inactin, surgically instrumented, and their body temperatures maintained using a thermally controlled surgical stage. A high fidelity pressure transducer (Millar Instruments, Houston, TX) was introduced into the left ventricle through the right carotid artery to measure left ventricular pressure, and blood pressure was recorded *via* a fluid filled catheter in the right femoral artery. A catheter in the right femoral vein was used for infusion of dobutamine, a β-adrenergic agonist.

RNA Seq analysis

Total RNA was isolated from whole hearts of 4 mo old male *Slc4a4*$^{flx/flx}$ and *Slc4a4*$^{flx/flx(Cre)}$ mice (n = 6 of each genotype). RNA Seq analysis was performed in the University of Cincinnati Genomics and Sequencing Core using the Illumina HiSeq 1000 platform, and sequence reads were aligned to the reference mouse genome using TopHat aligner[22]. Statistical analysis was performed using the negative-binomial model of read counts as carried out in the DeSeq Bioconductor package[23]. mRNA expression data are presented as Reads Per Kilobase per Million mapped reads (RPKM), which normalizes for the size of the mRNA and allows direct comparisons of transcript abundance.

Gene Ontology analysis

For Gene Ontology (GO) analyses, we used the GOrilla program[24] (http://cbl-gorilla.cs.technion.ac.il/). As discussed previously[7,25], two analysis options are available: (1) Two Unranked Lists, in which a target list of genes with a specific range of P values is compared against the list of all genes analyzed; and (2) a Single Rank List, with the entire gene set ranked according to P values, thereby avoiding the use of an arbitrary cutoff of P values. Both analyses were performed. However, because of the low number of genes with highly significant changes, we relied primarily on the Two List analysis, in which significance and enrichment are calculated based on the number of genes in each GO category that appear in the target list and background list. Enrichment is defined as = (b/n)/(B/N), where b is the number of genes in the intersection, n is the number of genes in the top of the user's input list or in the target set when appropriate, B is the total number of genes associated with a specific GO term, and N is the total number of genes. The program calculates statistical probabilities using the hypergeometric distribution[24]. In addition to a P value, the program provides an FDR q-value, which considers the total number of GO categories and corrects for the false discovery rate (FDR).

In vivo myocardial ischemia-reperfusion injury

Surgery to induce IR injury was performed on 4-5 mo old male mice (n = 4 for each genotype) as described previously[26]. Mice were anesthetized with ketamine-inactin and were mechanically ventilated using a rodent ventilator (Model 845, Harvard Apparatus) connected to an endotracheal tube. The heart was exposed by a left side limited thoracotomy and a 6-0 silk suture was passed beneath the left anterior descending artery (LAD) with a tapered needle[26]. A loose double knot was made with the suture and a 5 mm long piece of PE-10 tubing was placed through the loop. The loop was tightened around the artery and tubing to occlude blood flow. After 30 min, the knot was untied and the tubing was removed. The chest cavity was closed with continuous 4-0 silk sutures and the heart was reperfused for 3 h. The mice were euthanized and the chest cavity was opened to isolate the heart. The aorta was cannulated and perfused initially with PBS containing Heparin (10 units Heparin per ml) followed by a modified Krebs-Henseleit buffer (pH 7.4) containing 110 mmol/L NaCl, 16 mmol/L KCl, 16 mmol/L $MgCl_2$, 1.2 mmol/L $CaCl_2$, and 10 mmol/L $NaHCO_3$. Finally, the isolated heart was perfused with 10% buffered formalin and left in 10% buffered formalin for 48 h. The left ventricle was embedded in paraffin and sectioned, with great care taken to identify the exact location of the sections relative to the LAD occlusion site.

TUNEL assay

Cardiomyocyte death by apoptosis in hearts from mice subjected to IR injury (described above) was analyzed using the In Situ Cell Death Detection Kit, TMR red from Roche. Sections that were carefully oriented relative to the occlusion site were deparaffinized, hydrated and pretreated with proteinase K (20 μg/mL in 10 mmol/L tris/HCl, pH 7.4) for 30 min at 37 ℃. The sections were then incubated with the TUNEL mixture for 60 min at 37 ℃. The sections were rinsed with PBS and counterstained with 1:200 dilution of α-Sarcomeric actin antibody (Sigma, A2172) for 60 min at 37 ℃. The section was then rinsed and stained with 1:200 dilution of Fluorescein (FITC) anti-mouse secondary antibody (Jackson Immunoresearch, 115-095-146) for 60 min at 37 ℃. The sections were mounted with ProLong gold antifade mountant with DAPI from Life technologies. Images were taken under 40 × objective on a Olympus BX41 microscope equipped with a digital camera and MagnaFireTM software.

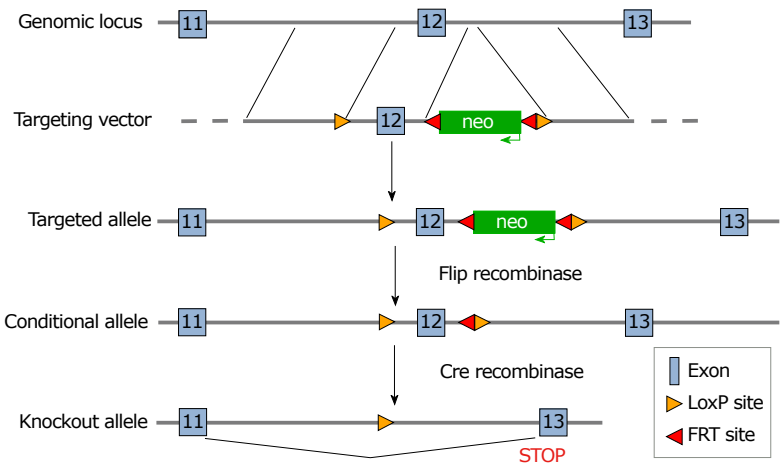

Figure 1 Targeting strategy for generation of *Slc4a4* cardiac myocyte conditional KO mice. The targeting construct contained the neomycin resistance gene (neo) to allow selection of ES cells after homologous recombination. The neo gene was flanked with flippase recognition target (FRT) sites, which allowed removal of neo when mice carrying the targeted allele were bred with transgenic mice expressing Flip recombinase. After confirming the deletion of neo, mice carrying the floxed allele were bred with mice expressing Cre recombinase controlled by the β-MHC promoter, which mediates the deletion of exon 12 of *Slc4a4* in cardiac myocytes.

Statistical analysis

Values are presented as means ± SEM. Individual comparisons were made using a two-tailed Student's *t*-test, and a *P* value < 0.05 was considered significant. For group comparisons, a mixed factor analysis of variance with repeated measures on the second factor was used. Statistical analyses of RNA Seq data and GO data are described in the respective sections above. Statistical methods were reviewed by coauthor Dr. Mario Medvedovic, Director of the Division of Biostatistics and Bioinformatics in the Department of Environmental Health.

RESULTS

Generation of a mouse model with cardiomyocyte-specific deletion of NBCe1 mRNA

A targeting construct in which coding exon 12 of the *Slc4a4* gene was flanked with LoxP sites was prepared (Figure 1) and electroporated into ES cells, which were then subjected to a positive-negative selection procedure. Cells carrying the floxed allele were injected into blastocyts and used to generate chimeric animals. After achieving germline transmission of the targeted allele, the neo gene was deleted by breeding the mice with a transgenic mouse expressing Flip recombinase.

To delete *Slc4a4* in cardiac myocytes, the *Slc4a4*$^{flx/flx}$ mouse was crossed with a transgenic mouse expressing Cre recombinase driven by the β-myosin heavy chain (β-MHC) promoter[19] to obtain *Slc4a4*$^{flx/+(Cre)}$ and *Slc4a4*$^{flx/+}$ mice. Further breeding was performed to obtain *Slc4a4*$^{flx/flx(Cre)}$ (KO) and *Slc4a4*$^{flx/flx}$ (WT) mice, which were mated to obtain experimental pairs. This allowed mice of both genotypes being used for experiments to be housed in the same cages, with sibling pairs often used for experiments. Male and female KO mice appeared normal, and WT and KO mice were indistinguishable in body weight, appearance, and behavior. Also, there was no significant difference in the heart weight: body weight ratios (WT: 4.38 ± 0.15 mg/g; KO: 4.56 ± 0.11 mg/g; *n* = 4 male and 4 female of each genotype at 4 mo of age).

Genotypes were determined by PCR analysis of tail DNA, which yielded a 176-base pair product for the WT allele and a 223-base pair product for the floxed allele (Figure 2A); a separate reaction was performed to test for the presence or absence of the Cre gene. The knockdown of *Slc4a4* mRNA in the heart was confirmed by qRT-PCR analysis of whole heart mRNA using primers from coding exons 11 and 12. This allowed a quantitative assessment of the percentage of NBCe1 transcripts that lack coding exon 12. Loss of this exon causes the sequences following codon 499, which encode most of the transmembrane domains, to be out of frame. As shown in Figure 2B, the amount of NBCe1 mRNA containing exon 12 was reduced by approximately 70% in whole hearts of *Slc4a4*$^{flx/flx(Cre)}$ mice relative to those of *Slc4a4*$^{flx/flx}$ mice. It should be noted that expression of NBCe1 is not restricted to cardiac myocytes, and has been shown to be expressed in both vascular and nerve tissues[27]. Thus, the reduction in functional NBCe1 mRNA in cardiac myocytes is likely to be greater than that indicated by qRT-PCR analysis of whole heart mRNA.

Cardiovascular performance in NBCe1 KO and WT mice under basal conditions and in response to β-adrenergic stimulation

Cardiovascular performance *in vivo* was analyzed under basal conditions and in response to β-adrenergic stimulation using dobutamine. Anesthetized and surgically instrumented mice were analyzed using a pressure transducer in the left ventricle to measure intraventricular pressures and a catheter in the right femoral artery to measure blood pressure and heart rate. There was no difference in heart rate (HR),

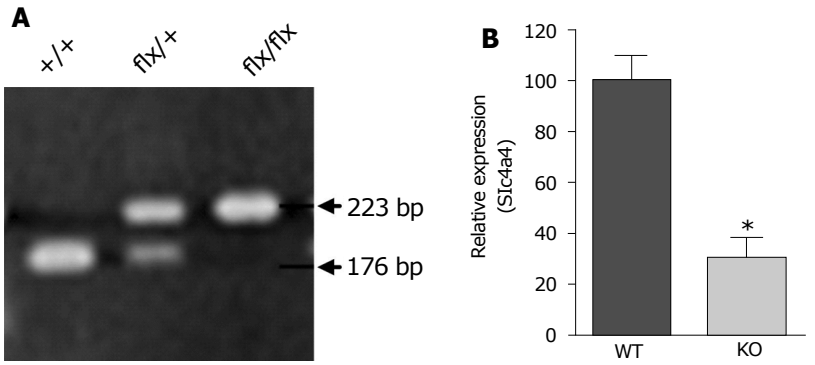

Figure 2 Polymerase chain reaction genotyping and quantitative reverse transcriptase-polymerase chain reaction of NBCe1 mRNA. A: PCR analysis of DNA from tail biopsies, using primers flanking the proximal LoxP site, showing bands for the alleles in *Slc4a4*$^{+/+}$, *Slc4a4*$^{flx/+}$ and *Slc4a4*$^{flx/flx}$ mice. The larger size of the band for the floxed allele is due to the presence of the LoxP site; B: Quantitative RT-PCR analysis of cDNA prepared from whole heart RNA (n = 6 for each genotype) showing a reduction of Slc4a4 mRNA in hearts of KO (*Slc4a4*$^{flx/flx(Cre)}$) relative to WT (*Slc4a4*$^{flx/flx}$ without *Cre*) mice. PCR: Polymerase chain reaction.

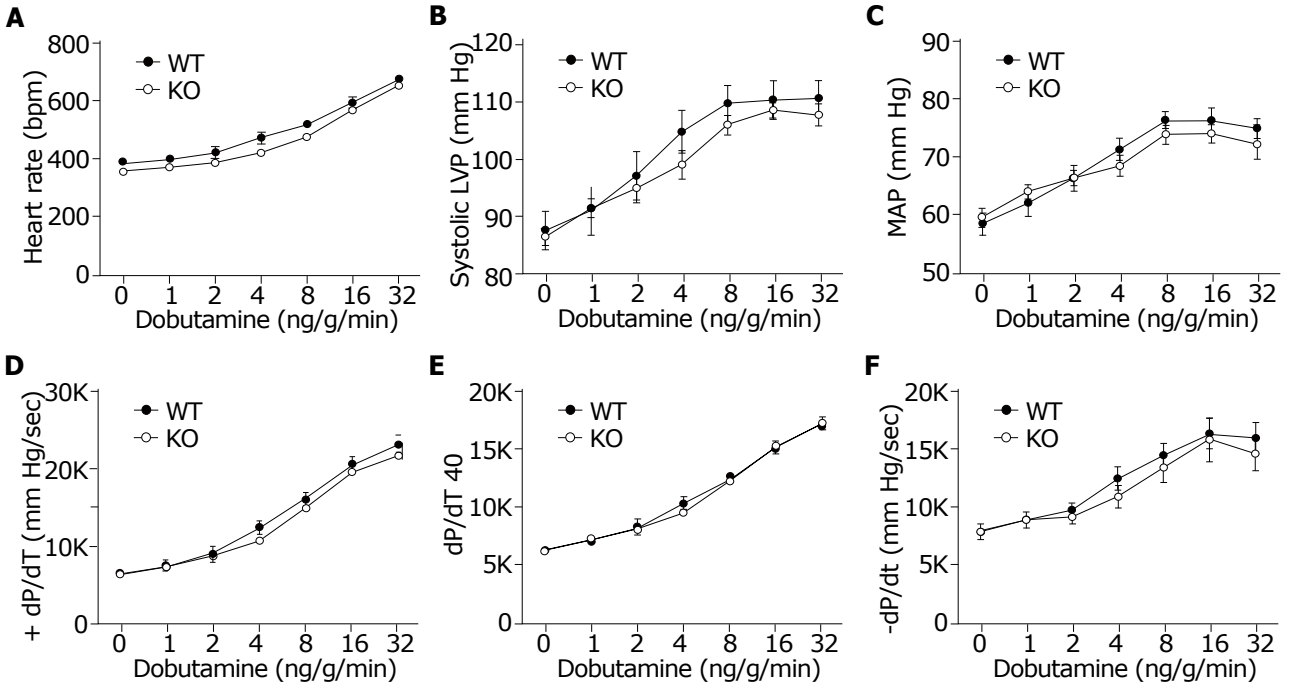

Figure 3 Cardiovascular performance in WT and KO mice. Intraventricular and intra-arterial pressure measurements were recorded using transducers in the left ventricle and right femoral artery of anesthetized 2-3 mo old WT (*Slc4a4*$^{flx/flx}$) and KO (*Slc4a4*$^{flx/flx(Cre)}$) mice under both basal conditions and in response to β-adrenergic stimulation (intravenous infusion of increasing doses of dobutamine). A: Heart rate; B: Systolic left ventricular pressure; C: Mean arterial pressure; D: Positive dP/dt in mm Hg/sec; E: Positive dP/dt at 40 mm Hg; F: Negative dP/dt in mm Hg/sec is shown for WT and KO mice. n = 8 WT (4 female, 4 male) and 8 KO (4 female, 4 male) mice.

systolic ventricular pressure, or mean arterial pressure (Figure 3A, 3B and 3C) between WT (*Slc4a4*$^{flx/flx}$) and KO (*Slc4a4*$^{flx/flx(Cre)}$) mice under basal conditions or in response to β-adrenergic stimulation. Left ventricular contractility (+dP/dT and +dP/dt$_{40}$) and relaxation (-dP/dt) (Figure 3D, 3E and 3F) were essentially the same in WT and KO mice, indicating normal cardiac function in NBCe1-deficient mice.

RNA sequencing of mRNA from NBCe1 KO and WT hearts

To identify patterns of differential gene expression changes in response to the loss of NBCe1 in cardiac myocytes, we performed RNA Seq analysis using mRNA from hearts of WT and KO mice. Between WT and KO hearts, there were 452 differentially expressed genes with $P < 0.05$. However, only a few of these genes had a highly significant FDR value. Many of the genes that fell within the range of $P < 0.05$ were expressed at very low levels or were absent in some samples. The genes that were expressed at low levels included sixteen major urinary proteins (Mups) and six cytochrome P450s, which were sharply induced in the KO. After removal of those genes with very low expression, the remaining 347 genes were subjected to GO analyses.

Because it has been proposed that the electrogenic

Table 1 Enriched Gene Ontology categories in NBCe1 cardiac conditional KO mice

GO category	*P*-value	Q-value	Enrichment	(N, B, n, b)
GO categories dealing with ion homeostasis				
GO:0006873 Cellular ion homeostasis	1.13E-4	5.68E-1	2.45	(21545, 579, 334, 22)
GO:0051453 Regulation of intracellular pH	1.92E-4	5.80E-1	5.86	(21545, 77, 334, 7)
GO:0030003 Cellular cation homeostasis	2.12E-4	4.58E-1	2.4	(21545, 564, 334, 21)
GO categories dealing with apoptosis				
GO:0043652 Engulfment of apoptotic cell	4.09E-4	4.42E-1	19.35	(21545, 10, 334, 3)
GO:1901030 Mitochondrial membrane permeabilization involved in apoptotic signaling	4.09E-4	4.12E-1	19.35	(21545, 10, 334, 3)
GO categories dealing with membrane compartments				
GO:0005783 Endoplasmic reticulum	2.82E-6	1.06E-3	2.03	(21545, 1493, 334, 47)
GO:0030315 T-tubule	3.45E-5	7.18E-3	7.65	(21545, 59, 334, 7)
GO:0016529 Sarcoplasmic reticulum	3.00E-4	3.30E-2	6.56	(21545, 59, 334, 6)
GO:0042383 Sarcolemma	4.84E-4	4.77E-2	4.41	(21545, 117, 334, 8)

GO categories were identified using the Two unranked list option of the GOrilla Gene Ontology program[24]. N is the total number of genes, B is the total number of genes associated with a specific GO term, n is the number of genes in the target set, b is the number of genes in the intersection. Enrichment = (b/n)/(B/N). Differential mRNA expression data were generated by RNA Seq analysis of hearts from 6 adult male mice for the NBCe1 KO (*Slc4a4*$^{flx/flx(Cre)}$) and NBCe1 WT (*Slc4a4*$^{flx/flx}$) genotypes.

activity of NBCe1 and its expression in t-tubules is likely to affect electrical activity of cardiac myocytes[1], we anticipated that there might be changes in genes involved in membrane excitability and cardiac conduction. In addition, because it has been suggested that NBCe1 activity can serve as a major mechanism for Na^+-loading, with subsequent effects on Ca^{2+}-handling and contractility[4,8], we were interested in whether the loss of NBCe1 might affect expression of genes encoding myofibrillar proteins, Ca^{2+}-handling proteins, and proteins that affect Na^+-loading.

As shown in Table 1, changes in Biological Function GO categories for cellular ion homeostasis, including subcategories for intracellular pH and cation homeostasis, were indicated, but the changes were modest and their statistical significance was poor (low FDR). Two Biological Function GO categories relating to apoptosis were identified, and their statistical significance was poor. However, when GO analysis was run using the single rank option for GOrilla GO analysis (see materials and methods), additional genes were identified for GO:0043652 (Engulfment of Apoptotic Cell) and an acceptable FDR value for this GO category was attained. There were no significant Molecular Function GO categories, but among Cellular Component GO categories there were a number dealing with membrane compartments (Table 1). These included GO categories for the endoplasmic and sarcoplasmic reticulum, t-tubules, and sarcolemma.

Genes for channels, pumps, and transporters that exhibited differential expression are shown in Table 2. Among K^+ channels, modest upregulation of *Kcnj2* and *Kcnj11* (both in the t-tubule GO category) was observed along with higher upregulation of *Kcna4* (K_v1.4; 1.50-fold increase), which is expressed in t-tubules and sarcolemma[28], and *Kcnk2* (TREK-1; 1.65x), which is expressed in intercalated discs[29]. Among Ca^{2+} channels, *Cacna1s* (Cav1.1; L-type α1S) was upregulated and *Cacnb1* (a beta subunit) was downregulated. Both Ca^{2+} channel subunits are in the t-tubule. However, they are major components of the skeletal muscle Ca^{2+} channel and are expressed at much lower levels in heart. The only other gene for a Ca^{2+}-handling protein that was changed was *Atp2a1*, the skeletal muscle sarcoplasmic reticulum (SR) Ca^{2+} pump, which is expressed at very low levels in heart.

Slc9a1 mRNA, encoding the NHE1 Na^+/H^+ exchanger, was slightly upregulated, and *Slc9a9*, an organellar Na^+/H^+ exchanger, was also upregulated. Other H^+-coupled transporters with altered expression (Table 2) were transporters for peptides (*Slc15a1, Slc15a2*), amino acids (*Slc36a1*), and lactate (*Slc16a3*). Additional transporters included two amino acid transporters (*Slc1a5 and Slc7a1*), an iron transporter (*Slc40a1*), and a zinc transporter (*Slc39a13*). The expression of NBCn1 (*Slc4a7*), the only other Na^+-HCO_3^- cotransporter expressed in heart, was not significantly changed (RPKM values: 6.67 ± 0.42 in WT; 6.99 ± 0.15 in KO).

Differentially expressed genes for proteins involved in apoptosis are shown in Table 3. Some of these were identified because of their inclusion in the apoptosis GO categories shown in Table 1 (*Xkr8*, *Rac3*, *Thbs1*, *Zfp13*, *Sh3glb1*, and *Siva1*). Others were identified based on literature searches and a P value ⩽ 0.01 (*Msrb3*, *Xlrl*, *Ier5*, *Hint1*, *and Stmn1*).

Reduced apoptosis in NBCe1 KO hearts in response to in vivo ischemia-reperfusion

To determine whether ablation of NBCe1 would provide protection against IR injury, WT and KO hearts were subjected to 30 min of ischemia by temporary ligation of the left anterior descending (LAD) artery, followed by 3 h of reperfusion. TUNEL staining was performed to detect apoptotic cell death and to quantify apoptotic nuclei in WT and KO heart sections. Apoptotic nuclei were detected primarily in the left ventricular free wall in both WT and KO heart sections (Figure 4A). However, there were significantly fewer apoptotic nuclei (Figure

Table 2 Ion channel and transporter genes altered in NBCe1-null hearts

Gene symbol	Description	Fold change	*P* value
Kcnj2	Inwardly-rectifying K^+ channel J2	1.18	0.02
Kcnj11	Inwardly-rectifying K^+ channel J11	1.14	0.03
Kcnk2	K^+ channel K2; TREK-1	1.65	0
Kcna4	K^+ channel, shaker-related 4; Kv1.4	1.50	0.05
Cacna1s	L type Ca^{2+} channel, alpha 1S subunit	1.44	0
Cacnb1	Ca^{2+} channel, beta 1 subunit	0.51	0
Atp2a1	Skeletal muscle SR Ca^{2+} pump	1.82	0.04
Slc9a1	Sarcolemmal Na^+/H^+ Exchanger	1.18	0.05
Slc9a9	Organellar Na^+/H^+ Exchanger	1.44	0.03
Slc16a3	Monocarboxylic acid transporter,	1.92	0.04
Slc1a5	Neutral amino acid transporter	0.81	0.04
Slc7a1	Cationic amino acid transporter, y+ system	1.24	0
Slc15a2	Proton/peptide transporter	1.87	0.01
Slc15a1	Oligopeptide transporter	0.56	0.03
Slc40a1	Iron transporter; ferroportin	0.86	0.02
Slc39a13	Zinc transporter	1.23	0.03
Slc36a1	Proton/amino acid symporter	0.83	0.05

Differential mRNA expression is presented as fold-changes in NBCe1-null hearts ($Slc4a4^{flx/flx(Cre)}$) relative to WT ($Slc4a4^{flx/flx}$) hearts.

Table 3 Differential expression of apoptosis genes in NBCe1-null hearts

Gene symbol	Description	Fold change	*P* value
Xkr8	X Kell Blood Group Precursor Related 8	0.61	0.015
Rac3	RAS-Related C3 Botulinum Substrate 3	0.36	0.016
Thbs1	Thrombospondin 1	0.79	0.020
Zfp13	Zinc Finger Protein 13	0.46	0.023
Sh3glb1	SH3-Domain GRB2-like B1 (Endophilin)	1.13	0.024
Siva1	SIVA1, Apoptosis-Inducing Factor	0.66	0.030
Msrb3	Methionine Sulfoxide Reductase B3	1.19	0.002
Xlrl	Xlr-like	1.77	0.003
Ier5	Immediate Early Response 5	0.80	0.005
Hint1	Histidine Triad Nucleotide Binding Protein 1	0.84	0.010
Stmn1	Stathmin 1	1.37	0.010

Differential mRNA expression is presented as fold-changes in NBCe1-null hearts ($Slc4a4^{flx/flx(Cre)}$) relative to WT ($Slc4a4^{flx/flx}$) hearts. The first six genes on this list were identified based on inclusion in the two apoptosis GO categories identified in Table 1.

4B) in KO (40.6 ± 6.4 apoptotic nuclei per mm^2) than in WT (142.0 ± 13.6 apoptotic nuclei per mm^2) heart sections.

DISCUSSION

On the basis of functional studies and expression data it is clear that NBCe1 serves as a major uptake mechanism for both Na^+ and HCO_3^- in cardiac myocytes[1,4]. Na^+-loading can affect both cardiac contractility and response to IR injury[4,8,15,16], and there is evidence that HCO_3^- has a major effect on contractility, both in isolated myocytes[5] and in the isolated work-performing heart[30]. Also, because NBCe1 is electrogenic and expressed in t-tubules, lateral sarcolemma, and intercalated discs[1], it has the potential to affect membrane potential and electrical activity of the myocyte. To begin testing the cardiovascular functions of NBCe1 we developed a mouse model carrying a floxed allele for NBCe1 and analyzed the effects of cardiomyocyte-specific ablation on cardiovascular performance and *in vivo* IR injury. In addition, we performed RNA Seq analysis to determine whether remodeling of cardiac systems occurs at the level of mRNA expression patterns in response to the loss of NBCe1.

The loss of NBCe1 did not impair cardiovascular performance, and heart weights did not differ between the two genotypes. NBCe1 mutant mice exhibited normal heart rates, blood pressures, and basal contraction and relaxation, and when they were treated with a β-adrenergic agonist, they exhibited normal increases in contraction and relaxation. The lack of any apparent detrimental effects supports the notion that inhibition of cardiac NBCe1 activity could be used for cardioprotection. These results also suggest that uptake of HCO_3^- by NBCe1 is not required for the stimulation of contraction observed in isolated myocytes and hearts in the presence of HCO_3^-[5,30], although it is possible that the high rate of HCO_3^- production from metabolically produced CO_2 *in vivo* prevents any deficit in intracellular HCO_3^- levels. Alternatively, reduced HCO_3^--efflux *via* Cl^-/HCO_3^- exchange or increased uptake *via* NBCn1 may be sufficient to maintain intracellular HCO_3^- homeostasis *in vivo* when NBCe1 was ablated. Also,

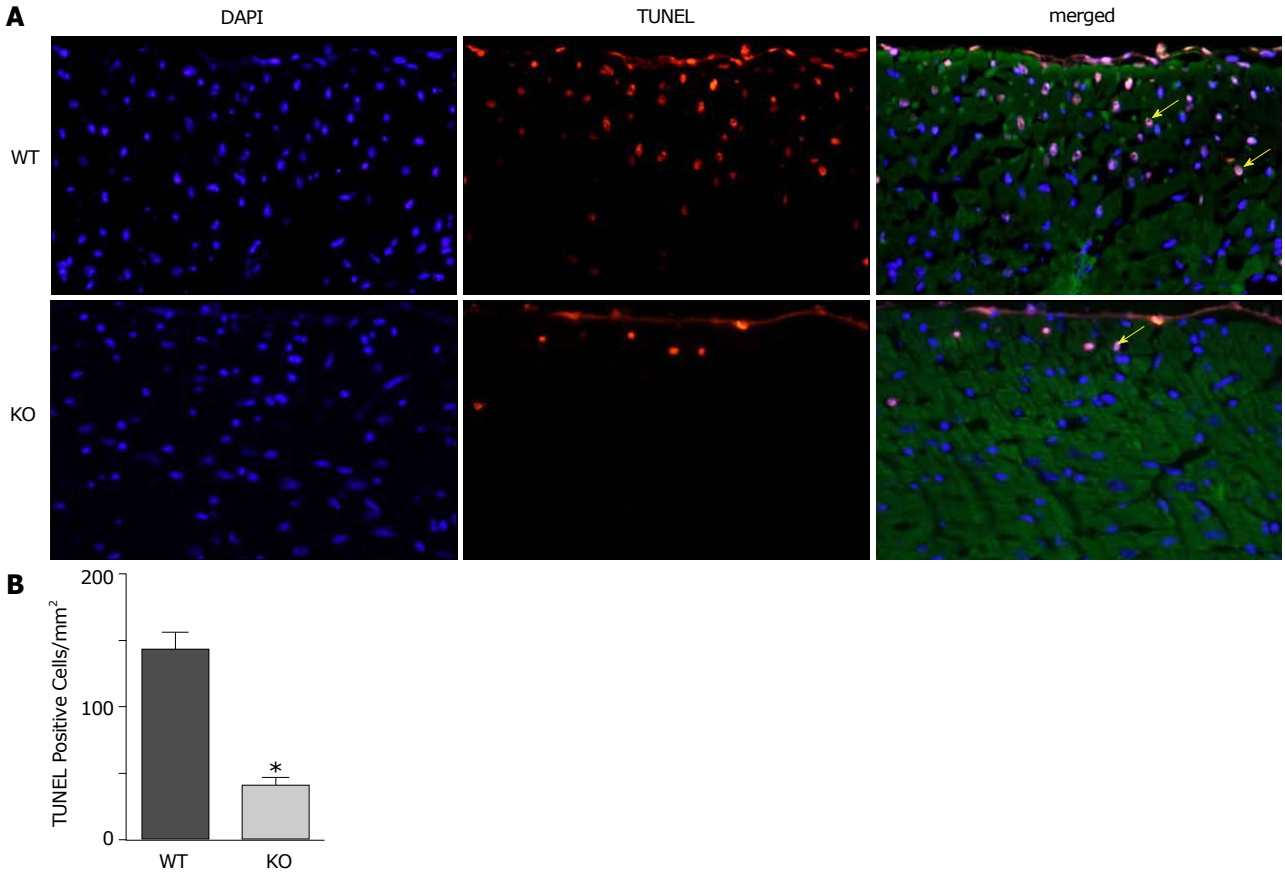

Figure 4 TUNEL staining to quantify apoptosis in WT and KO heart sections after ischemia and reperfusion. Mice were subjected to 30 min of ischemia by occlusion of the LAD, followed by 3 h of reperfusion, and heart sections were processed to analyze apoptosis. A: Representative images from WT and KO heart sections, taken from a region approximately 1 mm distal to the occlusion site, showing nuclei stained with DAPI (blue), TUNEL (red) and sarcomeric actin (green). Yellow arrows point to apoptotic nuclei (pink); B: Quantification of apoptotic nuclei. n = 4 mice of each genotype, $P \leqslant 0.05$.

the NHE1 Na^+/H^+ exchanger was slightly upregulated at the mRNA level and provides a powerful alternative mechanism of Na^+-loading and pH_i regulation. It should be noted that genetic ablation of NHE1 also caused no impairment of cardiovascular performance[31], and it had beneficial effects on cardiac energy metabolism, including increased glucose utilization and metabolic flexibility[31]. Interestingly, NBCe1 activity is involved in acute stimulation of glycolysis in astrocytes in response to membrane depolarization[32]. Thus, one could speculate that the increased glucose utilization observed in hearts of NHE1-null mice[31] might be due in part to a compensatory increase in NBCe1 activity.

Because they have opposing activities with respect to HCO_3^- fluxes, it is of interest to compare the results of ablating NBCe1, the predominant HCO_3^--uptake mechanism in heart, with the results of ablating the AE3 (*Slc4a3*) Cl^-/HCO_3^- exchanger. Both the very high mRNA expression levels of AE3[7] and its predominant role in recovery of myocytes from an alkaline load[33] demonstrate that it is the predominant HCO_3^--extrusion mechanism in the heart. In humans, heterozygous mutations in AE3 contribute to heart disease[34]. In mice, the loss of AE3 caused a mild impairment of force-frequency responses[35] and exacerbated heart disease caused by other genetic defects[21,36]. However, AE3-null mice exhibited normal cardiac contraction and relaxation under both basal conditions and after β-adrenergic stimulation[33]. Nevertheless, RNA Seq analysis indicated that AE3-null hearts undergo major remodeling of cardiac gene expression patterns involved in hypoxia responses and angiogenesis, energy metabolism, sarcomere function, and membrane excitability and electrical conduction[7].

Unlike the results of the AE3 RNA Seq study, RNA Seq analysis of NBCe1-null hearts revealed little evidence of cardiac remodeling at the mRNA level. For example, altered expression of genes involved in sarcomere function were very prominent in AE3 null-hearts[7], but no such changes were observed in NBCe1-null hearts, which is consistent with the normal contractility and β-adrenergic responses. Similarly, changes in energy metabolism genes were extensive in AE3-null hearts, but were not observed in NBCe1-null hearts, despite the known stimulatory effect of NBCe1 activity on glycolysis in astrocytes[32]. We also observed no changes in hypoxia response and angiogenesis genes, which were prominent in AE3-null hearts. However, there were several interesting changes related to membrane excitability.

One of the predictions by other investigators[1] was that the electrogenic activity of NBCe1 in the sarcolemma, t-tubules, and intercalated discs, with inward transport of one Na^+ and two HCO_3^- ions during depolarization, would affect membrane excitability. The changes in genes involved in membrane excitability and electrical conduction were extensive in AE3-null hearts, and included voltage-sensitive Na^+, K^+, and Ca^{2+} channels, and gap junction proteins involved in electrical coupling between myocytes. Few such changes were observed in NBCe1-null hearts. However, a number of K^+ channel genes were upregulated. These included *Kcna4*, encoding Kv1.4, and *Kcnk2*, encoding TREK-1. Kv1.4 is co-expressed with NBCe1 in t-tubules and the sarcolemma[28]. It mediates transient outward currents during the initial phase of depolarization[37] and might therefore counteract the lengthening of the action potential expected with a reduction in NBCe1 activity[38]. TREK-1 is expressed in intercalated discs[29] and plays an important role in regulating excitability of the sinoatrial node[39]. Thus, increased expression and activity of TREK-1 has the potential to counteract the electrical effects of the loss of NBCe1 activity in intercalated discs.

Although there were changes in two voltagesensitive Ca^{2+} channel subunits in t-tubules (*Cacna1s*, an α subunit expressed at low levels; *Cacnb1*, a β subunit, expressed at very low levels), both are primarily skeletal muscle isoforms. In contrast, *Cacna1c*, which encodes the major L-type Ca^{2+} channel in cardiac muscle (Cav1.2), was not changed (RPKM values: 26.8 ± 0.8 in WT; 26.2 ± 0.6 in KO). The only other gene for a Ca^{2+}-handling protein that was changed was *Atp2a1*, the skeletal muscle sarcoplasmic reticulum Ca^{2+} pump. However, *Atp2a1* is expressed at exceedingly low levels in heart (< 1 RPKM in WT), whereas *Atp2a2*, the cardiac Ca^{2+} pump was expressed at very high levels and was not changed (RPKM values: 2185 ± 47 in WT; 2183 ± 23 in KO). The major Na^+/Ca^{2+} exchanger (NCX1, *Slc8a1*) also was not significantly changed (RPKM values: 25.0 ± 0.6 in WT; 27.3 ± 0.7 in KO). These data provide little support for remodeling of Ca^{2+}-handling systems at the mRNA level.

A major objective was to determine whether genetic ablation of NBCe1 is cardioprotective during IR injury. The role of NHE1 in cardiac IR injury has been extensively studied using both inhibitors and genetic approaches[9-14], and it is generally accepted that the mechanism of protection involves reductions in Na^+-loading, Ca^{2+}-loading, and the rate of pH_i recovery during reperfusion. Since NBCe1, like NHE1, mediates both Na^+-loading and recovery from an acid load[40], a number of investigators have noted that NBCe1 activity could potentially contribute to IR injury. In fact, two groups have shown that inhibition of NBCe1 during reperfusion of mouse or rat hearts that were subjected to ischemia provides some protection against IR injury[15,16]. These results using isolated heart preparations support a role for NBCe1 in IR injury that is similar to that of NHE1 and indicate that a reduction in its activity can be cardioprotective.

Previous studies have shown that apoptotic cell death occurs mainly during reperfusion of ischemic tissue[41-43]. An increase in intracellular Ca^{2+} results in opening of the mitochondrial permeability transition pore[44], which then leads to apoptosis. In the current study, after WT and KO mice were subjected to 30 min of LAD occlusion and 3 h of reperfusion, apoptotic cell death and apoptotic nuclei were detected and quantified in heart sections taken from just below the point of occlusion. The significant reduction in the numbers of apoptotic nuclei in NBCe1 KO hearts following cardiac IR injury *in vivo* indicates that reduced NBCe1 activity is cardioprotective. Thus, both the studies using isolated hearts[15,16] and the current studies showing reduced apoptosis following *in vivo* IR injury support the hypothesis that a reduction in NBCe1 activity is cardioprotective. Given the severe effects of global NBCe1 ablation[18], only partial inhibition of NBCe1 is likely to be acceptable as part of a treatment strategy, however, it is possible that an NBCe1 inhibitor could be used in combination with other treatments.

As discussed above, the primary mechanism of NBCe1-mediated cardioprotection is likely to be the reductions in Na^+-loading, Ca^{2+}-loading, and the rate of pHi recovery during reperfusion. However, because a genetic ablation strategy was employed, rather than acute inhibition of NBCe1, it is possible that the long-term absence of NBCe1 has elicited remodeling that contributes to cardioprotection. This possibility is supported by the observation that genetic ablation of NHE1 reduces oxidative stress in the heart, high-fat diet-induced myocardial stress[31], and fatty liver disease[45], which are clear indications of long-term remodeling. A potentially interesting set of changes observed in the RNA Seq data were those involving genes with functions in apoptosis. The q-values for the apoptosis GO categories (Table 1) were not highly significant and these findings must therefore be considered with caution. Nevertheless, the observation provides suggestive evidence that ablation of the NBCe1 gene using the β-myosin promoter, which would be largely complete by birth, may cause changes in gene expression that tend to protect against apoptosis. For example, Siva1 (apoptosis-inducing factor) normally interacts with and inhibits Stathmin, thus promoting apoptosis[46,47]. Thus, down-regulation of Siva1 (0.66-fold, RPKM: 4.8 ± 0.3 in WT; 3.2 ± 0.2 in KO) and upregulation of Stathmin (1.37-fold, RPKM: 9.6 ± 0.5 in WT; 13.2 ± 1.2 in KO) would be expected to reduce apoptosis. Another interesting example is Xlrl, which was upregulated (1.77-fold, RPKM: 1.96 ± 0.34 in WT; 3.49 ± 0.17 in KO). Little is known about this gene, but Xlrl is almost identical to Xlr (95% amino acid identity and no gaps over their entire length of 208 amino acids), which protects against apoptosis[48]. Xlr was also upregulated (1.36-fold), but its levels of expression were lower.

The current study has a number of limitations. First, our mice were on a mixed 129/Svj and C57Bl6 background, rather than on a highly inbred background. The lack of a highly inbred background was likely

responsible for the relatively high variability in our RNA Seq data compared to the very low variability that we observed when performing RNA Seq analysis using mRNA from hearts of AE3-null and WT mice on a highly inbred background[7]. With much lower variability, it would have been possible to detect more subtle patterns of changes in gene expression. However, it was clear from the data that there were no extensive changes in gene expression patterns for sarcomeric or metabolic genes, and that the changes in ion channel genes were not extensive.

A second limitation is that the 30 min period of ischemia and 3 h of reperfusion were chosen to maximize our ability to detect apoptotic cell death, which plays a major role in ischemic injury. However, this protocol is not optimal for analysis of necrotic cell death, for detecting differences in cardiac function between WT and KO mice, or for detecting markers of myocardial infarction such as serum troponin levels. For such studies, a longer period of ischemia or a myocardial infarction model, with permanent occlusion of the LAD and long-term follow-up, would be necessary. In myocardial infarction studies it would also be useful to determine whether NBCe1 heterozygosity could provide some degree of cardioprotection, since any cardiac therapy using complete pharmacological inhibition of NBCe1 would have a severe impact on kidney function. Even limited cardioprotection caused by partial inhibition could be useful, however, as it might be possible to combine partial inhibition of NBCe1 with partial inhibition of the NHE1 Na^+/H^+ exchanger, which appear to act *via* similar mechanisms (see introduction).

An additional potential limitation was that our WT controls were *Slc4a4*$^{flx/flx}$ mice rather than *Slc4a4*$^{+/+(Cre+)}$ mice. A study published after we had performed our RNA Seq analysis reported that prolonged Cre expression driven by the α-myosin heavy chain promoter can be cardiotoxic[49]. However, we used a Cre transgene driven by the β-myosin promoter[19], which is expressed at much lower levels than the α-myosin promoter after birth. As an indication of cardiotoxicity, long-term expression of Cre via the α-myosin promoter caused approximately 7-fold increase in expression of atrial natriuretic factor mRNA and approximately 2.5-fold increase in expression of β-myosin mRNA[48]. However, these genes were not changed in the NBCe1 KO carrying Cre driven by the β-myosin promoter. Of greater relevance, 6 mo old mice expressing Cre *via* the α-myosin promoter exhibited an approximately 3-fold increase in apoptosis. In our own studies, however, only the NBCe1 cardiac-specific KO mice were carrying the Cre transgene, and they exhibited significantly less apoptosis than the *Slc4a4*$^{flox/flox}$ controls. These results clearly indicated a cardioprotective effect of NBCe1 ablation, despite the presence of Cre.

In summary, we have developed a conditional knockout mouse model for *Slc4a4* and have used it to test the effects of cardiac-specific ablation of NBCe1 in heart. The results show that loss of NBCe1 does not impair cardiovascular performance and that it significantly reduces the incidence of apoptosis following *in vivo* IR injury. These results are consistent with the results of previous studies using the isolated heart[15,16] and support the view that inhibition of NBCe1 during reperfusion has the potential to serve as a component of a cardioprotective treatment strategy.

ARTICLE HIGHLIGHTS

Research background

There is a strong rationale for the hypothesis that inhibition of NBCe1-mediated Na^+-HCO_3^- cotransport activity protects against cardiac ischemia-reperfusion injury. This suggests that inhibition of NBCe1 could become part of a cardioprotective strategy.

Research motivation

Previous studies have been performed using the isolated heart, but there are no *in vivo* studies supporting the hypothesis that loss of NBCe1 activity is cardioprotective. Such studies are critical if NBCe1 inhibition is to be developed as a therapeutic strategy.

Research objectives

The objective of this study was to test whether loss of NBCe1 in the heart would protect against cardiac ischemia-reperfusion injury *in vivo*.

Research methods

Gene targeting was used to develop a conditional knockout mouse model in which the NBCe1 gene was ablated in cardiomyocytes. Hemodynamic measurements were performed to assess the effects of cardiac-specific NBCe1 ablation on cardiovascular performance, RNA Seq analysis was used to study changes in the cardiac transcriptome, and histological techniques were used to analyze cardiomyocyte apoptosis in response to ischemia-reperfusion injury.

Research results

NBCe1 ablation did not impair cardiovascular performance and caused only limited changes in the cardiac transcriptome. However, it caused a significant reduction in apoptosis following *in vivo* cardiac ischemia-reperfusion injury.

Research conclusions

Loss of NBCe1 in heart does not cause any apparent adverse effects, but does have a cardioprotective effect following ischemia and reperfusion *in vivo*.

Research perspectives

Future studies should focus on whether NBCe1 ablation is cardioprotective following myocardial infarction and whether partial inhibition of NBCe1 can be combined with other treatments that reduce Na^+ and Ca^{2+} loading.

ACKNOWLEDGEMENTS

We thank Jeffery D Molkentin for providing the mouse model with the Cre transgene driven by the β-myosin promoter, Michelle L Nieman for help with the cardiovascular physiology experiments, and Glenn Doerman for preparing the figures.

REFERENCES

1 **Garciarena CD**, Ma YL, Swietach P, Huc L, Vaughan-Jones RD. Sarcolemmal localisation of Na+/H+ exchange and Na+-HCO3- co-transport influences the spatial regulation of intracellular pH in rat ventricular myocytes. *J Physiol* 2013; **591**: 2287-2306 [PMID: 23420656 DOI: 10.1113/jphysiol.2012.249664]

2 **Vaughan-Jones RD**, Spitzer KW, Swietach P. Intracellular pH regulation in heart. *J Mol Cell Cardiol* 2009; **46**: 318-331 [PMID: 19041875 DOI: 10.1016/j.yjmcc.2008.10.024]

3 **Lagadic-Gossmann D**, Buckler KJ, Vaughan-Jones RD. Role of bicarbonate in pH recovery from intracellular acidosis in the guinea-pig ventricular myocyte. *J Physiol* 1992; **458**: 361-384 [PMID: 1302269 DOI: 10.1113/jphysiol.1992.sp019422]

4 **Garciarena CD**, Youm JB, Swietach P, Vaughan-Jones RD. H^+-activated Na^+ influx in the ventricular myocyte couples Ca^{2+}-signalling to intracellular pH. *J Mol Cell Cardiol* 2013; **61**: 51-59 [PMID: 23602948 DOI: 10.1016/j.yjmcc.2013.04.008]

5 **Wang HS**, Chen Y, Vairamani K, Shull GE. Critical role of bicarbonate and bicarbonate transporters in cardiac function. *World J Biol Chem* 2014; **5**: 334-345 [PMID: 25225601 DOI: 10.4331/wjbc.v5.i3.334]

6 **Alvarez BV**, Fujinaga J, Casey JR. Molecular basis for angiotensin II-induced increase of chloride/bicarbonate exchange in the myocardium. *Circ Res* 2001; **89**: 1246-1253 [PMID: 11739292 DOI: 10.1161/hh2401.101907]

7 **Vairamani K**, Wang HS, Medvedovic M, Lorenz JN, Shull GE. RNA SEQ Analysis Indicates that the AE3 Cl-/HCO3- Exchanger Contributes to Active Transport-Mediated CO2 Disposal in Heart. *Sci Rep* 2017; **7**: 7264 [PMID: 28779178 DOI: 10.1038/s41598-017-07585-y]

8 **Shen X**, Cannell MB, Ward ML. Effect of SR load and pH regulatory mechanisms on stretch-dependent Ca(2+) entry during the slow force response. *J Mol Cell Cardiol* 2013; **63**: 37-46 [PMID: 23880608 DOI: 10.1016/j.yjmcc.2013.07.008]

9 **Moffat MP**, Karmazyn M. Protective effects of the potent Na/H exchange inhibitor methylisobutyl amiloride against post-ischemic contractile dysfunction in rat and guinea-pig hearts. *J Mol Cell Cardiol* 1993; **25**: 959-971 [PMID: 8263964 DOI: 10.1006/jmcc.1993.1108]

10 **Scholz W**, Albus U, Lang HJ, Linz W, Martorana PA, Englert HC, Schölkens BA. Hoe 694, a new Na+/H+ exchange inhibitor and its effects in cardiac ischaemia. *Br J Pharmacol* 1993; **109**: 562-568 [PMID: 8358557 DOI: 10.1111/j.1476-5381.1993.tb13607.x]

11 **Hendrikx M**, Mubagwa K, Verdonck F, Overloop K, Van Hecke P, Vanstapel F, Van Lommel A, Verbeken E, Lauweryns J, Flameng W. New Na(+)-H+ exchange inhibitor HOE 694 improves postischemic function and high-energy phosphate resynthesis and reduces Ca2+ overload in isolated perfused rabbit heart. *Circulation* 1994; **89**: 2787-2798 [PMID: 8205693 DOI: 10.1161/01.CIR.89.6.2787]

12 **Hartmann M**, Decking UK. Blocking Na(+)-H+ exchange by cariporide reduces Na(+)-overload in ischemia and is cardioprotective. *J Mol Cell Cardiol* 1999; **31**: 1985-1995 [PMID: 10591025 DOI: 10.1006/jmcc.1999.1029]

13 **Strömer H**, de Groot MC, Horn M, Faul C, Leupold A, Morgan JP, Scholz W, Neubauer S. Na(+)/H(+) exchange inhibition with HOE642 improves postischemic recovery due to attenuation of Ca(2+) overload and prolonged acidosis on reperfusion. *Circulation* 2000; **101**: 2749-2755 [PMID: 10851214 DOI: 10.1161/01.CIR.101.23.2749]

14 **Wang Y**, Meyer JW, Ashraf M, Shull GE. Mice with a null mutation in the NHE1 Na+-H+ exchanger are resistant to cardiac ischemia-reperfusion injury. *Circ Res* 2003; **93**: 776-782 [PMID: 12970112 DOI: 10.1161/01.RES.0000094746.24774.DC]

15 **Khandoudi N**, Albadine J, Robert P, Krief S, Berrebi-Bertrand I, Martin X, Bevensee MO, Boron WF, Bril A. Inhibition of the cardiac electrogenic sodium bicarbonate cotransporter reduces ischemic injury. *Cardiovasc Res* 2001; **52**: 387-396 [PMID: 11738055 DOI: 10.1016/S0008-6363(01)00430-8]

16 **Fantinelli JC**, Orlowski A, Aiello EA, Mosca SM. The electrogenic cardiac sodium bicarbonate co-transporter (NBCe1) contributes to the reperfusion injury. *Cardiovasc Pathol* 2014; **23**: 224-230 [PMID: 24721237 DOI: 10.1016/j.carpath.2014.03.003]

17 **Yamamoto T**, Shirayama T, Sakatani T, Takahashi T, Tanaka H, Takamatsu T, Spitzer KW, Matsubara H. Enhanced activity of ventricular Na+-HCO3- cotransport in pressure overload hypertrophy. *Am J Physiol Heart Circ Physiol* 2007; **293**: H1254-H1264 [PMID: 17416604 DOI: 10.1152/ajpheart.00964.2006]

18 **Gawenis LR**, Bradford EM, Prasad V, Lorenz JN, Simpson JE, Clarke LL, Woo AL, Grisham C, Sanford LP, Doetschman T, Miller ML, Shull GE. Colonic anion secretory defects and metabolic acidosis in mice lacking the NBC1 Na+/HCO3- cotransporter. *J Biol Chem* 2007; **282**: 9042-9052 [PMID: 17192275 DOI: 10.1074/jbc.M607041200]

19 **Parsons SA**, Millay DP, Wilkins BJ, Bueno OF, Tsika GL, Neilson JR, Liberatore CM, Yutzey KE, Crabtree GR, Tsika RW, Molkentin JD. Genetic loss of calcineurin blocks mechanical overload-induced skeletal muscle fiber type switching but not hypertrophy. *J Biol Chem* 2004; **279**: 26192-26200 [PMID: 15082723 DOI: 10.1074/jbc.M313800200]

20 **Lorenz JN**, Robbins J. Measurement of intraventricular pressure and cardiac performance in the intact closed-chest anesthetized mouse. *Am J Physiol* 1997; **272**: H1137-H1146 [PMID: 9087586 DOI: 10.1152/ajpheart.1997.272.3.H1137]

21 **Al Moamen NJ**, Prasad V, Bodi I, Miller ML, Neiman ML, Lasko VM, Alper SL, Wieczorek DF, Lorenz JN, Shull GE. Loss of the AE3 anion exchanger in a hypertrophic cardiomyopathy model causes rapid decompensation and heart failure. *J Mol Cell Cardiol* 2011; **50**: 137-146 [PMID: 21056571 DOI: 10.1016/j.yjmcc.2010.10.028]

22 **Trapnell C**, Pachter L, Salzberg SL. TopHat: discovering splice junctions with RNA-Seq. *Bioinformatics* 2009; **25**: 1105-1111 [PMID: 19289445 DOI: 10.1093/bioinformatics/btp120]

23 **Anders S**, Huber W. Differential expression analysis for sequence count data. *Genome Biol* 2010; **11**: R106 [PMID: 20979621 DOI: 10.1186/gb-2010-11-10-r106]

24 **Eden E**, Navon R, Steinfeld I, Lipson D, Yakhini Z. GOrilla: a tool for discovery and visualization of enriched GO terms in ranked gene lists. *BMC Bioinformatics* 2009; **10**: 48 [PMID: 19192299 DOI: 10.1186/1471-2105-10-48]

25 **Bradford EM**, Vairamani K, Shull GE. Differential expression of pancreatic protein and chemosensing receptor mRNAs in NKCC1-null intestine. *World J Gastrointest Pathophysiol* 2016; **7**: 138-149 [PMID: 26909237 DOI: 10.4291/wjgp.v7.i1.138]

26 **Xu Z**, Alloush J, Beck E, Weisleder N. A murine model of myocardial ischemia-reperfusion injury through ligation of the left anterior descending artery. *J Vis Exp* 2014; (86) [PMID: 24747599 DOI: 10.3791/51329]

27 **GTEx Consortium**. Human genomics. The Genotype-Tissue Expression (GTEx) pilot analysis: multitissue gene regulation in humans. *Science* 2015; **348**: 648-660 [PMID: 25954001 DOI: 10.1126/science.1262110]

28 **O'Connell KM**, Whitesell JD, Tamkun MM. Localization and mobility of the delayed-rectifer K+ channel Kv2.1 in adult cardiomyocytes. *Am J Physiol Heart Circ Physiol* 2008; **294**: H229-H237 [PMID: 17965280 DOI: 10.1152/ajpheart.01038.2007]

29 **Hund TJ**, Snyder JS, Wu X, Glynn P, Koval OM, Onal B, Leymaster ND, Unudurthi SD, Curran J, Camardo C, Wright PJ, Binkley PF, Anderson ME, Mohler PJ. β(IV)-Spectrin regulates TREK-1 membrane targeting in the heart. *Cardiovasc Res* 2014; **102**: 166-175 [PMID: 24445605 DOI: 10.1093/cvr/cvu008]

30 **Fülöp L**, Szigeti G, Magyar J, Szentandrássy N, Ivanics T, Miklós Z, Ligeti L, Kovács A, Szénási G, Csernoch L, Nánási PP, Bányász T. Differences in electrophysiological and contractile properties of mammalian cardiac tissues bathed in bicarbonate - and HEPES-buffered solutions. *Acta Physiol Scand* 2003; **178**: 11-18 [PMID: 12713510 DOI: 10.1046/j.1365-201X.2003.01114.x]

31 **Prasad V**, Lorenz JN, Miller ML, Vairamani K, Nieman ML, Wang Y, Shull GE. Loss of NHE1 activity leads to reduced oxidative stress in heart and mitigates high-fat diet-induced myocardial stress. *J Mol Cell Cardiol* 2013; **65**: 33-42 [PMID: 24080184 DOI: 10.1016/j.yjmcc.2013.09.013]

32 **Ruminot I**, Gutiérrez R, Peña-Münzenmayer G, Añazco C, Sotelo-Hitschfeld T, Lerchundi R, Niemeyer MI, Shull GE, Barros LF. NBCe1 mediates the acute stimulation of astrocytic glycolysis by extracellular K+. *J Neurosci* 2011; **31**: 14264-14271 [PMID: 21976511 DOI: 10.1523/JNEUROSCI.2310-11.2011]

33 **Sowah D**, Brown BF, Quon A, Alvarez BV, Casey JR. Resistance to cardiomyocyte hypertrophy in ae3-/- mice, deficient in the AE3

Cl-/HCO3- exchanger. *BMC Cardiovasc Disord* 2014; **14**: 89 [PMID: 25047106 DOI: 10.1186/1471-2261-14-89]

34 **Thorsen K**, Dam VS, Kjaer-Sorensen K, Pedersen LN, Skeberdis VA, Jurevičius J, Treinys R, Petersen IMBS, Nielsen MS, Oxvig C, Morth JP, Matchkov VV, Aalkjær C, Bundgaard H, Jensen HK. Loss-of-activity-mutation in the cardiac chloride-bicarbonate exchanger AE3 causes short QT syndrome. *Nat Commun* 2017; **8**: 1696 [PMID: 29167417 DOI: 10.1038/s41467-017-01630-0]

35 **Prasad V**, Lorenz JN, Lasko VM, Nieman ML, Al Moamen NJ, Shull GE. Loss of the AE3 Cl(-)/HCO(-) 3 exchanger in mice affects rate-dependent inotropy and stress-related AKT signaling in heart. *Front Physiol* 2013; **4**: 399 [PMID: 24427143 DOI: 10.3389/fphys.2013.00399]

36 **Prasad V**, Bodi I, Meyer JW, Wang Y, Ashraf M, Engle SJ, Doetschman T, Sisco K, Nieman ML, Miller ML, Lorenz JN, Shull GE. Impaired cardiac contractility in mice lacking both the AE3 Cl-/HCO3- exchanger and the NKCC1 Na+-K+-2Cl- cotransporter: effects on Ca2+ handling and protein phosphatases. *J Biol Chem* 2008; **283**: 31303-31314 [PMID: 18779325 DOI: 10.1074/jbc.M803706200]

37 **Schmitt N**, Grunnet M, Olesen SP. Cardiac potassium channel subtypes: new roles in repolarization and arrhythmia. *Physiol Rev* 2014; **94**: 609-653 [PMID: 24692356 DOI: 10.1152/physrev.00022.2013]

38 **Aiello EA**, De Giusti VC. Regulation of the cardiac sodium/bicarbonate cotransporter by angiotensin II: potential Contribution to structural, ionic and electrophysiological myocardial remodelling. *Curr Cardiol Rev* 2013; **9**: 24-32 [PMID: 23116057 DOI: 10.2174/157340313805076340]

39 **Unudurthi SD**, Wu X, Qian L, Amari F, Onal B, Li N, Makara MA, Smith SA, Snyder J, Fedorov VV, Coppola V, Anderson ME, Mohler PJ, Hund TJ. Two-Pore K+ Channel TREK-1 Regulates Sinoatrial Node Membrane Excitability. *J Am Heart Assoc* 2016; **5**: e002865 [PMID: 27098968 DOI: 10.1161/JAHA.115.002865]

40 **Vaughan-Jones RD**, Villafuerte FC, Swietach P, Yamamoto T, Rossini A, Spitzer KW. pH-Regulated Na(+) influx into the mammalian ventricular myocyte: the relative role of Na(+)-H(+) exchange and Na(+)-HCO Co-transport. *J Cardiovasc Electrophysiol* 2006; **17** Suppl 1: S134-S140 [PMID: 16686668 DOI: 10.1111/j.1540-8167.2006.00394.x]

41 **Gottlieb RA**, Burleson KO, Kloner RA, Babior BM, Engler RL. Reperfusion injury induces apoptosis in rabbit cardiomyocytes. *J Clin Invest* 1994; **94**: 1621-1628 [PMID: 7929838 DOI: 10.1172/JCI117504]

42 **Takashi E**, Ashraf M. Pathologic assessment of myocardial cell necrosis and apoptosis after ischemia and reperfusion with molecular and morphological markers. *J Mol Cell Cardiol* 2000; **32**: 209-224 [PMID: 10722798 DOI: 10.1006/jmcc.1999.1067]

43 **Freude B**, Masters TN, Robicsek F, Fokin A, Kostin S, Zimmermann R, Ullmann C, Lorenz-Meyer S, Schaper J. Apoptosis is initiated by myocardial ischemia and executed during reperfusion. *J Mol Cell Cardiol* 2000; **32**: 197-208 [PMID: 10722797 DOI: 10.1006/jmcc.1999.1066]

44 **Halestrap AP**, Clarke SJ, Javadov SA. Mitochondrial permeability transition pore opening during myocardial reperfusion--a target for cardioprotection. *Cardiovasc Res* 2004; **61**: 372-385 [PMID: 14962470 DOI: 10.1016/S0008-6363(03)00533-9]

45 **Prasad V**, Chirra S, Kohli R, Shull GE. NHE1 deficiency in liver: implications for non-alcoholic fatty liver disease. *Biochem Biophys Res Commun* 2014; **450**: 1027-1031 [PMID: 24976401 DOI: 10.1016/j.bbrc.2014.06.095]

46 **Li N**, Jiang P, Du W, Wu Z, Li C, Qiao M, Yang X, Wu M. Siva1 suppresses epithelial-mesenchymal transition and metastasis of tumor cells by inhibiting stathmin and stabilizing microtubules. *Proc Natl Acad Sci USA* 2011; **108**: 12851-12856 [PMID: 21768358 DOI: 10.1073/pnas.1017372108]

47 **Ma Y**, Liu T, Song X, Tian Y, Wei Y, Wang J, Li X, Yang X. Siva 1 inhibits proliferation, migration and invasion by phosphorylating Stathmin in ovarian cancer cells. *Oncol Lett* 2017; **14**: 1512-1518 [PMID: 28789373 DOI: 10.3892/ol.2017.6307]

48 **Kang TH**, Noh KH, Kim JH, Bae HC, Lin KY, Monie A, Pai SI, Hung CF, Wu TC, Kim TW. Ectopic expression of X-linked lymphocyte-regulated protein pM1 renders tumor cells resistant to antitumor immunity. *Cancer Res* 2010; **70**: 3062-3070 [PMID: 20395201 DOI: 10.1158/0008-5472.CAN-09-3856]

49 **Pugach EK**, Richmond PA, Azofeifa JG, Dowell RD, Leinwand LA. Prolonged Cre expression driven by the α-myosin heavy chain promoter can be cardiotoxic. *J Mol Cell Cardiol* 2015; **86**: 54-61 [PMID: 26141530 DOI: 10.1016/j.yjmcc.2015.06.019]

P- Reviewer: Anan R, Montecucco F, Salvadori M, Ueda H
S- Editor: Ji FF **L- Editor**: Filipodia **E- Editor**: Wu YXJ

World Journal of Cardiology

Submit a Manuscript: http://www.f6publishing.com

World J Cardiol 2018 September 26; 10(9): 110-118

DOI: 10.4330/wjc.v10.i9.110

ISSN 1949-8462 (online)

ORIGINAL ARTICLE

Clinical Trials Study

Accuracy of myocardial viability imaging by cardiac MRI and PET depending on left ventricular function

Peter Hunold, Heinz Jakob, Raimund Erbel, Jörg Barkhausen, Christina Heilmaier

Peter Hunold, Jörg Barkhausen, Clinic for Radiology and Nuclear Medicine, University Hospital Schleswig-Holstein, Campus Lübeck, Lübeck 23538, Germany

Heinz Jakob, Department of Thoracic and Cardiovascular Surgery, West German Heart Center, University of Duisburg-Essen, University Hospital Essen, Essen 45122, Germany

Raimund Erbel, Department of Cardiology, West German Heart Center, University of Duisburg-Essen, University Hospital Essen, Essen 45122, Germany

Christina Heilmaier, Department of Radiology and Nuclear Medicine, Stadtspital Triemli, Zürich 8063, Switzerland

ORCID number: Peter Hunold (0000-0003-4416-5934); Heinz Jakob (0000-0002-4743-5066); Raimund Erbel (0000-0001-9884-0785); Jörg Barkhausen (0000-0001-8937-1198); Christina Heilmaier (0000-0002-9595-9999).

Author contributions: Hunold P and Heilmaier C designed research; Hunold P, Heilmaier C, Barkhausen J, Erbel R and Jakob H acquired data; Hunold P, Heilmaier C and Barkhausen J analyzed data; Heilmaier C and Hunold P wrote the paper; Barkhausen J, Erbel R and Jakob H revised and approved final manuscript version

Institutional review board statement: This study was reviewed and approved by the Institutional review board of the Medical Faculty of the University Essen, Germany (No. 00-142-1497).

Clinical trial registration statement: N/A.

Informed consent statement: All patients gave written informed consent to participate in the study prior to study inclusion and agreed to the evaluation and publication of their anonymized data.

Conflict-of-interest statement: None of the authors states a conflict of interest concerning firms and products reported in this study.

Manuscript source: Invited manuscript

Correspondence to: Peter Hunold, MD, Assistant Professor, Vice Chairman, Clinic for Radiology and Nuclear Medicine, University Hospital Schleswig-Holstein, Campus Lübeck, Ratzeburger Allee 160, Lübeck 23538, Germany. peterhunold@icloud.com
Telephone: +49-451-50017010
Fax: +49-451-50017004

Received: March 29, 2018
Peer-review started: March 29, 2018
First decision: April 23, 2018
Revised: June 28, 2018
Accepted: August 5, 2018
Article in press: August 5, 2018
Published online: September 26, 2018

Abstract

AIM

To compare myocardial viability assessment accuracy of cardiac magnetic resonance imaging (CMR) compared to [^{18}F]-fluorodeoxyglucose (FDG)- positron emission tomography (PET) depending on left ventricular (LV) function.

METHODS

One-hundred-five patients with known obstructive coronary artery disease (CAD) and anticipated coronary revascularization were included in the study and examined by CMR on a 1.5T scanner. The CMR protocol consisted of cine-sequences for function analysis and late gadolinium enhancement (LGE) imaging for viability

assessment in 8 mm long and contiguous short axis slices. All patients underwent PET using [^{18}F]-FDG. Myocardial scars were rated in both CMR and PET on a segmental basis by a 4-point-scale: Score 1 = no LGE, normal FDG-uptake; score 2 = LGE enhancement < 50% of wall thickness, reduced FDG-uptake (⩾ 50% of maximum); score 3 = LGE ⩾ 50%, reduced FDG-uptake (< 50% of maximum); score 4 = transmural LGE, no FDG-uptake. Segments with score 1 and 2 were categorized "viable", scores 3 and 4 were categorized as "non-viable". Patients were divided into three groups based on LV function as determined by CMR: Ejection fraction (EF), < 30%: *n* = 45; EF: 30%-50%: *n* = 44; EF > 50%: *n* = 16). On a segmental basis, the accuracy of CMR in detecting myocardial scar was compared to PET in the total collective and in the three different patient groups.

RESULTS

CMR and PET data of all 105 patients were sufficient for evaluation and 5508 segments were compared in total. In all patients, CMR detected significantly more scars (score 2-4) than PET: 45% *vs* 40% of all segments (P < 0.0001). In the different LV function groups, CMR found more scar segments than PET in subjects with EF< 30% (55% *vs* 46%; P < 0.0001) and EF 30%-50% (44% *vs* 40%; P < 0.005). However, CMR revealed less scars than PET in patients with EF > 50% (15% *vs* 23%; P < 0.0001). In terms of functional improvement estimation, *i.e.*, expected improvement after revascularization, CMR identified "viable" segments (score 1 and 2) in 72% of segments across all groups, PET in 80% (P < 0.0001). Also in all LV function subgroups, CMR judged less segments viable than PET: EF < 30%, 66% *vs* 75%; EF = 30%-50%, 72% *vs* 80%; EF > 50%, 91% *vs* 94%.

CONCLUSION

CMR and PET reveal different diagnostic accuracy in myocardial viability assessment depending on LV function state. CMR, in general, is less optimistic in functional recovery prediction.

Key words: Magnetic resonance imaging; Positron-emission tomography; Myocardial infarction; Coronary artery disease; Myocardium; Ventricular dysfunction

Core tip: Both cardiac magnetic resonance imaging (CMR) and [^{18}F]-fluorodeoxyglucose-positron emission tomography (PET) are considered standard methods and reliable in myocardial viability imaging in coronary artery disease. However, CMR in general detects more scar and is, therefore, less optimistic in functional recovery prediction. Moreover, CMR and PET reveal different diagnostic accuracy depending on left ventricular (LV) function state: Particularly in severe and moderate LV function impairment, where revascularization is performed to improve function, CMR detects more scar and less viable myocardium - most probably due to higher spatial resolution. This aspect has not been reported, yet. Irrespective of LV function, PET might overestimate the improvement of regional and global function after revascularization.

Hunold P, Jakob H, Erbel R, Barkhausen J, Heilmaier C. Accuracy of myocardial viability imaging by cardiac MRI and PET depending on left ventricular function. *World J Cardiol* 2018; 10(9): 110-118 Available from: URL: http://www.wjgnet.com/1949-8462/full/v10/i9/110.htm DOI: http://dx.doi.org/10.4330/wjc.v10.i9.110

INTRODUCTION

Left ventricular (LV) dysfunction due to myocardial ischemia is one of the most common manifestations in chronic coronary artery disease (CAD), but does not necessarily represent non-viable, irreversibly injured tissue[1-4]. Although large multicenter studies such as the positron-emission-tomography (PET) and recovery following revascularization PARR-2 trial[5,6] or the surgical treatment for ischemic heart failure STICH-trial have been performed, even today there is no general consensus as to when assigning patients to either optimized medical treatment alone or to a combination of medical treatment plus revascularization procedures [(percutaneous coronary intervention or coronary artery bypass graft (CABG) surgery)][7-12]. Arriving at the optimal management strategy for these patients is a complex multifactorial process that includes not only viability but also processes such as ischemia and remodeling[4,7, 8,13-15].

Currently, several imaging modalities are used for the evaluation of myocardial viability, each of them assessing different myocardial features: *e.g.*, low-dose dobutamine stress echocardiography (DSE), nuclear techniques such as PET or single-photon-emission-computed-tomography (SPECT) as well as cardiac magnetic resonance imaging (CMR). Traditionally, nuclear techniques were regarded as gold standard for viability testing owing to their high sensitivity and negative predictive value (NPV) [*e.g.*, fluorodeoxyglucose (FDG)-PET 92% and 87%, respectively][7,12,16,17]. For this purpose mainly three tracers are used evaluating cell membrane integrity, perfusion and intact mitochondria ([^{201}Tl] thallium- or [^{99m}Tc] technetium-SPECT)[18] or maintained metabolism ([^{18}F] FDG-PET)[2].

With recent advances of the hard and software, especially the introduction of non-breath-hold sequences and arrhythmia rejection protocols[19,20], CMR has become a versatile alternative to nuclear imaging, coming along with an excellent spatial resolution[17]. While late gadolinium enhancement (LGE) allows visualization of the transmural extent of the scar by achieving signal intensity differences of nearly 500% between irreversibly injured and viable myocardium[14,18,21],

dobutamine stress CMR analyzes contractile reserve of dysfunctional myocardium similar to DSE[2,7]. Although the low specificity of LGE-CMR is well known, which is mainly attributable to the variable functional recovery in segments with LGE covering 25%-75% of the wall[1,14,22], its general high diagnostic accuracy for detecting myocardial scars has been proven in different studies[2,7,14,22-25]. However, so far, the value of CMR and PET has not been defined considering different LV function states. The aim of this study therefore was to evaluate the diagnostic accuracy of LGE-CMR viability assessment and PET and to compare them in patient groups with different LV functions.

MATERIALS AND METHODS

Study population

The local institutional review board (Ethics Committee of the Medical Faculty, University Essen) approved the study protocol and informed written consent has been given by all participants.

Within 30 mo, 105 patients (87 men, 18 women; mean age, 61 ± 11 years) with known obstructive CAD as proven by catheter coronary angiography and indication for CABG surgery were enrolled in the study. All of them underwent nuclear myocardial viability testing for clinical indication. After completion of the nuclear imaging contrast-enhanced CMR was performed; all imaging examinations took place within 6 ± 4 d before scheduled CABG surgery.

CMR: Study protocol

CMR scans were performed on a 1.5T scanner (Magnetom Sonata, Siemens Medical Solutions, Erlangen, Germany). Patients were examined in supine position. The spine array coil (two elements) and a body flex phased array coil (two elements) were combined for signal reception.

The CMR protocol consisted of a LV functional study by an electrocardiography (ECG)-triggered breath-hold segmented steady-state free precession (SSFP) cine sequence [repetition time (TR)/echo time (TE), 3.0/1.5 ms; flip angle, 60°; bandwidth, 975 Hertz per pixel]. Slice thickness was 8 mm. At first, three standard long axis views were acquired (four-chamber view, two-chamber view, LV three-chamber view); thereafter, the entire LV was covered by contiguous short axis slices without interslice gap. LGE images were acquired after administration of 0.2 mmol/kg bw Gadolinium-DTPA (Magnevist™, Bayer AG, Leverkusen, Germany) at a flow rate of 2 mL/s. Again, three long and all short axis slices were scanned utilizing an established ECG-triggered segmented 2D inversion-recovery gradient-recalled echo sequence (TR/TE, 8/4 ms; flip angle, 25°) during breath-hold[21]. LGE images were acquired 8 to 15 min after contrast media injection. To null the signal of normal myocardium the inversion time (TI, non-selective inversion pulse) had to be manually adjusted between 200 and 260 ms. The rectangular field-of-view (FOV) provided an in-plane resolution of 1.6 × 1.3 mm^2 for all sequences.

CMR: Image analysis

Two experienced radiologists, who were blinded to nuclear study results, analyzed all CMR data in a consensus reading. SSFP images were reviewed as cine-loops on an interactive workstation. LV volumetry was done using the ARGUS™ software (Siemens Medical Systems, Erlangen, Germany) by manual drawing of the endocardial contours on all short axes in end-diastolic and end-systolic phase including the papillary muscles to the LV lumen[26]. End-diastolic volumes (EDV) and end-systolic volumes (ESV) were measured by slice summation; ejection fraction (EF) was calculated using the equation: EF = (EDV - ESV)/EDV.

For quantification of myocardial viability, all short axis images were segmented using a 6-segment model. The LGE extent was assessed and quantified in each short axis segment by the 4-point scoring system given in Table 1. As recommended in the guidelines, a cutoff value of 50%-transmurality was set to discriminate myocardium with a chance to functionally recover after revascularization ("viable", score 1 and 2) from myocardium without beneficial functional prognosis ("non-viable", score 3 and 4)[15,27] .

Nuclear studies: Imaging protocol

The PET study was done under fasting conditions (at least 4 h) and after oral administration of two doses of acipimox 500 mg (Olbemox™, Pharmacia, Erlangen, Germany) and 75 g of glucose. Imaging was performed using a high-resolution PET camera (Siemens ECAT HR+, Erlangen, Germany). Forty minutes after intravenous application of [^{18}F]-FDG (370 MBq) PET data was acquired in a 2-dimensional fashion: (1) transmission scan (duration, 10 min) 60 min after injection; (2) emission scan (duration, 30 min). After attenuation and scatter correction the emission data was reconstructed in an iterative fashion (OSEM algorithm, 2 iterations, 32 subsets, Gauss filter FWHM 6 mm). Furthermore, the 2-dimensional data stack was reformatted into a 3-dimensional volume to create 8 mm long and short axis slices corresponding to the acquired MR data.

Nuclear studies: Image analysis

As with CMR data, myocardial FDG-uptake was evaluated using the same 4-point scale (Table 1) for each myocardial segment. Preserved or increased glucose utilization and subsequent FDG-uptake indicated cell survival, while reduced FDG-uptake defined myocardial scar.

Comparison and statistical analysis

For statistical analyses SPSS Statistics software (version 22, IBM Corp., Amonk, NY, United States) was

Table 1 Scoring system for evaluation of myocardial viability in cardiac magnetic resonance imaging and positron emission tomography

Score	CMR	PET
1	No enhancement	Normal FDG uptake
2	Enhancement < 50% of wall thickness	Reduced FDG uptake, ⩾ 50% of maximum
3	Enhancement ⩾ 50% of wall thickness	Reduced FDG uptake, < 50% of maximum
4	Transmural enhancement	No FDG uptake

Based on the data by Kim *et al*[22], score 1 and 2 represent viable myocardium, while score 3 and 4 are regarded as non-viable tissue ("scar") in view of expected functional improvement after revascularization. Per definition, reduced or completely missing viability encompassed decreased or no FDG-uptake. CMR: Cardiac magnetic resonance imaging; PET: Positron emission tomography; FDG: Fluorodeoxyglucose.

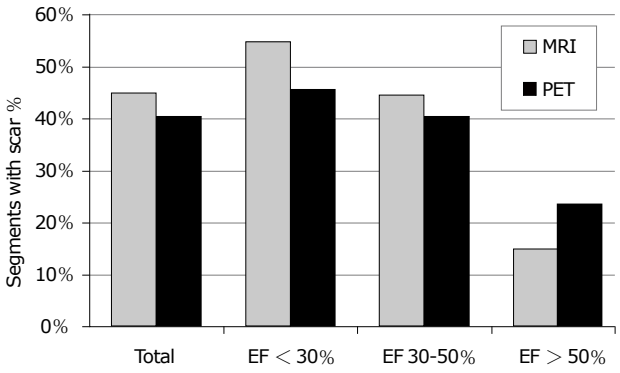

Figure 1 Histogram showing the frequency of scar detection in cardiac magnetic resonance imaging (grey bars) and positron emission tomography (black bars). In total, cardiac magnetic resonance imaging (CMR) found scars in 45% of all segments compared to PET in 40%. CMR depicted significantly more scars in patients with severely (EF < 30%) and moderately (EF, 30%-50%) impaired left ventricular function. However, PET suggested more scars in EF > 50% group. PET: Positron emission tomography; EF: Ejection fraction.

used. Statistical significance was assumed with $P < 0.05$. Moreover, Bonferroni correction was performed, yielding an adapted level of significance of $P = 0.008$.

At first, 3 different patient groups were composed based on the global LV function as assessed by CMR: (1) severely impaired LV function (EF < 30%); (2) moderately decreased LV function (EF 30%-50%); and (3) non-compromised LV function (EF > 50%). After that, CMR viability scores were compared segment-based to PET scores in two ways: first, normal segments (score 1) and segments with any kind of scar (score 2-4) were analyzed. Secondly, according to data published by Kim *et al*[22], evaluation of segments with no or little scar (scores 1 and 2, "viable"), which are expected to improve after revascularization, were compared to segments with score 3 and 4 ("non-viable"). In each case, sensitivity, specificity, positive predictive value (PPV), NPV, and accuracy were evaluated in contingency tables for CMR as test variable compared to PET. Diagnostic accuracy of CMR and PET were compared for the three LV function groups separately. Parametric data is expressed as mean ± SD. Two-tailed Fisher's exact test was applied to compare frequencies of scar detection (scores 2-4) and functional recovery estimation (scores 1 and 2) between CMR and PET. Cohen's Kappa was calculated for the agreement of CMR and PET in detecting scar and functional recovery estimation.

RESULTS

All patients successfully finished the study protocol, therefore complete data sets of 105 subjects underwent analysis. Depending on the long axis diameter, the LV was covered in CMR by 8 to 14 short axis slices. The 3D PET data set was then separated accordingly into the same number of slices yielding a total of 5508 segments. Mean CMR volumetric measures were: EDV, 198 ± 69 mL (range, 63-386 mL) and ESV, 137 ± 66 mL (range, 24-316 mL), resulting in a mean EF of 34% ± 14% (range, 9%-78%). Forty-five patients had an EF < 30%, 44 patients 30%-50%, and 16 patients > 50%.

Scar assessment by CMR and PET depending on LV function

As demonstrated by Figure 1, CMR detected myocardial scars (score 2-4) in 45% of all segments, while PET depicted scars in 40% of all segments ($P < 0.0001$). Inter-observer agreement (Cohen's Kappa) between CMR and PET in scar detection was 0.39 (fair to moderate). Analysis of the different patient groups revealed that CMR found more scars than PET in subjects with EF < 30% (55% *vs* 46%; $P < 0.0001$) and EF 30%-50% (44% *vs* 40%; $P < 0.005$). However, CMR revealed less scars than PET in patients with EF > 50% (15% *vs* 23%; $P < 0.0001$). Statistical values (sensitivity, specificity, PPV, NPV, and accuracy) within the 3 different patient groups are summarized in Table 2. Viable segments which can be expected to improve after revascularization (score 1 and 2) were detected by CMR in 72% (3949/5508) compared to non-viable segments (score 3 and 4) in 28% (1559/5508). For PET, viability of segments was declared in 80% (4396/5508) and non-viability in 20% (1112/5508). CMR and PET significantly differed in depicting viable and non-viable segments ($P < 0.0001$). Inter-observer agreement (Cohen's Kappa) between CMR and PET in functional recovery estimation was 0.48 (moderate). Analysis of the different patient groups Analysis of the different subgroups revealed that CMR judged segments as

Table 2 Myocardial scar detection by cardiac magnetic resonance imaging (contingency table)

	Sensitivity	Specificity	PPV	NPV	Accuracy
All patients	69%	71%	62%	77%	70%
EF< 30%	79%	66%	66%	79%	72%
EF 30%-50%	64%	69%	58%	74%	67%
EF > 50%	25%	89%	41%	79%	74%

Detection of myocardial scar (score 2-4) by cardiac magnetic resonance imaging (CMR) as test parameter compared to positron emission tomography (PET). Analysis was done for the whole patient collective as well as in the three patient subgroups with different ejection fraction (EF). In patients with moderately or severely compromised EF CMR outperformed PET. NPV: Negative predictive value; PPV: Positive predictive value.

Table 3 Functional recovery as detected by cardiac magnetic resonance imaging shown as contingency table

	Sensitivity	Specificity	PPV	NPV	Accuracy
All patients	72%	83%	51%	92%	81%
EF < 30%	74%	79%	55%	90%	78%
EF 30%-50%	73%	82%	50%	93%	81%
EF > 50%	30%	92%	19%	95%	89%

The contingency table shows the detection of tissue with potential functional recovery (score 1 and 2) by cardiac magnetic resonance imaging (CMR) as test variable compared to positron emission tomography (PET). Calculation was performed for the whole patient collective as well as separately for the three patient subgroups with different EF. Except for patients with not compromised left ventricular function sensitivity, specificity, PPV, NPV and accuracy were higher in CMR. EF: Ejection fraction; NPV: Negative predictive value; PPV: Positive predictive value.

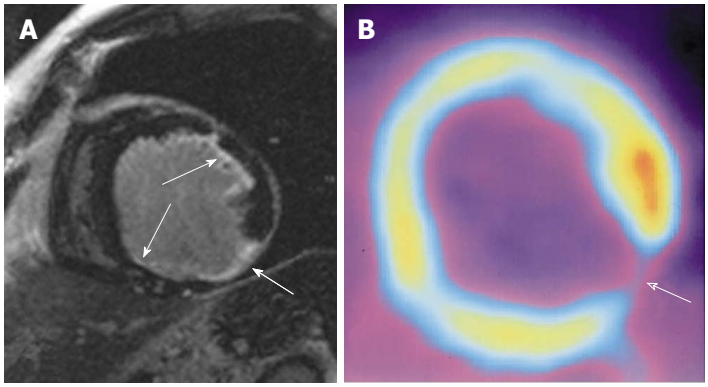

Figure 2 A sixty-seven-year-old man with severe coronary artery disease and history of myocardial infarction. A: Short axis inversion-recovery gradient-recalled echo cardiac magnetic resonance imaging (CMR) image of the mid- to apical-portion of the left ventricular shows a small area of transmural late gadolinium enhancement (LGE) in the inferolateral wall (broad arrow). CMR viability scores: Anterior: 2; anterolateral: 2; inferolateral: 4, inferior: 2; B: The positron emission tomography (PET) image of the corresponding slice reveals an uptake defect (broad arrow) in the same segment suggesting a transmural scar. PET viability scores: anterior: 2; inferolateral: 4. Small subendocardial scars with LGE in CMR (A) in the anterolateral and inferior wall (small arrows) were overseen in PET.

viable in 66% in patients with severely compromised LV function, in 72% in subjects with moderately reduced LV function and in 91% in patients with non-compromised LV function. For PET, these values were 75%, 80%, and 94% respectively. Comparison of CMR and PET showed that CMR declared significantly less segments as viable than PET in patients with severely or moderately reduced LV function (for all, $P < 0.0001$). In patients with uncompromised LV function no statistical significance was evident between both modalities after Bonferroni correction ($P = 0.03$).

Table 3 provides statistical values for CMR in the estimation of functional recovery (MRI score 1 and 2) compared to PET. Comparison of Tables 2 and 3 reveals that overall performance of CMR was better in Table 3, when small scars (< 50% transmurality) were excluded. Figure 2 gives an example of a transmural scar detected both by CMR and PET as well as of small subendocardial scars that were found by CMR but overseen in PET. Figure 3 shows diagrams of the volumetric measures in relation to the total extent of scar (mean scar score).

DISCUSSION

Results from myocardial viability testing play an important role in clinical decision making especially in patients with impaired myocardial function, who might require invasive treatment. Albeit several studies reported on patients who benefited from restoration of blood flow despite pre-interventional proof of non-viable tissue and without post-operative functional

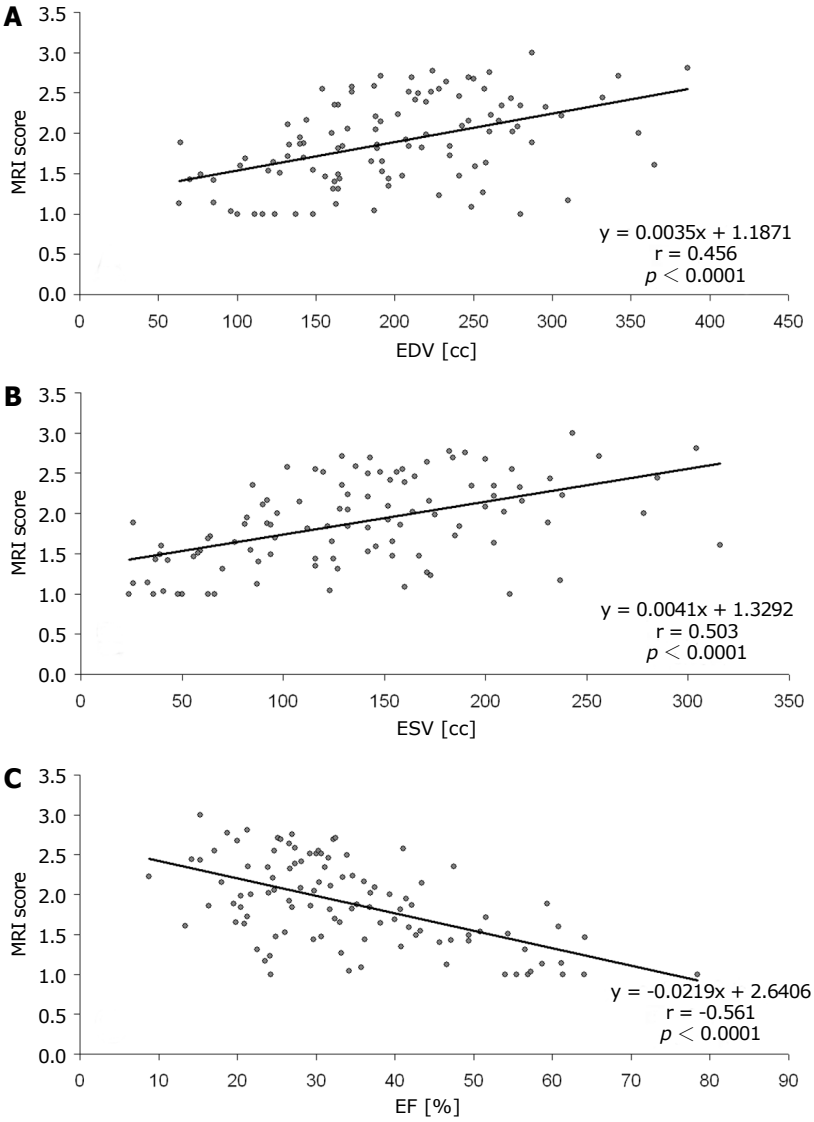

Figure 3 Correlation of left ventricular volumes and function to the MRI-derived extent of myocardial scar (summarized as mean magnetic resonance imaging score per patient). A: End-diastolic volumes (EDV); B: End-systolic volumes (ESV); C: Ejection fraction (EF).

recovery consequently[11,28,29], general consensus exists that information on the transmural extent of myocardial scar is of importance because it holds a close relationship with recovery of segmental function at follow-up[3]. We, therefore, sought to evaluate the diagnostic accuracy of LGE-CMR viability assessment and PET in patient groups with different LV functions. The main findings were: (1) in subjects with severely or moderately reduced LV function, CMR detects considerably more myocardial scars than PET; (2) scars, which are only seen in PET in patients with non-compromised LV function are probably false-positive results or artifacts; and (3) in patients with impaired LV function (EF < 50%), CMR demonstrates more non-viable myocardium compared to PET and is generally less optimistic concerning functional recovery after revascularization procedures.

Within the last decade CMR has more and more replaced nuclear imaging techniques in myocardial viability assessment. In particular, CMR seems to be useful in identifying patients, who most likely will not benefit from coronary revascularization[11]. Kühl *et al*[11] demonstrated that none of the segments which were classified as viable by PET/SPECT and nonviable by CMR showed functional recovery 6 mo after revascularization procedures, while 42% of segments described as viable by CMR and non-viable by PET/SPECT still improved[7].

To our knowledge, the present study is the first to compare CMR and PET differentiated in groups depending on LVEF. In patients with severely or moderately reduced LVEF, our study revealed a high sensitivity, specificity and NPV, indicating that CMR is good in detecting myocardial scars. Especially, the high NPV is of great importance in decision-making: if CMR indicates non-viable tissue, low likelihood for functional improvement after revascularization would be expected,

which might prevent patients from unnecessary invasive procedures and potential peri-interventional risks. Moreover, CMR demonstrated considerably more nonviable myocardial tissue than PET with better sensitivity, PPV, NPV and accuracy (excluding small scars with < 50% transmural extent, score 2; Tables 2 and 3). One reason for that most probably is the significantly higher spatial resolution of CMR compared to PET, which is of benefit in finding subendocardial scars and in analyzing the thinned myocardial walls in subjects with severely reduced LVEF. Another explanation might be related to the fact that FDG-uptake represents viability, so that small amounts of viable cells lead to visible FDG-uptake indicating viability[11,29,30], although structural changes may already be present (*e.g*., expansion of extracellular spaces), leading to altered gadolinium kinetics. In addition to that, PET evaluates myocardial viability semiquantitatively: FDG-uptake in a given segment is expressed relative to the segment with maximum FDG-uptake. As a consequence, in thinned myocardium already small rims of reduced FDG-uptake may decrease relative percentage of FDG-uptake to below the threshold value set for viability, albeit viable tissue exists[11], resulting in false-negative evaluation of myocardial viability.

PET detected more scars in subjects with noncompromised LVEF (> 50%), similar to what Klein *et al*[30] described in their study. These surplus segments seen in PET only are most likely false-positive results or artifacts: As LVEF is only marginally or not impaired, only small amounts of non-viable subendocardial tissue are expected. Larger scars would have had more impact on myocardial function. However, a considerable number of non-viable cells is needed for detectable reduction of the relative FDG-uptake below the threshold-value considered for viability, which seems less probable in small scars[31-33]. Owing to the lower spatial resolution of PET it appears unlikely that these small scars were depicted by PET with higher sensitivity than by CMR[3,17]. This is further underlined by studies describing that more than half of the small subendocardial scars depicted by CMR cannot be delineated in PET[30]. Moreover, a minimum of 2 g irreversibly injured myocardium can be detected by LGE-CMR compared to a minimum tissue of 10 g required in PET[33]. Because of that recent studies have denominated LGE-CMR as method of choice for small subendocardial unrecognized myocardial infarction scars[34,35]. Other shortcomings of PET are its radiation exposure, the long examination time and the allocation of appropriate tracers[11]. CMR has evolved as a valuable alternative to PET for evaluation of viable and infarcted myocardium by different techniques (morphology, edema, function, perfusion and scar) in a single examination[2]. Estimated examination time for a complete CMR work-up is 30-60 min. Whether the recently emerging combination of PET and CMR (PET/CMR-hybrid) might be an alternative to CMR alone in assessment of myocardial viability will be the task of future studies[36,37].

We are aware of the following limitations of our study: First, the possibility of anatomical misalignment between different imaging modalities cannot be excluded. Within the last years, hybrid PET/CT-systems had increasingly replaced single PET-scanners. However, as published in a review by Anagnostopoulos *et al*[38] the impact of PET/CT-imaging on clinical outcomes in patients suffering from CAD is still unclear. They therefore recommended that until further studies are performed anatomical or functional imaging should be done sequentially by cardiac CT or PET depending on the pre-test probability of CAD[38]. In patients with higher probability PET should be the first line modality as its ability to guide patient management decisions regarding revascularization or medical treatment has been shown[39]. Therefore, we think that our results can be regarded representative, even though we are aware of the limitations of comparing semi-quantitative assessment of radiotracer uptake in PET as comparator for evaluating LGE-CMR. Furthermore, we defined myocardial scar as area with decreased FDG-uptake, even though reduced FDG-uptake might also be caused by stunned myocardium. The most appropriate approach would have been to perform both a functional and perfusion scan, in which stunned myocardium would have been detected as area with reduced FDP-uptake but normal perfusion (perfusion-metabolism reverse mismatch)[33]. However, for the given clinical indication in our patients the functional scan was sufficient and therefore no perfusion data was available. Another technical limitation might be that we did not use a glucose-insulin clamp to standardize the glucose metabolism within the whole myocardium. Like others[36,37], in our institution PET imaging is done under fasting condition and oral administration of two doses of acipimox and 75 g glucose prior to FDG application. Therefore, we believe the number of false-negative segments to be negligible. However, the lack of clinical approval of acipimox in the United States hampers representativeness of our data abroad. Moreover, no correction technique was applied for PET. And finally, a detailed segment-to-segment attenuation comparison was only partly done in our study, but would have been of interest to get deeper information on exact differences between PET and CMR regarding scar detection, *e.g.*, considering the location of scar keeping in mind that the exact delineation of the inferior LV segments is often impaired in PET[30,40]. This has to be investigated by further studies.

In conclusion, our study demonstrates differences in diagnostic accuracy of CMR and PET differentiating between patient groups according to LV ejection fraction. Advantages of CMR compared to PET were found in detecting scars and non-viable tissue in subjects with severely or moderately reduced LVEF. CMR is generally less optimistic concerning functional recovery after revascularization procedures, which is of

great importance in clinical decision-making.

ARTICLE HIGHLIGHTS

Research background

Cardiac magnetic resonance imaging (CMR) and positron emission tomography (PET) have been established for myocardial viability imaging in coronary artery disease (CAD). However, differences in accuracy have been reported. It has been shown that CMR provides higher sensitivity in detecting small scars due to the significantly higher spatial resolution. So far, no data are available on differences in diagnostic accuracy depending on left ventricular (LV) function although it might be suggested that LV volumes and wall thickness, for example, might have an impact on the sensitivity.

Research motivation

The above mentioned missing data have been collected in our large study and have now been made available. This study might help to better understand the advantages and disadvantages of the two different methods.

Research objectives

The primary objective of this research was to compare contrast-enhanced CMR and fluorodeoxyglucose-PET for the evaluation of myocardial viability in known CAD under different LV function conditions.

Research methods

One-hundred-five CAD patients were examined by CMR and PET. Myocardial scars were rated in both CMR and PET on a segmental basis in each 8 mm thick short axis slice concerning presence and extent of myocardial scar after myocardial infarction. For each of the evaluated 5518 segments, direct comparison was performed and three patient groups with different LV function were analyzed. In particular two aspects, diagnostic accuracy has been evaluated: (1) scar detection; and (2) functional improvement estimation by the two methods.

Research results

As expected, CMR has a higher sensitivity for scar detection and, therefore, is less optimistic than PET in the prediction of functional recovery after revascularization. In the different LV function groups, CMR found more scar segments than PET in subjects with EF < 30% and EF 30%-50% (44% *vs* 40 %; $P < 0.005$), whereas CMR revealed less scars than PET in patients with EF > 50%.

Research conclusions

There are differences in the diagnostic accuracy between both modalities that have not been described, yet. This new knowledge helps to understand the strengths and weaknesses of the two modalities. One should keep in mind that particularly in severely impaired LV function - where viability really matters - CMR is able to detect more scars. In those cases, using CMR instead of PET could prevent unnecessary revascularizations and accompanying complications.

Research perspectives

This study could initiate more research on particular myocardial viability imaging aspects to better sort outpatient conditions that influence the accuracy of available techniques.

REFERENCES

1 **Tomlinson DR**, Becher H, Selvanayagam JB. Assessment of myocardial viability: comparison of echocardiography versus cardiac magnetic resonance imaging in the current era. *Heart Lung Circ* 2008; **17**: 173-185 [PMID: 18222726 DOI: 10.1016/j.hlc.2007.10.005]

2 **Grover S**, Srinivasan G, Selvanayagam JB. Evaluation of myocardial viability with cardiac magnetic resonance imaging. *Prog Cardiovasc Dis* 2011; **54**: 204-214 [PMID: 22014488 DOI: 10.1016/j.pcad.2011.06.004]

3 **Wu YW**, Tadamura E, Kanao S, Yamamuro M, Marui A, Komeda M, Toma M, Kimura T, Togashi K. Myocardial viability by contrast-enhanced cardiovascular magnetic resonance in patients with coronary artery disease: comparison with gated single-photon emission tomography and FDG position emission tomography. *Int J Cardiovasc Imaging* 2007; **23**: 757-765 [PMID: 17364219 DOI: 10.1007/s10554-007-9215-y]

4 **Shabana A**, El-Menyar A. Myocardial viability: what we knew and what is new. *Cardiol Res Pract* 2012; **2012**: 607486 [PMID: 22988540 DOI: 10.1155/2012/607486]

5 **Abraham A**, Nichol G, Williams KA, Guo A, deKemp RA, Garrard L, Davies RA, Duchesne L, Haddad H, Chow B, DaSilva J, Beanlands RS; PARR 2 Investigators. 18F-FDG PET imaging of myocardial viability in an experienced center with access to 18F-FDG and integration with clinical management teams: the Ottawa-FIVE substudy of the PARR 2 trial. *J Nucl Med* 2010; **51**: 567-574 [PMID: 20237039 DOI: 10.2967/jnumed.109.065938]

6 **Beanlands RS**, Nichol G, Huszti E, Humen D, Racine N, Freeman M, Gulenchyn KY, Garrard L, deKemp R, Guo A, Ruddy TD, Benard F, Lamy A, Iwanochko RM; PARR-2 Investigators. F-18-fluorodeoxyglucose positron emission tomography imaging-assisted management of patients with severe left ventricular dysfunction and suspected coronary disease: a randomized, controlled trial (PARR-2). *J Am Coll Cardiol* 2007; **50**: 2002-2012 [PMID: 17996568 DOI: 10.1016/j.jacc.2007.09.006]

7 **Schinkel AF**, Bax JJ, Poldermans D, Elhendy A, Ferrari R, Rahimtoola SH. Hibernating myocardium: diagnosis and patient outcomes. *Curr Probl Cardiol* 2007; **32**: 375-410 [PMID: 17560992 DOI: 10.1016/j.cpcardiol.2007.04.001]

8 **Ling LF**, Marwick TH, Flores DR, Jaber WA, Brunken RC, Cerqueira MD, Hachamovitch R. Identification of therapeutic benefit from revascularization in patients with left ventricular systolic dysfunction: inducible ischemia versus hibernating myocardium. *Circ Cardiovasc Imaging* 2013; **6**: 363-372 [PMID: 23595888 DOI: 10.1161/CIRCIMAGING.112.000138]

9 **Tarakji KG**, Brunken R, McCarthy PM, Al-Chekakie MO, Abdel-Latif A, Pothier CE, Blackstone EH, Lauer MS. Myocardial viability testing and the effect of early intervention in patients with advanced left ventricular systolic dysfunction. *Circulation* 2006; **113**: 230-237 [PMID: 16391157 DOI: 10.1161/CIRCULATIONAHA.105.541664]

10 **Slart RH**, Bax JJ, van Veldhuisen DJ, van der Wall EE, Dierckx RA, de Boer J, Jager PL. Prediction of functional recovery after revascularization in patients with coronary artery disease and left ventricular dysfunction by gated FDG-PET. *J Nucl Cardiol* 2006; **13**: 210-219 [PMID: 16580957 DOI: 10.1007/BF02971245]

11 **Kühl HP**, Lipke CS, Krombach GA, Katoh M, Battenberg TF, Nowak B, Heussen N, Buecker A, Schaefer WM. Assessment of reversible myocardial dysfunction in chronic ischaemic heart disease: comparison of contrast-enhanced cardiovascular magnetic resonance and a combined positron emission tomography-single photon emission computed tomography imaging protocol. *Eur Heart J* 2006; **27**: 846-853 [PMID: 16434414 DOI: 10.1093/eurheartj/ehi747]

12 **Uebleis C**, Hellweger S, Laubender RP, Becker A, Sohn HY, Lehner S, Haug A, Bartenstein P, Cumming P, Van Kriekinge SD, Slomka PJ, Hacker M. The amount of dysfunctional but viable myocardium predicts long-term survival in patients with ischemic cardiomyopathy and left ventricular dysfunction. *Int J Cardiovasc Imaging* 2013; **29**: 1645-1653 [PMID: 23744128 DOI: 10.1007/s10554-013-0254-2]

13 **Schinkel AF**, Valkema R, Geleijnse ML, Sijbrands EJ, Poldermans D. Single-photon emission computed tomography for assessment of myocardial viability. *EuroIntervention* 2010; **6** Suppl G: G115-G122 [PMID: 20542817]

14 **Selvanayagam JB**, Kardos A, Francis JM, Wiesmann F, Petersen SE, Taggart DP, Neubauer S. Value of delayed-enhancement cardiovascular magnetic resonance imaging in predicting myocardial viability after surgical revascularization. *Circulation* 2004; **110**: 1535-1541 [PMID: 15353496 DOI: 10.1161/01.CIR.0000142045.22628.74]

15 **Nagel E**, Schuster A. Myocardial viability: dead or alive is not the question! *JACC Cardiovasc Imaging* 2012; **5**: 509-512 [PMID: 22595158 DOI: 10.1016/j.jcmg.2012.03.005]

16 **Bax JJ**, Poldermans D, Elhendy A, Boersma E, Rahimtoola SH. Sensitivity, specificity, and predictive accuracies of various

noninvasive techniques for detecting hibernating myocardium. *Curr Probl Cardiol* 2001; **26**: 147-186 [PMID: 11276916 DOI: 10.1067/mcd.2001.109973]
17 **Nekolla SG**, Martinez-Moeller A, Saraste A. PET and MRI in cardiac imaging: from validation studies to integrated applications. *Eur J Nucl Med Mol Imaging* 2009; **36** Suppl 1: S121-S130 [PMID: 19104798 DOI: 10.1007/s00259-008-0980-1]
18 **Weinsaft JW**, Klem I, Judd RM. MRI for the assessment of myocardial viability. *Magn Reson Imaging Clin N Am* 2007; **15**: 505-525, v-vi [PMID: 17976589 DOI: 10.1016/j.mric.2007.08.007]
19 **Uecker M**, Zhang S, Voit D, Karaus A, Merboldt KD, Frahm J. Real-time MRI at a resolution of 20 ms. *NMR Biomed* 2010; **23**: 986-994 [PMID: 20799371 DOI: 10.1002/nbm.1585]
20 **Zhang S**, Uecker M, Voit D, Merboldt KD, Frahm J. Real-time cardiovascular magnetic resonance at high temporal resolution: radial FLASH with nonlinear inverse reconstruction. *J Cardiovasc Magn Reson* 2010; **12**: 39 [PMID: 20615228 DOI: 10.1186/1532-429X-12-39]
21 **Simonetti OP**, Kim RJ, Fieno DS, Hillenbrand HB, Wu E, Bundy JM, Finn JP, Judd RM. An improved MR imaging technique for the visualization of myocardial infarction. *Radiology* 2001; **218**: 215-223 [PMID: 11152805 DOI: 10.1148/radiology.218.1.r01ja50215]
22 **Kim RJ**, Wu E, Rafael A, Chen EL, Parker MA, Simonetti O, Klocke FJ, Bonow RO, Judd RM. The use of contrast-enhanced magnetic resonance imaging to identify reversible myocardial dysfunction. *N Engl J Med* 2000; **343**: 1445-1453 [PMID: 11078769 DOI: 10.1056/NEJM200011163432003]
23 **Mahrholdt H**, Klem I, Sechtem U. Cardiovascular MRI for detection of myocardial viability and ischaemia. *Heart* 2007; **93**: 122-129 [PMID: 17170353 DOI: 10.1136/hrt.2005.071290]
24 **Romero J**, Xue X, Gonzalez W, Garcia MJ. CMR imaging assessing viability in patients with chronic ventricular dysfunction due to coronary artery disease: a meta-analysis of prospective trials. *JACC Cardiovasc Imaging* 2012; **5**: 494-508 [PMID: 22595157 DOI: 10.1016/j.jcmg.2012.02.009]
25 **Hunold P**, Brandt-Mainz K, Freudenberg L, Vogt FM, Neumann T, Knipp S, Barkhausen J. [Evaluation of myocardial viability with contrast-enhanced magnetic resonance imaging--comparison of the late enhancement technique with positronemission tomography]. *Rofo* 2002; **174**: 867-873 [PMID: 12101477 DOI: 10.1055/s-2002-32697]
26 **Miller S**, Simonetti OP, Carr J, Kramer U, Finn JP. MR Imaging of the heart with cine true fast imaging with steady-state precession: influence of spatial and temporal resolutions on left ventricular functional parameters. *Radiology* 2002; **223**: 263-269 [PMID: 11930076 DOI: 10.1148/radiol.2231010235]
27 **Kramer CM**, Barkhausen J, Flamm SD, Kim RJ, Nagel E; Society for Cardiovascular Magnetic Resonance Board of Trustees Task Force on Standardized Protocols. Standardized cardiovascular magnetic resonance (CMR) protocols 2013 update. *J Cardiovasc Magn Reson* 2013; **15**: 91 [PMID: 24103764 DOI: 10.1186/1532-429X-15-91]
28 **Hombach V**, Merkle N, Bernhard P, Rasche V, Rottbauer W. Prognostic significance of cardiac magnetic resonance imaging: Update 2010. *Cardiol J* 2010; **17**: 549-557 [PMID: 21154256]
29 **Samady H**, Elefteriades JA, Abbott BG, Mattera JA, McPherson CA, Wackers FJ. Failure to improve left ventricular function after coronary revascularization for ischemic cardiomyopathy is not associated with worse outcome. *Circulation* 1999; **100**: 1298-1304 [PMID: 10491374 DOI: 10.1161/01.CIR.100.12.1298]
30 **Klein C**, Nekolla SG, Bengel FM, Momose M, Sammer A, Haas F, Schnackenburg B, Delius W, Mudra H, Wolfram D, Schwaiger M. Assessment of myocardial viability with contrast-enhanced magnetic resonance imaging: comparison with positron emission tomography. *Circulation* 2002; **105**: 162-167 [PMID: 11790695 DOI: 10.1161/hc0202.102123]
31 **Wang L**, Yan C, Zhao S, Fang W. Comparison of (99m)Tc-MIBI SPECT/18F-FDG PET imaging and cardiac magnetic resonance imaging in patients with idiopathic dilated cardiomyopathy: assessment of cardiac function and myocardial injury. *Clin Nucl Med* 2012; **37**: 1163-1169 [PMID: 23154474 DOI: 10.1097/RLU.0b013e3182708794]
32 **Wagner A**, Mahrholdt H, Holly TA, Elliott MD, Regenfus M, Parker M, Klocke FJ, Bonow RO, Kim RJ, Judd RM. Contrast-enhanced MRI and routine single photon emission computed tomography (SPECT) perfusion imaging for detection of subendocardial myocardial infarcts: an imaging study. *Lancet* 2003; **361**: 374-379 [PMID: 12573373 DOI: 10.1016/S0140-6736(03)12389-6]
33 **Rischpler C**, Langwieser N, Souvatzoglou M, Batrice A, van Marwick S, Snajberk J, Ibrahim T, Laugwitz KL, Nekolla SG, Schwaiger M. PET/MRI early after myocardial infarction: evaluation of viability with late gadolinium enhancement transmurality vs. 18F-FDG uptake. *Eur Heart J Cardiovasc Imaging* 2015; **16**: 661-669 [PMID: 25680385 DOI: 10.1093/ehjci/jeu317]
34 **Achenbach S**, Barkhausen J, Beer M, Beerbaum P, Dill T, Eichhorn J, Fratz S, Gutberlet M, Hoffmann M, Huber A, Hunold P, Klein C, Krombach G, Kreitner KF, Kühne T, Lotz J, Maintz D, Mahrholdt H, Merkle N, Messroghli D, Miller S, Paetsch I, Radke P, Steen H, Thiele H, Sarikouch S, Fischbach R. Consensus recommendations of the German Radiology Society (DRG), the German Cardiac Society (DGK) and the German Society for Pediatric Cardiology (DGPK) on the use of cardiac imaging with computed tomography and magnetic resonance imaging. *Rofo* 2012; **184**: 345-368 [PMID: 22426867 DOI: 10.1055/s-0031-1299400]
35 **Krumm P**, Zitzelsberger T, Weinmann M, Mangold S, Rath D, Nikolaou K, Gawaz M, Kramer U, Klumpp BD. Cardiac MRI left ventricular global function index and quantitative late gadolinium enhancement in unrecognized myocardial infarction. *Eur J Radiol* 2017; **92**: 11-16 [PMID: 28624007 DOI: 10.1016/j.ejrad.2017.04.012]
36 **Nensa F**, Poeppel T, Tezgah E, Heusch P, Nassenstein K, Mahabadi AA, Forsting M, Bockisch A, Erbel R, Heusch G, Schlosser T. Integrated FDG PET/MR Imaging for the Assessment of Myocardial Salvage in Reperfused Acute Myocardial Infarction. *Radiology* 2015; **276**: 400-407 [PMID: 25848898 DOI: 10.1148/radiol.2015140564]
37 **Nensa F**, Schlosser T. Cardiovascular hybrid imaging using PET/MRI. *Rofo* 2014; **186**: 1094-1101 [PMID: 25184216 DOI: 10.1055/s-0034-1385009]
38 **Anagnostopoulos C**, Georgakopoulos A, Pianou N, Nekolla SG. Assessment of myocardial perfusion and viability by positron emission tomography. *Int J Cardiol* 2013; **167**: 1737-1749 [PMID: 23313467 DOI: 10.1016/j.ijcard.2012.12.009]
39 **Rohatgi R**, Epstein S, Henriquez J, Ababneh AA, Hickey KT, Pinsky D, Akinboboye O, Bergmann SR. Utility of positron emission tomography in predicting cardiac events and survival in patients with coronary artery disease and severe left ventricular dysfunction. *Am J Cardiol* 2001; **87**: 1096-1099, A6 [PMID: 11348609]
40 **Slart RH**, Bax JJ, van Veldhuisen DJ, van der Wall EE, Dierckx RA, Jager PL. Imaging techniques in nuclear cardiology for the assessment of myocardial viability. *Int J Cardiovasc Imaging* 2006; **22**: 63-80 [PMID: 16372139 DOI: 10.1007/s10554-005-7514-8]

P- Reviewer: Nacak M, Tomizawa N **S- Editor**: Ji FF
L- Editor: A **E- Editor**: Wu YXJ

World Journal of Cardiology

Submit a Manuscript: http://www.f6publishing.com

World J Cardiol 2018 September 26; 10(9): 119-122

DOI: 10.4330/wjc.v10.i9.119

ISSN 1949-8462 (online)

LETTERS TO THE EDITOR

Snugger method - The Oldenburg modification of perceval implantation technique

Ahmed Mashhour, Konstantin Zhigalov, Marcin Szczechowicz, Sabreen Mkalaluh, Jerry Easo, Harald Eichstaedt, Dmitry Borodin, Jürgen Ennker, Alexander Weymann

Ahmed Mashhour, Konstantin Zhigalov, Marcin Szczechowicz, Sabreen Mkalaluh, Jerry Easo, Harald Eichstaedt, Dmitry Borodin, Jürgen Ennker, Alexander Weymann, Department of Cardiac Surgery, European Medical School Oldenburg-Groningen, Carl von Ossietzky University Oldenburg, Oldenburg 26133, Niedersachsen, Germany

ORCID number: Ahmed Mashhour (0000-0003-4496-3610); Konstantin Zhigalov (0000-0002-6440-3736); Marcin Szczechowicz (0000-0002-0711-7354); Sabreen Mkalaluh (0000-0003-0250-0060); Jerry Easo (0000-0001-9445-5716); Harald Eichstaedt (0000-0001-5106-3886); Dmitry Borodin (0000-0003-4716-0653); Jürgen Ennker (0000-0002-9946-6147); Alexander Weymann (0000-0003-2966-6159).

Author contributions: Mashhour A wrote the paper and collected the data; Zhigalov K, Szczechowicz M, Mkalaluh S and Borodin D collected the data; Eichstaed H, Easo J, Ennker J and Weymann A developed the technique, performed the surgeries and revised the paper.

Conflict-of-interest statement: The authors have no conflicts of interest to declare.

Manuscript source: Unsolicited Manuscript

Correspondence to: Alexander Weymann, MD, PhD, Consultant Cardiac Surgeon, Surgeon, Department of Cardiac Surgery, European Medical School Oldenburg-Groningen, Carl von Ossietzky University Oldenburg, Rahel-Strauß-Street 10, Oldenburg 26133, Niedersachsen, Germany. weymann.alexander@klinikum-oldenburg.de
Telephone: +49-441-4032820
Fax: +49-441-4032830

Received: April 14, 2018
Peer-review started: April 16, 2018
First decision: June 6, 2018
Revised: July 9, 2018
Accepted: August 26, 2018
Article in press: August 26, 2018
Published online: September 26, 2018

Abstract

We present a modified implantation technique of the Perceval® sutureless aortic valve (LivaNova, London, United Kingdom) that involves the usage of snuggers for the guiding sutures during valve deployment. Both limbs of each guiding suture are pulled through an elastic tube, which is fixed with a Pean clamp, which tightens the sutures and fixes the prosthesis to the aortic annulus during valve deployment. This method proved safe and useful in over 120 cases. Valve implantation was facilitated and the need for manipulation by the assistant or the nurse was eliminated.

Key words: Aortic valve; Surgical; Perceval; Snugger; Sutureless aortic valve

Core tip: In this article, we are presenting a modified implantation technique of the Perceval sutureless aortic valve prosthesis to enhance proper positioning of the prosthesis and aid the reproducibility of the implantation procedure. The modification involves using snuggers to fix the valve prosthesis to the aortic annulus during deployment.

Mashhour A, Zhigalov K, Szczechowicz M, Mkalaluh S, Easo J, Eichstaedt H, Borodin D, Ennker J, Weymann A. Snugger

method - The Oldenburg modification of perceval implantation technique. *World J Cardiol* 2018; 10(9): 119-122 Available from: URL: http://www.wjgnet.com/1949-8462/full/v10/i9/119.htm DOI: http://dx.doi.org/10.4330/wjc.v10.i9.119

TO THE EDITOR

Introduction

Surgery of the aortic valve replacement (AVR) is still recommended in certain patients with aortic valve disease. Two approaches have become quite popular; surgical and trans-catheter aortic valve replacement (SAVR and TAVR, respectively), whereby TAVR is mostly reserved for elderly patients with higher surgical risk[1,2]. Although not considered in the current guidelines, the sutureless variety of SAVR has been proven to reduce the overall surgical risk by significantly reducing operative and cross-clamp times, while demonstrating lower incidence of known complications of TAVR with comparable or even better results, especially in intermediate-risk patients[3-5].

The Perceval valve (Sorin Group Italia Srl, Saluggia, Italy) is a self-anchoring, self-expanding, sutureless, surgical aortic bioprosthesis. The valve leaflets are mounted to an elastic nickel-titanium alloy stent[3]. The stent anchors the valve *via* six sinusoidal posts to the aortic root at the sinuses of Valsalva, while the valve prosthesis seals the left ventricular outflow tract (LVOT) through an intra-annular and a supra-annular sealing ring. Correctly positioned, the leaflets of the valve prosthesis are aligned with those of the native aortic valve and the inflow ring of the prosthesis lies at the level of the insertion plane of the native leaflets[6]. The intra-annular ring of the Perceval valve prosthesis is supplied with three eyelets to pass guiding sutures which are previously made at the hinge points of the native aortic valve leaflets.

The valve prosthesis is then inserted into the aortic root over these guiding sutures and deployed "hand-held" in position. We describe a modification of this technique, where the prosthesis is virtually "fixed" onto the aortic annulus during deployment, which guarantees correct positioning of the prosthesis and aid the reproducibility of the implantation procedure.

Implantation technique according to the manufacturer (Sorin group)

The aortotomy should be in a transverse manner at least 3.5 cm above the aortic annulus to facilitate aortic closures. The native aortic valve is excised as with other SAVR prostheses. Although a complete decalcification of the aortic annulus is not necessary, a regular annular profile is essential for proper sealing. Sizing of the aortic annulus should be performed using the dedicated sizers. Now, the prepared prosthesis can be put in place. To ensure correct placement and alignment, a suture is made at hinge point of each leaflet perpendicular to the annulus, so that the three sutures are approximately 120° equidistant. The suture points should be 2-3 mm afar from each side of the insertion plane of the leaflets. After each suture is taken, the needle should be cut off and both ends of the thread secured with a clamp.

Each of the guiding sutures is then passed through one of the eyelets of the prosthesis. After that, the valve prosthesis is parachuted into the aorta sliding on the guiding threads which are kept straight with a gentle pull maintaining alignment with the aorta. Correct position of the prosthesis is reached when it is descended until it is stopped at the insertion points of the threads and the commissural struts of the prosthesis are aligned with the native commissures.

The valve is then released in two steps. First, the inflow section is released by rotating the control button on the delivery device until a click is heard and felt. At this stage, it is important to ensure that the sinusoidal struts correspond to the sinuses of Valsalva and that the stent of the prosthesis does not obstruct the coronary ostia. Second, the outflow section is released by withdrawing the sliding sheath off the holder avoiding rotational movement. It is important to keep the holder in an axial position to aorta all the time.

After visual assessment of the correct position and alignment of the prosthesis, patency of the coronary ostia and that no annulus is visible below and above the valve inflow ring, the inflow ring should be postdilated (4 atmospheric pressure for 30 s) using a dedicated catheter. While the postdilation balloon is inflated, warm sterile saline is poured within the aortic root to ensure optimal valve sealing and optimized anchoring. The guiding sutures are removed and the aortotomy is closed as usual taking care not to capture the stent of the prosthesis within the closure suture.

How we do it

Preparations of the prosthesis and the aortic root as well as the sizing procedure and prosthesis selection are similar to the method described above. The guiding sutures are also placed as described. We use 3/0 double-armed poly-propylene sutures. The suture is made with one needle from the LVOT side to the aorta side of the hinge point of each leaflet leaving 2-3 mm on each side as recommended above. The other needle is passed through the eyelet of the Perceval prosthesis before both needles are cut off.

Now, instead of directly securing the thread with a clamp, both ends are passed through an elastic tube making a snugger. While holding the prosthesis holder in place and axial to the aortic root, the snuggers are tightened. While tightening each snugger, both ends of the thread are pulled upwards. This "pull" is partially opposed by a light downward pressure on the prosthesis in the direction of the insertion of the guiding suture. The snugger is then pulled tight and secured with a Pean clamp (Figure 1).

This is repeated with the other two guiding sutures.

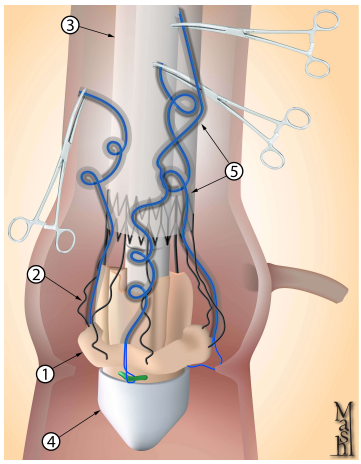

Figure 1 Graphic presentation of the prosthesis in place after tightening the snares and securing with clamps. 1 represents valve prosthesis; 2 represents valve stent; 3 represents shaft of the dual holder device; 4 represents tip of the dual holder device; 5 represents the snares.

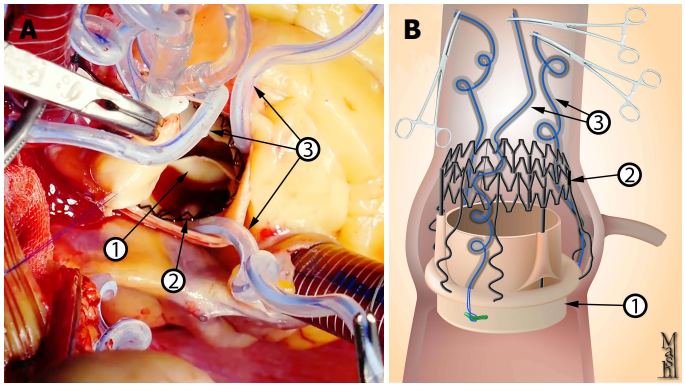

Figure 2 Intraoperative picture. A: Graphic presentation of the prosthesis after deployment; B: Prosthesis. Notice that the snare should not lie between the ring of the prosthesis and the annulus of the aorta. 1 represents valve prosthesis; 2 represents valve stent; 3 represents the snares.

The assistant should retract the aortic wall slightly open, so that the descent of the elastic tube into the tightened position is done under direct vision. It is important that the snuggers are tight enough; however, care should be taken that the elastic tube ends above the sealing ring of the inflow stent of the prosthesis and not trapped between the ring and the aortic annulus (Figure 2), as this could lead to incomplete deployment of the prosthesis, difficult withdrawal of the elastic tube and, potentially, dislodgement of the prosthesis during withdrawal of the elastic tube.

Next, the prosthesis is deployed in the same fashion described above. In this step, the assistant can help stabilize the prosthesis and hold the aorta open to aid visualization. Checking for correct positioning *etc.* as well as postdilation and irrigation with warm saline are also performed as described above.

Now, the snuggers a loosened and the elastic tubes are withdrawn. This should be done slowly and under direct vision taking care not to dislodge the prosthesis. The threads are then pulled out carefully. The prosthesis is checked again for proper anchoring and correct seat, and the aortotomy is closed.

Comment

As rapid-deployment prosthesis, one of the main benefits of the Perceval prosthesis is reducing operative and cross-clamp times through simplifying the surgical implantation technique. However, absolute stability is required during valve deployment to ensure proper seating of the prosthesis within the aortic root. Otherwise, valve malposition could occur[7].

On the contrary, in the technique described in this work, after tightening the snuggers, the prosthesis and the aortic annulus are fixed together eliminating the need for extra manipulations by the assistant or the nurse, so that the surgeon can self-sufficiently deploy the valve with one hand holding the delivery device and the other hand rotating the control button to release the valve.

Moreover, while tightening each snugger, the surgeon should pay attention to this one guiding suture; a step which is repeated with each suture at a time. On the contrary, the standard technique recommended by the manufacturer requires ensuring that the prosthesis is seated in the right position in respect to the three guiding sutures simultaneously.

According to the manufacturer's recommendations, traction sutures should be released prior to the deployment of the valve. We did not consider this step necessary as the snuggers would literally fix the valve prosthesis to the aortic annulus at three points forcing it into planarity and thus eliminating any distorting leverage exerted by the traction sutures. The continued presence of the traction sutures allows better visualization of the aortic annulus during prosthesis deployment.

In the manufacturer's recommendations, in case of a hypoplastic coronary ostium, the first guiding suture should be in the corresponding sinus. We did not encounter this in our case series. We also did not find any reports on the use of Perceval prosthesis in cases with a hypoplastic coronary ostium. Indeed, this should not be problematic. Nevertheless, the modification proposed in this work would add more security to the implantation, as the snuggers push the prosthesis down as far as possible, guaranteeing freedom of the hypoplastic ostium.

The use of snuggers, was reported once to facilitate a total endoscopic AVR[8]. However, to our knowledge, the use of snuggers to fixate the Perceval prosthesis during deployment in the way described in this work has not been described before. Until now, we have used this modification in over 120 patients with 100% primary success and excellent postoperative results.

REFERENCES

1 **Nishimura RA**, Otto CM, Bonow RO, Carabello BA, Erwin JP 3rd, Fleisher LA, Jneid H, Mack MJ, McLeod CJ, O'Gara PT, Rigolin VH, Sundt TM 3rd, Thompson A. 2017 AHA/ACC Focused Update of the 2014 AHA/ACC Guideline for the Management of Patients With Valvular Heart Disease: A Report of the American College of Cardiology/American Heart Association Task Force on Clinical Practice Guidelines. *Circulation* 2017; **135**: e1159-e1195 [PMID: 28298458 DOI: 10.1161/CIR.0000000000000503]

2 **Baumgartner H**, Falk V, Bax JJ, De Bonis M, Hamm C, Holm PJ, Iung B, Lancellotti P, Lansac E, Rodriguez Muñoz D, Rosenhek R, Sjögren J, Tornos Mas P, Vahanian A, Walther T, Wendler O, Windecker S, Zamorano JL; ESC Scientific Document Group. 2017 ESC/EACTS Guidelines for the management of valvular heart disease. *Eur Heart J* 2017; **38**: 2739-2791 [PMID: 28886619 DOI: 10.1093/eurheartj/ehx391]

3 **Fischlein T**, Meuris B, Hakim-Meibodi K, Misfeld M, Carrel T, Zembala M, Gaggianesi S, Madonna F, Laborde F, Asch F, Haverich A; CAVALIER Trial Investigators. The sutureless aortic valve at 1 year: A large multicenter cohort study. *J Thorac Cardiovasc Surg* 2016; **151**: 1617-1626.e4 [PMID: 26936009 DOI: 10.1016/j.jtcvs.2015.12.064]

4 **Laborde F**, Fischlein T, Hakim-Meibodi K, Misfeld M, Carrel T, Zembala M, Madonna F, Meuris B, Haverich A, Shrestha M; Cavalier Trial Investigators. Clinical and haemodynamic outcomes in 658 patients receiving the Perceval sutureless aortic valve: early results from a prospective European multicentre study (the Cavalier Trial)†. *Eur J Cardiothorac Surg* 2016; **49**: 978-986 [PMID: 26245628 DOI: 10.1093/ejcts/ezv257]

5 **Kadam PD**, Chuan HH. Erratum to: Rectocutaneous fistula with transmigration of the suture: a rare delayed complication of vault fixation with the sacrospinous ligament. *Int Urogynecol J* 2016; **27**: 505 [PMID: 26811110 DOI: 10.1007/s00192-016-2952-5]

6 **Folliguet TA**, Laborde F, Zannis K, Ghorayeb G, Haverich A, Shrestha M. Sutureless perceval aortic valve replacement: results of two European centers. *Ann Thorac Surg* 2012; **93**: 1483-1488 [PMID: 22541180 DOI: 10.1016/j.athoracsur.2012.01.071]

7 **Santarpino G**, Pfeiffer S, Concistrè G, Fischlein T. A supra-annular malposition of the Perceval S sutureless aortic valve: the 'χ-movement' removal technique and subsequent reimplantation. *Interact Cardiovasc Thorac Surg* 2012; **15**: 280-281 [PMID: 22535542 DOI: 10.1093/icvts/ivs148]

8 **Vola M**, Fuzellier JF, Gerbay A, Campisi S. First in Human Totally Endoscopic Perceval Valve Implantation. *Ann Thorac Surg* 2016; **102**: e299-e301 [PMID: 27645967 DOI: 10.1016/j.athoracsur.2016.03.045]

P- Reviewer: Iacoviello M, Dai X, Falconi M **S- Editor**: Dou Y
L- Editor: A **E- Editor**: Wu YXJ

Published by **Baishideng Publishing Group Inc**
7901 Stoneridge Drive, Suite 501, Pleasanton, CA 94588, USA
Telephone: +1-925-223-8242
Fax: +1-925-223-8243
E-mail: bpgoffice@wjgnet.com
Help Desk: http://www.f6publishing.com/helpdesk
http://www.wjgnet.com